Aus der Klinik für Neurologie
der Medizinischen Fakultät Charité – Universitätsmedizin Berlin

DISSERTATION

Relationships of ongoing activity, stimulus response variability, and behavioral performance in the human brain

zur Erlangung des akademischen Grades
Doctor medicinae (Dr. med.)

vorgelegt der Medizinischen Fakultät
Charité – Universitätsmedizin Berlin

von

Matthias Reinacher

aus Gießen

Gutachter: 1. Priv.-Doz. Dr. med. P. Ritter

2. Prof. Dr. A. Daffertshofer

3. Prof. Dr. M. Breakspear

Datum der Promotion: 23.06.2013

Contents

1 List of selected publications

The synopsis will refer to the studies conducted within the scope of this thesis as follows:

- **Study 1**: **Reinacher, M.**, Becker, R., Villringer, A. & Ritter, P. Oscillatory brain states interact with late cognitive components of the somatosensory evoked potential. *Journal of Neuroscience Methods* **183**, 49–56 (2009).

  Impact Factor (2010): 2.10

- **Study 2**: Becker, R., **Reinacher, M.**, Freyer, F., Villringer, A. & Ritter, P. How Ongoing Neuronal Oscillations Account for Evoked fMRI Variability. *The Journal of Neuroscience* **31**, 11016–11027 (2011).

  Impact Factor (2010): 7.27

- **Study 3**: Freyer, F., **Reinacher, M.**, Nolte, G., Dinse, H. R. & Ritter, P. Repetitive tactile stimulation changes resting–state functional connectivity—implications for treatment of sensorimotor decline. *Frontiers in Human Neuroscience* **6**, Article 144 (2012).

  Impact Factor (2010): 1.94

2 Synopsis

2.1 Abstract

The question of the function and meaning of brain rhythms, especially in the processing of stimuli and generation of stimulus–based (evoked) brain signals, has long been and still is a topic of great interest and debate. We tested different aspects of putative interactions between ongoing activity, evoked activity, and behavioral performance, using electroencephalography (EEG) and, partly, simultaneous functional magnetic resonance imaging (fMRI). We employed novel, online data analysis approaches allowing to maximize the signal of interest and the difference across conditions in a noisy, artefact–prone environment.

We discovered interactions between ongoing α and μ rhythms and the respective evoked potentials (EPs) in the examined sensory systems, indicating their involvement in stimulus processing and higher cognitive functions. Furthermore, we found effects of α rhythm power on evoked fMRI responses, both by linear superposition and by more complex, non–linear relationships, helping to explain the source of trial–by–trial variance in functional neuroimaging data and cast further light on the origin and nature of these rhythms.

Finally, we observed increased spatial acuity and changes in resting–state functional connectivity of the μ rhythm after a specific form of high–frequency repetitive somatosensory stimulation, showing that this form of stimulation changes intrinsic network properties of distant brain regions without the need for active participation of the subject. These data might provide a neurophysiological basis for the previously observed improvements in sensorimotor training in response to that stimulation, which make it a candidate for rehabilitation paradigms for e.g. stroke patients. Importantly, it also shows that assessment of functional connectivity might be used as a tool to study the efficacy of different sensory and motor training paradigms.

2.2 Introduction

Since they were first observed in 1929 [1], ongoing, spontaneous brain rhythms such as the α rhythm have been a subject of constant research and of numerous theories regarding their origin and functional meaning. They exhibit a number of striking features: Among others, some of them are visible in the EEG even to the naked human eye, and a link to intrinsic functional states and behavior has also already been noted by Berger [1], the most prominent being the so–called "α blocking" in an eyes–open compared to an eyes–closed condition. For a detailed overview, please see the book by Shaw [2]. The α rhythm interacts with components of the visual evoked potential (VEP) [3], and thus shows involvement with the processing of incoming stimuli and activity evoked by them.

Another interesting feature of brain–derived signals is the high variance in evoked signals despite input or stimulus being constant. On a single–cell level, this has been shown to be, to great extent, due to ongoing activity linearly superimposed on evoked activity [4]. In whole–brain human fMRI studies, ongoing activity from the somatomotor cortex of one hemisphere has been shown to explain much of the variance of motor task responses in the other hemisphere [5]. However, the blood oxygenation level–dependent (BOLD) fMRI signal is, as its name suggests, derived from metabolic properties of blood flow, and the exact origin of response variance is not clear—namely, whether this variance stems from neuronal sources, or might merely be a vascular or metabolic "by–product". Thus, an interesting question here is a putative neuronal basis of this activity, and whether this can be attributed to ongoing neuronal activity that is accessible to measurement with EEG, like the classic α rhythm introduced above.

A specific form of high–frequency repetitive somatosensory stimulation (RSS), following the Hebbian principle "what fires together, wires together" has been shown to induce lasting improvement in a somatosensory detection task [6] and improve outcome of somatomotor training paradigms [7], without active involvement of the participant. This makes this class of paradigms a likely candidate to supplement e.g. active–participation motor training in stroke rehabilitation. However, neurophysiological correlates of the latter effect are not yet clear. We addressed this question, testing functional connectivity of the somatosensory μ rhythm, which, given its tight links to the sensorimotor cortical network [8], seems a good candidate for assessment of changes in the network's connectivity properties.

2.3 Aims

The general aim of this thesis was to research the putative functional role of ongoing brain rhythms and specifically their relationship to the processing of

evoked, stimulus–based activity. More specifically, we wanted to test whether ongoing α and μ rhythms had effects on evoked potentials (EPs) in their respective sensory domains, and test the α rhythm as one potential source of stimulus response variance in BOLD fMRI signals.

To achieve this goal, we aimed to develop a setup capable of real–time, online detection of EEG signatures, and then to methodologically advance it in combination with an existing EEG–fMRI setup to the point where this detection becomes possible in the noisy, complex environment of simultaneous EEG–fMRI. This setup allowed us to design and implement experiments examining the relationship between ongoing activity in EEG and evoked, stimulus–based activity in both EEG and fMRI.

Finally, we implemented a setup to reproduce previously reported improvements in behavioral performance after RSS [6], in order to test the effects of this type of stimulation on resting–state connectivity parameters of brain rhythms.

2.4 Methods

I will provide an overview of the methods used for the studies carried out in the context of this thesis. For more detailed descriptions, please refer to the Methods sections of the attached publications.

From a general point of view, Study 1 and Study 2 deal with the question of the influence of ongoing (intrinsic) activity on evoked brain signals, and share much of their EEG–based methodology, even though they were carried out in a different sensory domain (i.e. on the somatosensory μ rhythm in Study 1 and the visual α rhythm in Study 2). Study 2 adds fMRI data acquisition to the online EEG approach of Study 1.

Study 3 deals with the question of functional connectivity changes in the somatosensory system after RSS.

Subjects and experimental design

All studies were carried out with healthy volunteers. Prior to the experiments, subjects gave written informed consent in accordance with the declaration of Helsinki [9]. All studies were approved by the local ethics committee.

Study 1

Subjects sat in a comfortable chair, wearing earplugs to minimize noise exhibition, and asked to relaxedly fixate a point 1.5 m in front of them. Vibrotactile stimuli were applied to their right index and middle finger using a custom–made piezoceramic vibrator affixed with adhesive tape. Two experiments were conducted: A pre–experiment designed to block–wise modulate the μ rhythm and identify blind source separation (BSS) components correlated with this

rhythm, and the main experiment, consisting of a μ–triggered vibrotactile frequency discrimination oddball task.

Study 2

Subjects lying in the bore of the MR scanner were presented with visual stimuli via a projection screen. Similar to Study 1, two experiments were performed: A pre–experiment designed to modulate the occipital α rhythm to determine BSS components correlated with the rhythm, and a main experiment consisting of an α–triggered visual oddball task.

Study 3

Subjects sitting in a comfortable chair in a dimly lit room were instructed to stay awake and to watch a silent animal documentary on a distant computer screen. Three sessions of the experiment were conducted: A *pre* session of resting–state EEG recording, a *RSS* session of high–frequency somatosensory stimulation, and a *post* session again of resting–state EEG recording.

Data acquisition and online analysis

EEG recording

In all studies, EEG data was recorded using 32–channel MR–compatible EEG amplifiers (BrainAmp MR, Brain Products, Munich, Germany) and EEG caps (EasyCap, FMS, Herrsching–Breitbrunn, Germany). Scalp electrodes were arranged according to the international 10–20 system with the reference electrode positioned at position FCz.

In Study 1 and Study 3, two amplifiers and a corresponding EEG cap were used for a 64–channel setup. In Study 2, one amplifier and a corresponding cap were used for a 32–channel setup.

fMRI recording

In Study 2, a combined EEG–fMRI setup was used to study metabolic changes associated with stimulation during different states of brain rhythms. A 1.5 T scanner was used for fMRI recordings (Magnetom Vision, Siemens, Erlangen, Germany). For this study, a modified T2*–weighted EPI–BOLD sequence ('stepping stone') was used, optimized for EEG–fMRI and minimization of Image Acquisition Artefacts (IAAs) during simultaneous acquisition [10]. Also, the clock of the EEG amplifier was synchronized to the MR gradient system clock to ensure time–invariant sampling and thus far better artifact removal using Average Artefact Subtraction [11].

Online EEG analysis

In Studies 1 and 2, an online analysis approach was used to maximize the difference between conditions, and to ensure sufficient signal–to–noise ratio for the signal of interest. This approach consisted of two steps:

First, a spatial filter was determined to maximize the signal of interest and minimize unwanted artefacts in the EEG (e.g. eye movements and the heart beat–related ballistocardiogram). This required a pre–experiment in which the spontaneous rhythm was manipulated. In Study 1, this consisted of a block–wise eyes–open/eyes–closed task, in Study 2 of block–wise continuous vibrotactile stimulation vs. rest. Using a computationally effective form of BSS (TDSEP, [12]), we identified the component that correlated best with pre–experiment paradigm and hence the rhythm itself.

Second, the EEG time series resulting from this spatial filter was used for real–time detection of ongoing activity. In Study 2, incoming IAA–contaminated EEG was artefact–corrected in real–time using a vendor–supplied plugin for the RecView software (Brain Products, Munich, Germany). In both studies, the EEG was fed to an in–house developed plugin that analyzed frequency content using a short–term Fast Fourier Transform (FFT), and triggered stimulation based on different parameters set before the experiment. Using this approach, we maximized the difference between the control condition and a condition with strong ongoing α or μ rhythm, while keeping inter–stimulus intervals (ISIs) large enough to allow the event–related desynchronization to fully return to baseline. This was also important in Study 2, since adequate ISIs had to be ensured for the event–related fMRI BOLD analysis.

Data analysis

EEG data

EEG data analysis was mainly carried out in MATLAB (The Mathworks Inc., Natick, MA, USA) using the open–source toolbox EEGLAB [13].

Study 1

The impact of ongoing μ rhythm power on the somatosensory evoked potential (SEP) was examined. We compared the SEPs of the two aforementioned conditions, as well as the topography of different SEP components. We tested for differences in the SEPs using Student's t–Test.

Study 2

Raw IAA–contaminated EEG data was first corrected using Vision Analyzer (BrainProducts, Munich, Germany). Then, we compared the visual evoked potentials (VEPs) as in [3] and time–frequency analyses of trials to validate

the online approach in the noisy EEG–fMRI setting. Our analysis then predominantly focused on the metabolic BOLD changes, as described below.

Study 3

For the *RSS* session, we used ICA to determine components related to the somatosensory stimulation, and to exclude artefacts like eye movements, scalp muscle artefacts and gross movement artefact. For this, we evaluated SEPs and event–related spectral perturbation. We then used the resulting somato–IC to determine each subject's individual μ peak frequency. We defined three sub–bands with respect to this individual frequency: lower higher, and peak bands, as well as a broad β band. Please refer to the attached publication for their exact definition.

For the *pre* and *post* sessions, we calculated resting–state power spectra for each band using Welch's method. We then calculated Imaginary Coherency [14] as a measure of functional connectivity between each possible channel pair. We tested for differences between *pre* and *post* sessions using Student's t–Test, after normalizing the data using Fisher's Z–transformation.

fMRI data

In Study 2, we assessed the effect of α rhythm–dependent stimulation on evoked BOLD responses. fMRI data preprocessing and analysis was performed using the open–source analysis suite SPM5 [15].

Using SPM, we built a General Linear Model modeling the expected hemodynamic responses to the experimental paradigm. We analyzed the following conditions: The high–α state stimulation condition, the state–independent stimulation condition that served as a control condition, i.e. stimuli were shown irrespectively of α power, and the high–α inter–stimulus condition, which identified periods of high α activity in periods without visual stimulation within the second condition. The resulting prediction was correlated to the fMRI data, yielding a measure of how well the model was able to predict the actual data. Then, we calculated contrasts showing alpha–dependent effects on stimulation and baseline.

We then compared stimulus response amplitudes of the different regressors within significant regions to be able to determine if the α baseline modulation could account for the stimulus response modulation, i.e. a linear superposition of α and stimulus effects on the BOLD signal is possible as explanation for the observed variance.

2.5 Results

Study 1

We successfully demonstrated the feasibility of online detection and classification of μ rhythm states. We found an interaction between μ rhythm and late components of the SEP—namely, significantly larger N140 and P260 components after stimulation in high–μ state. Interestingly, these components exhibit a largely fronto–central topography, corresponding to their putative connection to higher cognitive processing and attention [16], whereas the increase in μ rhythm power is located unilaterally over the somatosensory cortex, as expected.

Study 2

Concerning EEG data, we found effects on the late EP component similar to those in [3], and verified that α rhythm dependent stimulation was properly achieved despite noise and artefact issues typical for the MR environment.

We were able to observe α–dependent BOLD stimulus response signal decreases in posterior, thalamic, and cerebellar areas. Of these areas, a subset mainly in visual areas showed a corresponding BOLD baseline decrease in correlation with α rhythm power, implying a linear superposition of ongoing and resting–state fMRI activity. Another subset, mainly comprised of thalamic, cerebellar and smaller occipital and precuneal areas, exhibited α–dependent stimulus response modulation, but not baseline modulation, thus indicating a more complex, non–linear relationship between stimulus variance and α rhythm.

Study 3

RSS led to an increase in tactile acuity, namely a significant reduction of the 2–point discrimination threshold. These results are closely in line with earlier studies using the identical protocol [6], ensuring stimulation efficacy as the basis for further analysis.

Comparing the *pre* and *post* sessions, we found significant changes in functional connectivity measured by Imaginary Coherency in the upper μ frequency band. Significant channel pairs were located over central cortical areas contralateral to the somatosensory stimulation, i.e. at the site of expected stimulation effects. We found only isolated single channel pairs in the other bands.

2.6 Discussion

Methodologically, we were able to set up a real–time, online EEG analysis tool capable of detecting EEG signatures and their features during experiment run–time. Using Blind Source Separation and advances in EEG–fMRI recording techniques, we successfully adapted this setup to the special environment of simultaneous EEG–fMRI, dealing with the inherently noisy and artefact–ridden MRI situation. This existing setup can now be adapted to new questions, such as analysing not only amplitude, but also the phase of ongoing activity, to mention one example.

We discovered effects of ongoing μ rhythm power on late, cognitive components of the SEP. This finding was in line with earlier findings of our group concerning the occipital α rhythm and the visual evoked potential [3]. Thus, we postulate that the interaction with late components of the EP might be a universal feature of ongoing rhythms and the respective EPs in sensory systems. Interestingly, the topography of the components modulated was not consistent with the topography of the ongoing rhythm itself—speaking against a direct causative role of the rhythm's fluctuation in the EP effect, but rather for an indirect top–down or bottom–up influence, or a third party driving both ongoing rhythm and EP component amplitude. It has been suggested that the μ rhythm at least partially represents top–down modulation of somatomotor areas by executive areas [17], which fits well with the N140 and P260 components' involvement with attention [16] and their fronto–central topography.

Regarding the fMRI results from Study 2, we provide evidence that, indeed, intrinsic neuronal activity as captured by ongoing EEG rhythms is at least partly responsible for evoked fMRI response variance. We were able to confirm our linear superposition hypothesis for distinct brain regions, while also discovering areas where fMRI responses are modulated, but such a direct, additive link was not found. One explanation for this might be the U–shaped relations between ongoing activity and behaviour found in certain conditions such as near–threshold stimuli [18]. In our results, however, linear superposition was the dominant mechanism in terms of statistical robustness. It is noteworthy in this context that the concepts of linear superposition and functional roles of ongoing activity are not mutually exclusive [19].

The RSS paradigm used in Study 3 has been extensively researched, and has been shown to not only improve tactile acuity [6], but also cause reorganization of cortical maps [20] via a proposed Hebbian–like learning process. It also improves motor test results in stroke patients and stabilizes training effects compared to the same training without stimulation [7], indicating an involvement of different functional areas of the sensorimotor system in the emergence of these results. We provide neurophysiological evidence of an effect on the resting–state network properties of the brain in form of altered functional connectivity between these areas after stimulation. This may ac-

count for the improvements and functional changes noted above. Assessment of changes in functional connectivity could prove to be a valuable tool for the evaluation of both sensory and motor training paradigms in the rehabilitation not only of stroke patients, but also in physiological, age–related decline of sensorimotor capabilities [21].

Concluding, we have identified several ways how ongoing brain activity such as the α and μ rhythms, evoked, stimulus–based activity, and behavioral performance interact. We provide evidence in support of the assumption that intrinsic, ongoing brain activity is responsible for evoked signal variance in different sensory and recording modalities, and we show that high–frequency RSS elicits changes in resting–state functional connectivity and thus in network properties of the brain.

As a general outlook, the research done in the scope of this study could be extended by taking the experiment done in Study 2 into different sensory modalities, stressing our hypothesis that ongoing activity accounts for variance in evoked responses across different sensory systems and recording modalities. Also, integration of behavioral tests by combining online, rhythm–driven stimulation and more complex tasks and paradigms will provide further, exciting insights into the relevance of ongoing activity for different aspects of human performance, and possibly lead to new tools and treatments counteracting the effects of disease and physiological aging on complex human brain function.

2.7 References

[1] Berger, H. Über das Elektrenkephalogramm des Menschen. *Archiv für Psychiatrie und Nervenkrankheiten* **87**, 527–570 (1929).

[2] Shaw, J. *The brain's alpha rhythms and the mind* (Elsevier B.V., Amsterdam, 2003).

[3] Becker, R., Ritter, P. & Villringer, A. Influence of ongoing alpha rhythm on the visual evoked potential. *NeuroImage* **39**, 707–716 (2008).

[4] Arieli, A., Sterkin, A., Grinvald, A. & Aertsen, A. Dynamics of ongoing activity: explanation of the large variability in evoked cortical responses. *Science* **273**, 1868–1871 (1996).

[5] Fox, M. D., Snyder, A. Z., Zacks, J. M. & Raichle, M. E. Coherent spontaneous activity accounts for trial-to-trial variability in human evoked brain responses. *Nature Neuroscience* **9**, 23–25 (2006).

[6] Godde, B., Stauffenberg, B., Spengler, F. & Dinse, H. R. Tactile coactivation-induced changes in spatial discrimination performance. *The Journal of Neuroscience* **20**, 1597–1604 (2000).

[7] Smith, P. S., Dinse, H. R., Kalisch, T., Johnson, M. & Walker-Batson, D. Effects of repetitive electrical stimulation to treat sensory loss in persons poststroke. *Archives of Physical Medicine and Rehabilitation* **90**, 2108–2111 (2009).

[8] Salmelin, R., Hámáaláinen, M., Kajola, M. & Hari, R. Functional Segregation of Movement-Related Rhythmic Activity in the Human Brain. *NeuroImage* **2**, 237–243 (1995).

[9] WMA Declaration of Helsinki - Ethical Principles for Medical Research Involving Human Subjects (2008). URL `http://www.wma.net/en/30publications/10policies/b3/index.html`.

[10] Anami, K., Mori, T., Tanaka, F., Kawagoe, Y., Okamoto, J., Yarita, M., Ohnishi, T., Yumoto, M., Matsuda, H. & Saitoh, O. Stepping stone sampling for retrieving artifact-free electroencephalogram during functional magnetic resonance imaging. *NeuroImage* **19**, 281–295 (2003).

[11] Mandelkow, H., Halder, P., Boesiger, P. & Brandeis, D. Synchronization facilitates removal of MRI artefacts from concurrent EEG recordings and increases usable bandwidth. *NeuroImage* **32**, 1120–1126 (2006).

[12] Ziehe, A., Muller, K. R., Nolte, G., Mackert, B. M. & Curio, G. Artifact reduction in magnetoneurography based on time-delayed second-order

correlations. *IEEE Transactions on Biomedical Engineering* **47**, 75–87 (2000).

[13] Delorme, A. & Makeig, S. EEGLAB: an open source toolbox for analysis of single-trial EEG dynamics including independent component analysis. *Journal of Neuroscience Methods* **134**, 9–21 (2004).

[14] Nolte, G., Bai, O., Wheaton, L., Mari, Z., Vorbach, S. & Hallett, M. Identifying true brain interaction from EEG data using the imaginary part of coherency. *Clinical Neurophysiology* **115**, 2292–2307 (2004).

[15] SPM - Statistical Parametric Mapping. URL `http://www.fil.ion.ucl.ac.uk/spm/`.

[16] Kenntner-Mabiala, R., Andreatta, M., Wieser, M. J., Mühlberger, A. & Pauli, P. Distinct effects of attention and affect on pain perception and somatosensory evoked potentials. *Biological Psychology* **78**, 114–122 (2008).

[17] Pineda, J. A. The functional significance of mu rhythms: translating "seeing" and "hearing" into "doing". *Brain Research Reviews* **50**, 57–68 (2005).

[18] Linkenkaer-Hansen, K., Nikulin, V. V., Palva, S., Ilmoniemi, R. J. & Palva, J. M. Prestimulus oscillations enhance psychophysical performance in humans. *The Journal of Neuroscience* **24**, 10186–10190 (2004).

[19] Fox, M. D., Snyder, A. Z., Vincent, J. L. & Raichle, M. E. Intrinsic fluctuations within cortical systems account for intertrial variability in human behavior. *Neuron* **56**, 171–184 (2007).

[20] Pleger, B., Foerster, A. F., Ragert, P., Dinse, H. R., Schwenkreis, P., Malin, J. P., Nicolas, V. & Tegenthoff, M. Functional imaging of perceptual learning in human primary and secondary somatosensory cortex. *Neuron* **40**, 643–653 (2003).

[21] Kalisch, T., Tegenthoff, M. & Dinse, H. R. Repetitive electric stimulation elicits enduring improvement of sensorimotor performance in seniors. *Neural Plasticity* **2010**, Article 690531 (2010).

3 Declaration of contribution to publications

- **Study 1**: **Reinacher, M.**, Becker, R., Villringer, A. & Ritter, P. Oscillatory brain states interact with late cognitive components of the somatosensory evoked potential. *Journal of Neuroscience Methods* **183**, 49–56 (2009).

  Contribution in percent: 75

  Detailed contribution: Designed the study, conducted the experiments, analysed the data, wrote the paper, oversaw the review process.

- **Study 2**: Becker, R., **Reinacher, M.**, Freyer, F., Villringer, A. & Ritter, P. How Ongoing Neuronal Oscillations Account for Evoked fMRI Variability. *The Journal of Neuroscience* **31**, 11016–11027 (2011).

  Contribution in percent: 35

  Detailed contribution: Participated in the design of the experiment, conducted the experiments, participated in analysing the data, participated in writing the paper & review process.

- **Study 1**: Freyer, F., **Reinacher, M.**, Nolte, G., Dinse, H. R. & Ritter, P. Repetitive tactile stimulation changes resting–state functional connectivity—implications for treatment of sensorimotor decline. *Frontiers in Human Neuroscience* **6**, Article 144 (2012).

  Contribution in percent: 30

  Detailed contribution: Participated in analysing the data and writing the paper. Participated in the review process.

Matthias Reinacher _____

4 Attached copies of publications

4.1 Study 1

- **Reinacher, M.**, Becker, R., Villringer, A. & Ritter, P. Oscillatory brain states interact with late cognitive components of the somatosensory evoked potential. *Journal of Neuroscience Methods* **183**, 49–56 (2009).

  Reprinted from Journal of Neuroscience Methods, reference above, with permission from Elsevier.

Journal of Neuroscience Methods 183 (2009) 49–56

Contents lists available at ScienceDirect

Journal of Neuroscience Methods

journal homepage: www.elsevier.com/locate/jneumeth

Oscillatory brain states interact with late cognitive components of the somatosensory evoked potential

Matthias Reinacher[a], Robert Becker[a], Arno Villringer[a,b,c], Petra Ritter[a,c,*]

[a] Bernstein Center for Computational Neuroscience, Berlin and Department of Neurology, Charité Universitaetsmedizin Berlin, Berlin, Germany
[b] Max Planck Institute for Brain and Cognitive Sciences, Leipzig, Germany
[c] Berlin School of Mind and Brain & Mind and Brain Institute, Philosophical Institute, Humboldt University, Berlin, Germany

ARTICLE INFO

Article history:
Received 3 June 2009
Received in revised form 26 June 2009
Accepted 27 June 2009

Keywords:
Rolandic rhythm
Alpha rhythm
Somatosensory
SEP
EEG
Ongoing
Evoked

ABSTRACT

The question of interaction between ongoing neuronal activity and evoked responses has been addressed for different species, sensory systems and measurement modalities. Among other findings, there is converging evidence for an interaction of occipital alpha-rhythm amplitude with the visual evoked potential. Here, we test the hypothesis that the modulatory role of an ongoing rhythm might not be confined to the visual system and the occipital alpha rhythm, but instead may be generalized to other sensory systems. Using an online EEG analysis approach, we investigated the influence of the Rolandic alpha-rhythm on the somatosensory evoked potential (SEP). We triggered vibrotactile stimulation during periods of high Rolandic alpha-rhythm amplitude. Analysis revealed significant effects of pre-stimulus Rolandic alpha amplitude on the amplitude of the N140 and P260 components of the SEP, known to be linked to cognitive processing, but not on early sensory components. The N140–P260 complex shows a different focus in topography than the early sensory components and the pre-stimulus Rolandic alpha rhythm. These results indicate an involvement of Rolandic alpha-rhythm in higher cognitive processing. In more general terms – and in the context of similar studies in the visual system – our findings suggest that modulation of late EP components by ongoing rhythms might be a characteristic and possibly universal feature of sensory systems.

1. Introduction

Ever since their first observation, ongoing brain oscillations such as the occipital alpha-rhythm (Berger, 1929) and the Rolandic alpha (μ) rhythm generated in sensorimotor areas (Gastaut, 1952; Kuhlman, 1978) have been widely investigated with respect to their cellular origin, sites of generation, and the question whether they bear functional significance for information processing in the brain (Niedermeyer and Lopes da Silva, 2004). Numerous phenomena indicating such significance became evident:

Rhythms are modulated by behavior resulting in well-known phenomena such as the classic occipital "alpha blocking" during eyes opening, the event-related desynchronization (ERD) of the occipital alpha-rhythm during visual stimulation and of the Rolandic alpha-rhythm during sensorimotor tasks (Arroyo et al., 1993; Chatrian et al., 1959; Cheyne et al., 2003; Jasper and Penfield, 1949; Pfurtscheller and Aranibar, 1980; Pfurtscheller and Berghold, 1989; Salmelin et al., 1995; Salmelin and Hari, 1994) and the (re)synchronization (ERS) of these rhythms following an event and after cessation of a task or stimulation (Neuper et al., 2006). Alpha-rhythm amplitudes increase during higher memory load (Jensen et al., 2002) and decrease with higher attentional demand (Ray and Cole, 1985; Rihs et al., 2007; Sauseng et al., 2005; Thut et al., 2006; Worden et al., 2000). Sleep deprivation as a method of inducing fatigue alters both alpha-rhythm and auditory- and motor-evoked fields (Boonstra et al., 2005).

Specific properties of the alpha rhythms correlate with behavioral performance measures. For example, good perceptual (Hanslmayr et al., 2005a) and memory (Klimesch, 1997) performance are related to strong alpha-rhythm ERD. Pre-stimulus alpha power is lower before perceived as compared to unperceived visual stimuli (Ergenoglu et al., 2004). Intermediate amplitudes of the Rolandic alpha-rhythm facilitate somatosensory stimulus perception in near-threshold stimulation conditions (Linkenkaer-Hansen et al., 2004). Pre-stimulus Rolandic alpha-rhythm predicts detection of a target stimulus against stronger masking stimuli (Schubert et al., 2008).

Furthermore, controlled manipulation of the alpha-rhythm alters behavior. Both rapid-rate transcranial magnetic stimulation (rTMS) at individual alpha frequency (Klimesch et al., 2003)

* Corresponding author at: Bernstein Center for Computational Neuroscience, Berlin and Department of Neurology, Charité Universitaetsmedizin Berlin, Berlin, Germany. Tel.: +49 30 450560005.
E-mail address: petra.ritter@charite.de (P. Ritter).

0165-0270/$ – see front matter © 2009 Elsevier B.V. All rights reserved.
doi:10.1016/j.jneumeth.2009.06.036

and neurofeedback-mediated increase in alpha-rhythm amplitude resulting in enhanced ERD (Hanslmayr et al., 2005b) are associated with improved performance in a mental rotation task.

Combining electroencephalography (EEG) and functional magnetic resonance imaging (fMRI), several studies have shown that higher occipital alpha-rhythm amplitudes (de Munck et al., 2007; Difrancesco et al., 2008; Feige et al., 2005; Goldman et al., 2002; Goncalves et al., 2005; Laufs et al., 2003a,b; Moosmann et al., 2003) as well as higher Rolandic alpha-rhythm amplitudes (Ritter et al., 2009) are associated with a decreased blood oxygen level dependent (BOLD) fMRI signal in specific cortical areas, indicating less net neuronal activity. In line with these findings, alpha activity has been associated with cortical inhibition (Klimesch et al., 2007; Neuper et al., 2006).

A long-debated question has been the interaction between ongoing (oscillatory) activity, such as EEG rhythms, and event- or stimulus-related activity as measured by evoked potentials (EPs). Several theories on the nature of the relationship between ongoing and evoked activities have been proposed (see detailed overviews in Becker et al. (2008), Sauseng et al. (2007) and note the current debate in *Neuroimage* (Klimesch et al., 2009; Risner et al., 2009; Ritter and Becker, 2009).

Prevailing theories are: (1) The evoked response is – at least partially – generated by the phase alignment of an ongoing rhythm with respect to the event or stimulus (Makeig et al., 2002; Sayers et al., 1974). This "phase-reset" theory implies that identical neuronal assemblies generate evoked response and rhythm. (2) The evoked response is independent of the ongoing rhythm and adds linearly to the ongoing activity ("evoked" theory) (Arieli et al., 1996), implying different neuronal assemblies. (3) The evoked response interacts with (contrary to the evoked theory), but is not generated by the ongoing rhythm (contrary to the phase reset theory). Possible scenarios for this "interaction" theory are: The neuronal assembly generating the rhythm exerts influence over the neuronal assembly generating the EP and vice versa. A third neuronal assembly modulates both – neuronal assemblies that generate the rhythm and neuronal assemblies that generate the EP.

In previous studies, we reported an interaction of the occipital alpha-rhythm and a late (220–310 ms post stimulus) component of the visual evoked potential (VEP) in a passive viewing task (Becker et al., 2008) and in an oddball task (Becker et al., 2009). Since the late component is composed of frequencies lower than the alpha-rhythm and arises during maximum ERD, a phase reset as constituting mechanism (theory 1) is unlikely. A possible explanation has been offered by the magnetoencephalography (MEG) works of (Nikulin et al., 2007) and (Mazaheri and Jensen, 2008), proposing non-zero mean characteristics of Rolandic and occipital alpha-rhythm as a mechanism by which late evoked components are generated. Concerning late somatosensory evoked field (SEF) components, Nikulin et al. (2007) focus on a time window 250–600 ms post stimulus. In their study, both late SEF amplitude effects and Rolandic alpha-rhythm non-zero mean characteristics exhibited highly consistent topographies over primary somatosensory areas contralateral to stimulation, supporting the theory that the observed SEF effects are caused by the rhythm.

So far, processing of supra-threshold somatosensory stimuli in an oddball task has not been investigated for the relation between pre-stimulus Rolandic alpha-rhythm amplitude and the somatosensory evoked potential (SEP).

Hence the goal of this study is two-fold: first, to investigate whether modulation of EP components in an oddball task by the pre-stimulus alpha rhythm, as found in Becker et al. (2009), is restricted to the visual system and the occipital alpha rhythm, or rather may be a more general phenomenon, being also inherent in other modalities, such as somatosensation. Second, to investigate topographies of alpha-rhythm state changes and presumptive EP amplitude effects, to infer whether the rhythm per se may give rise to the observed effect.

2. Methods

2.1. Subjects

15 subjects with no history of neurological or psychiatrical disease (10 female/5 male, mean age 27.1 years ± 4.7 years) participated in the study. All experiments were performed in compliance with the relevant laws and institutional guidelines. Subjects were sitting comfortably in a chair, wearing earplugs to minimize noise exhibition as well as prevent auditory frequency discrimination due to different vibration-related sounds generated by the stimulus device in the experiment. Subjects were asked to keep their eyes open, to fixate a point 1.5 m in front of them in a relaxed manner and to avoid excessive eye movements.

2.2. EEG recording

We used a 64-electrode cap (Easy-Cap, FMS, Herrsching-Breitbrunn, Germany) for EEG recordings, carrying 61 scalp electrodes placed following the international 10–20 system, with a hardwired reference at position FCz. Furthermore, two electrocardiogram (ECG) electrodes and one vertical electrooculogram (vEOG) electrode below the left eye were recorded. Electrode impedances were maintained below 10 kΩ by applying an abrasive electrode paste (ABRALYT 2000; FMS, Herrsching-Breitbrunn, Germany). Two 32-channel high dynamic range EEG amplifiers (BrainAmp MR Plus, BrainProducts GmbH, Munich, Germany) were used, as well as the BrainVision Recorder and RecView software by the same company for recording and online analysis of EEG data. Sampling rate was 5 kHz, recording resolution 0.5 μV with 16 bit dynamic range. In the analog pre-filter, no highpass filter setting was used, thus also recording direct current (DC), and a lowpass setting of 250 Hz.

2.3. Stimulation equipment

We used an in-house built programmable vibrotactile stimulator (Medizinisch-Technische Labore, Charité Universitätsmedizin Berlin, Germany) driving a custom-made piezoceramic vibrator, measuring 22 mm in diameter. The vibrator was affixed to the subjects' right index and middle finger using adhesive tape. The subjects' right hands were positioned on a pad on the table in front of them to avoid stimulation of e.g. upper leg. Stimulation was carried out by a computer using MATLAB (The Mathworks, Natick, MA, USA) and the Cogent 2000 toolbox (developed by the Cogent 2000 team at the FIL and the ICN and Cogent Graphics developed by John Romaya at the LON at the Wellcome Department of Imaging Neuroscience). Stimulation markers were written in the EEG recording for each stimulus and subject response.

2.4. Pre-experiment to determine individual Rolandic alpha topography

All subjects underwent a vibrotactile stimulation paradigm designed to desynchronize the Rolandic alpha-rhythm prior to the main experiment, in order to identify blind source separation (BSS) components maximally correlated with Rolandic alpha-rhythm ERD and subsequent synchronization. We recorded EEG during a passive block-wise vibrotactile stimulation task (t = 8 min, 12 blocks each consisting of 20 s rest and 20 s stimulation with f = 70 Hz, stimulus duration t = 400 ms and stimulus repetition rate f = 2 Hz). Data was subsequently analyzed using custom MATLAB procedures, partly based on EEGLAB (Delorme and Makeig, 2004). After

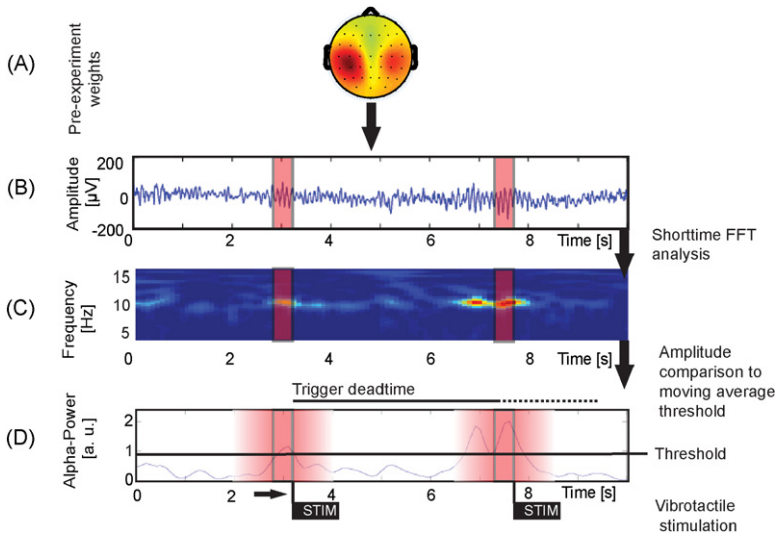

Fig. 1. Stimulation protocol for the alpha-triggered condition of the main experiment. (A) In the pre-experiment a BSS component is identified representing Rolandic alpha rhythm. (B) In the main experiment, EEG activity is weighted by the BSS component weights. (C) The EEG is time–frequency decomposed using a short time FFT with a sliding window of 2048 sample points/410 ms. (D) Alpha-band amplitude is compared to a sliding average baseline of one minute and stimulation is triggered when amplitude exceeds 1.5 SD of the baseline. A trigger dead-time of 4–6 s after stimulation controls for sufficient inter-stimulus interval lengths.

down sampling to 200 Hz, a BSS decomposition using the TDSEP algorithm was calculated. We chose this algorithm due to its ability to separate small physiological signals from 'noisy' recordings (Ziehe et al., 2000), its robustness, and its small computational load compared to iterative procedures. The amplitude of the resulting BSS components' alpha band was correlated with the task function described above, and components exhibiting highest negative correlation, i.e. those reflecting Rolandic alpha-rhythm ERD/ERS following the task function, were identified. A semi-automatic approach to component identification was employed, consisting of plotting the component topographies alongside their respective correlation values. Based on their topography, those components were ignored representing signatures of extracerebral origin, e.g. eye movements or muscle artifact. After exclusion of those 'artifact' components, we chose the component best representing Rolandic alpha-rhythm based on its topography (i.e. maximal weights in pericentral areas) and its correlation with the task (reflecting task-related ERD and ERS). We weighted the topography of the component higher than the task correlation, i.e. we chose from those components exhibiting typical Rolandic alpha-rhythm topographies the one that correlated best. The chosen component was then used as a spatial filter for real-time calculation of Rolandic alpha-rhythm amplitude in the main experiment, as described below.

2.5. Main experiment

We employed a vibrotactile frequency discrimination oddball task. Two stimuli were used, a standard stimulus $f = 40$ Hz and $t = 900$ ms, and a deviant stimulus differing in frequency, $f = 70$ Hz ($f = 120$ Hz in one subject due to excessive error rate). Subjects were asked to keep their eyes open, to concentrate on their right index and middle finger, and to quickly press a button on an in-house built response box with their left thumb as soon as they detected the deviant stimulus.

Two conditions were used for the main experiment. In the 'alpha-triggered' condition, the alpha-band amplitude in the component described above is continually measured by an in-house plug-in to the RecView software, using a short time fast Fourier transform (FFT) approach. RecView transmits data chunks of approximately 100 samples, corresponding to 20 ms, to the plug-in which maintains a buffer corresponding to the FFT window size of 2048 sample points (410 ms). Each time a data chunk arrives, the plug-in calculates the amplitude spectrum of the FFT window in the alpha band, and adds the value to an ongoing moving average baseline of one minute length. The plug-in sends a signal to the stimulation computer when the calculated value exceeds 1.5 standard deviations (SD) of this baseline, triggering a stimulus. After stimulation, no triggers were delivered in a window of 4–6 s, even if the alpha amplitude exceeded the threshold, ensuring sufficient and jittered minimum inter-stimulus intervals ('trigger dead-time'). The plug-in was adjusted to trigger deviant stimuli independent of ongoing alpha activity in 20% of total stimulations. See Fig. 1 for a graphical illustration of the process. We chose this online stimulation approach for the following reasons: It allows us to increase the difference between conditions, i.e. to create a "high alpha" condition with a more pronounced alpha activity as opposed to a random-stimulation and offline-sorting approach. The chosen approach is thought to increase the expected effect strength allowing us to study subtler effects of the rhythm on the EP, and to keep inter-stimulus intervals (ISIs) large enough to disregard attenuation of EP components and expectancy effects due to repetitive stimulation.

In the control condition, trains of stimuli not dependent of ongoing activity as in the alpha-triggered condition, but with identical ISIs were delivered by the following procedure: Logs recorded by the stimulation computer were used as stimulation protocols for the control condition, "replaying" the earlier stimulation, but with no relation to ongoing activity.

To control for order effects, we split the experiment in 8 blocks of 6 min each, and pseudo-randomly assigned 'alpha-triggered' and control runs to the blocks. Also alpha-triggered run logs were randomly assigned to each control run. Constraints were: 1st block had to be alpha-triggered, each alpha-triggered run to be used no more than twice and a finally balanced distribution of 'alpha-triggered' and control runs.

2.6. EEG preprocessing

EEG data was loaded into BrainVision Analyzer (BrainProducts GmbH, Munich, Germany), filtered with a bandpass filter of 0.5–40 Hz, down sampled to 1 kHz, and exported for fur-

ther processing in EEGLAB. Artifact rejection was carried out using an exclusion threshold of 125 μV for EEG/EOG channel data and improbability of data as estimated by joint-probability and kurtosis-of-activity analysis using EEGLAB preset defaults. Two datasets were discarded due to insufficient trial numbers after artifact rejection, resulting in 13 datasets with, on average, 121 ± 19 trials in the alpha-triggered condition and 125 ± 21 trials in the control condition, with a mean inter-stimulus interval for standard triggers of 10.29 ± 1.32 s and 10.15 ± 1.33 s, respectively. For analysis of EPs, the data was further down sampled to 500 Hz, and re-referenced to electrodes FT9 and FT10 to allow for better analysis of signals generated centrally at the vertex. Trials were segmented in −2 s to 2 s epochs time-locked to the stimulus. A baseline correction of the data using a time window from −2 s to 0 s was applied. Only standard trials with no errant motor response (false positive in oddball task) were considered for analysis.

2.7. ICA decomposition

We calculated an ICA decomposition of the segmented, artifact-rejected data to allow further correction of artifacts, using the Infomax algorithm as implemented in EEGLAB. The ICA decomposition time courses and topographies were inspected visually, and components clearly related to stimulus-related artifacts were identified (1 or 2 components per subject), contributing between 0.01% and 1.06% to the total variance of the signal (mean 0.26%, SD 0.23%). These components were removed; the remaining components were subsequently backprojected and further analysis was carried out in channel space.

2.8. EEG analysis and statistical evaluation

To assess accuracy of triggering in the alpha-triggered condition, time–frequency decompositions (using short time fast Fourier transform) of the data were calculated using the BSS component used for triggering.

The grand-average EP was calculated for each condition, and compared in a time window from −300 ms to 1300 ms relative to the stimulus. Channels exhibiting highest baseline-to-peak EP amplitudes for the different EP components (P50, P100, N140 and P260) under the control condition were further statistically evaluated.

A one-sample *T*-test was performed for each data point in the pre-defined EP window for each channel of interest depending on the respective EP component. We corrected for multiple comparisons by using the false discovery rate (FDR) method. We used this approach since we only had two conditions in our experiment, and had specific spatial hypotheses (based on the EP topography under control condition) for the possible localization of effects for each EP component. Multivariate approaches such as PCA (Boonstra et al., 2007) and PLS (McIntosh et al., 1996, 2004; McIntosh and Lobaugh, 2004) are certainly able to capture information about spatiotemporal brain dynamics in a more data-driven way, and will be considered for further analyses.

Topography maps for the components of the EP were calculated from the data, as well as difference maps between conditions.

3. Results

3.1. Evaluation of the pre-stimulus alpha amplitude

In the alpha-triggered condition, a significant increase of pre-stimulus alpha amplitude over baseline is present in all subjects, showing that our online amplitude analysis approach has successfully identified periods of high Rolandic alpha-rhythm amplitude.

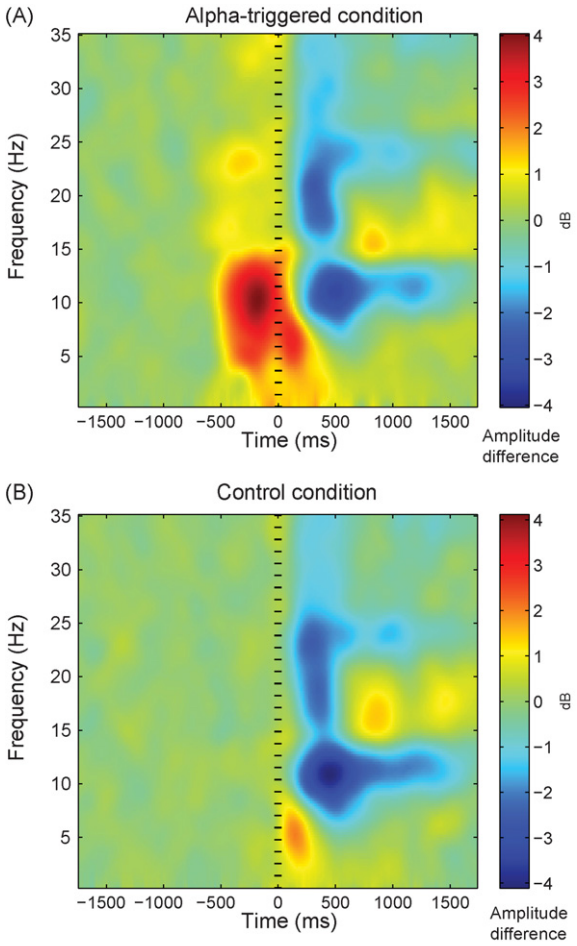

Fig. 2. The grand-average time–frequency plot of the main-experiment data weighted with the BSS component weights identified in the pre-experiment. (A) Alpha-triggered condition; (B) control condition.

The grand-average time–frequency plot of both conditions of the main-experiment data, weighted with the BSS component used for stimulation, is shown in Fig. 2. The grand-average topography of the BSS component weights is shown in Fig. 3A, the difference plot for the pre-stimulus (−400 ms to −100 ms) alpha-rhythm amplitude across conditions is shown in Fig. 3B.

3.2. Grand-average EP time courses

Analysis of the grand-average EPs (Fig. 4) revealed a typical evoked response following vibrotactile stimulation, with distinct P50, P100, N140, and P260 components as well as a stimulus-offset EP after cessation of stimulation at 900 ms.

The P50 component for both conditions exhibits maximal amplitude in electrode CP5 located over the contralateral somatosensory cortex, in accordance with its presumed generation in the primary somatosensory cortex (SI).

The amplitudes of the P100, N140 and P260 components were maximal at the central recording sites Cz and FCz for both conditions. A significant (FDR-corrected alpha ≤ 0.05) difference across conditions for the N140 and P260 components was detected in electrode FCz (N140: 14 data points/28 ms, P260: 10 data points/20 ms) with amplitudes being higher in the alpha-triggered condition. Further significant differences were found at 548 ms (5 data points/10 ms), at 632 ms (6 data points/12 ms), and in the offset EP at 1184 ms (2 data points/4 ms).

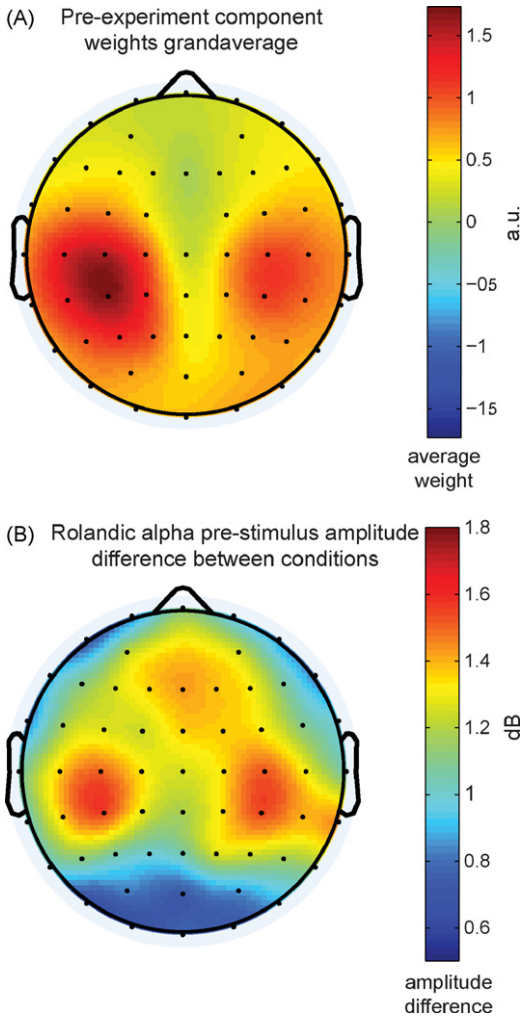

Fig. 3. Grand-averages of Rolandic alpha-rhythm topographies: (A) mean BSS components as identified in the pre-experiment; (B) difference plot for pre-stimulus (−400 ms to −100 ms) alpha-rhythm across conditions.

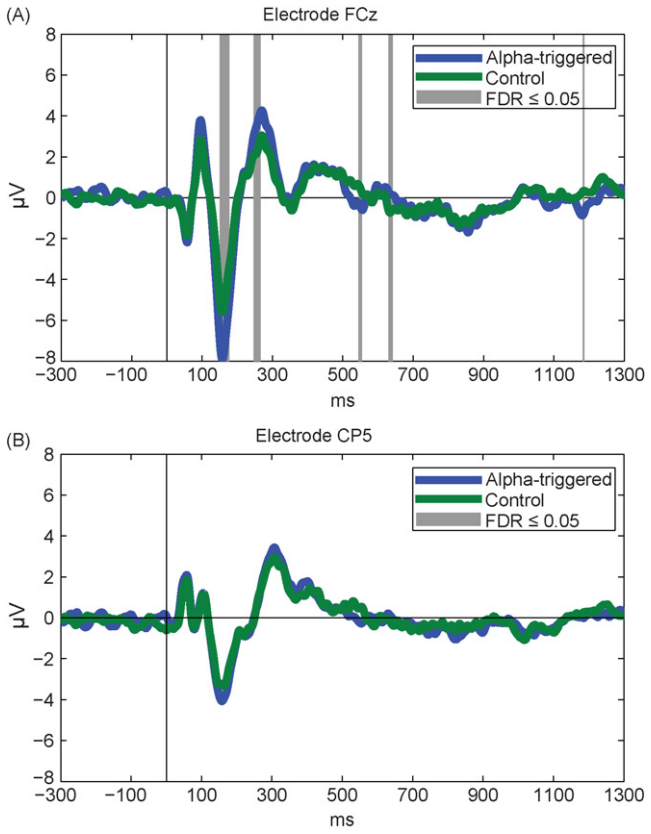

Fig. 4. Time courses of the grand-average EPs: (A) channel FCz exhibiting largest effects concerning the difference between conditions; (B) channel CP5 exhibiting most pronounced early SEP responses.

3.3. *Topography of components and differences*

Analysis of EP topographies showed a pericentral, contralateral topography for the P50 component, a central topography for the P100, a central-contralateral topography for the N140, and a frontocentral topography for the P260 component (Fig. 5).

The significant amplitude differences in the N140 and P260 components exhibited central and frontocentral topographies, respectively.

4. Discussion

We have shown that: (1) high pre-stimulus Rolandic alpha-rhythm amplitudes are associated with increased amplitudes of the N140 and P260 component but show no interaction with early components of the somatosensory evoked response. (2) Topographies of pre-stimulus Rolandic alpha-rhythm and interaction sites differ.

4.1. *Pre-stimulus Rolandic alpha interacts with late (cognitive) SEP components*

The N140–P260 complex of the SEP is related to higher cognitive processing (Kenntner-Mabiala et al., 2008; Miltner et al., 1989). The somatosensory negative evoked response 'N1' (around 100 ms post stimulus) can be found with varying latencies and hence is known under different labels: N120, N130, N140, N145, and N150 (Garcia-Larrea et al., 1995). The component is susceptible to the attentional state of the subject (Desmedt and Robertson, 1977; Eimer et al., 2003; Nakajima and Imamura, 2000). Latency and amplitude increase with the degree of attentional demand, and the component is not detected in an unattended stimulation paradigm. It is regarded as a complex response representing different neurophysiological processes (Garcia-Larrea et al., 1995) and it is thought to originate in higher order sensory (e.g. SII) and executive areas, such as prefrontal cortex (PFC) (Mountcastle, 1984).

The N140 is significantly enhanced for perceived as compared to unperceived stimuli in near-threshold stimulation experiments (Schubert et al., 2006; Zhang and Ding, 2009). Concerning the link between the Rolandic alpha-rhythm and the N140 component, an inverted-U relationship has recently been shown for the condition of near perception threshold electrical somatosensory stimulation (Zhang and Ding, 2009). Our study, in contrast, employed a supra-threshold vibrotactile oddball task and compared a high pre-stimulus alpha amplitude state with an average pre-stimulus alpha control condition. Our finding of a high Rolandic alpha amplitude state before stimulation being associated with increased N140 amplitudes as compared to average pre-stimulus alpha activity may hence not be regarded as contradictory to the results of Zhang and Ding (2009), who found intermediate pre-stimulus Rolandic alpha amplitudes to be associated with highest N140 amplitudes.

High pre-stimulus amplitudes are related to larger late EP components according to our data, and larger N140 amplitudes are related to increased attention and improved perception according to the results of others (Garcia-Larrea et al., 1995; Zhang and Ding, 2009). Alpha-rhythm desynchronizes over areas representing attended receptive fields, and high alpha amplitudes can be found in

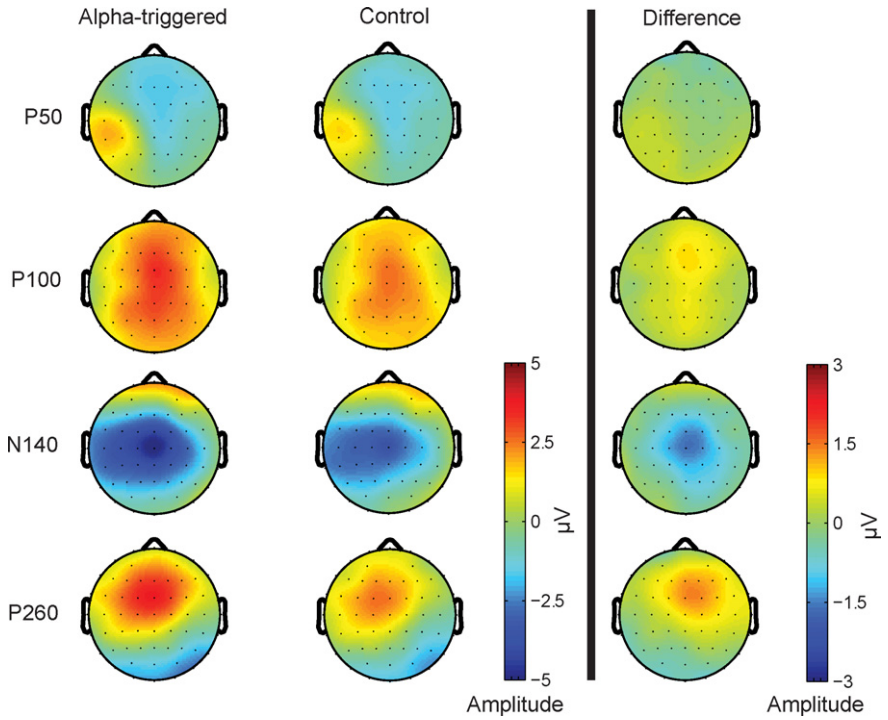

Fig. 5. Topographies of EP components and differences between conditions.

inhibited, i.e. non-active cortex areas (Klimesch et al., 2007; Neuper et al., 2006; Pfurtscheller, 1992). In the light of the latter findings, our result of increased cognitive processing – as reflected in an increased N140–P260 complex – with higher pre-stimulus alpha amplitudes may seem counterintuitive. However, it is in line with the theory "that good cognitive performance is related to large resting power but small 'test' power during task performance (i.e. a large extent of alpha suppression)" (Hanslmayr et al., 2005b). In other words, the amount of alpha ERD may be most important for cognitive performance.

Our findings of interaction between the N140–P260 complex and the Rolandic alpha rhythm, together with the strong known link of the N140–P260 complex to higher cognitive processing, suggests the Rolandic alpha-rhythm to be also related to cognitive functions. However, the directions of interaction between the ongoing rhythm, the cognitive EP components and executive areas of the brain are not easily identified. Possible models include: (1) Rolandic alpha-rhythm modulations are controlled in a top-down manner from executive areas, indicating that the rhythm reflects "control" or "priming" of primary sensory areas, for example by altering the balance between inhibition and excitation. Since we believe the cognitive EP components to be generated in higher order areas, this would imply a common underlying modulation by e.g. PFC as the cause for the observed interaction. (2) Rolandic alpha-rhythm modulates executive areas in a bottom-up manner, resulting in modulation of the cognitive components. This model, however, is contradicted by the finding of a causal influence from the PFC on primary somatosensory areas concerning the alpha band in the pre-stimulus time interval (Zhang and Ding, 2009).

Subjects can learn to volitionally control Rolandic rhythms, implying control of executive areas over sensorimotor areas. Accordingly, the Rolandic alpha-rhythm has been suggested to partially reflect top-down modulation of sensorimotor areas by executive areas (for a review, see Pineda, 2005), in the sense of "priming" sensory areas based on task relevance, attention, and affection.

In contrast to the distinct link to cognitive SEP components, we did not find a relation between pre-stimulus Rolandic alpha-rhythm and the early components of the SEP, in line with Nikouline et al. (2000).

4.2. Role of the alpha-rhythm for EP generation

Similar as in our study of occipital alpha-rhythm and the VEP, the late SEP is composed of signals lower in frequency than the alpha band (the main interaction effect is observed around 4 Hz), and hence a pure phase reset of ongoing Rolandic alpha-rhythm is unlikely to be the cause for the observed effect. The topographical distinction between rhythm and effect, and interaction of the rhythm with two separate EP components of different polarity, also speak against a pure baseline shift effect for the present data as proposed by (Mazaheri and Jensen, 2008; Nikulin et al., 2007). However, alpha-like oscillations are also present at frontocentral interaction sites, so that a possible contribution of this effect to our results should not easily be dismissed.

In the light of the different theories on EP generation, we regard an interaction of ongoing rhythm and late EP components, possibly by a common modulation from executive areas of the brain, for the most likely explanation of the effect present in our data.

5. Conclusions

High pre-stimulus Rolandic alpha-rhythm states are associated with increased amplitudes of the somatosensory evoked cognitive N140–P260 complex. The different topographies of ongoing rhythm and the components indicate an interaction of rhythm and late EP components. Our findings support the theory that the Rolandic alpha-rhythm might reflect top-down modulation from higher order executive areas. In more general terms, and in the context of similar studies in the visual system, our findings suggest that modulation of late EP components by ongoing rhythms might be a characteristic feature of sensory systems.

Acknowledgements

This work was supported by the German Federal Ministry of Education and Research BMBF (Berlin NeuroImaging Center; Bernstein Center for Computational Neuroscience), the German Research Foundation DFG (Berlin School of Mind and Brain) and the Robert Bosch Foundation.

References

Arieli A, Sterkin A, Grinvald A, Aertsen A. Dynamics of ongoing activity: explanation of the large variability in evoked cortical responses. Science 1996;273:1868–71.
Arroyo S, Lesser RP, Gordon B, Uematsu S, Jackson D, Webber R. Functional significance of the mu rhythm of human cortex: an electrophysiologic study with subdural electrodes. Electroencephalogr Clin Neurophysiol 1993;87:76–87.
Becker R, Reinacher M, Freyer F, Villringer A, Ritter P. Spontaneous neuronal EEG signatures of the human brain account for variability in evoked fMRI responses. In: 15th annual meeting, organization for human brain mapping; 2009.
Becker R, Ritter P, Villringer A. Influence of ongoing alpha rhythm on the visual evoked potential. Neuroimage 2008;39:707–16.
Berger H. Über das Elektroenkephalogramm des Menschen. Arch Psychiat Nervenkr 1929;87:527–70.
Boonstra TW, Daffertshofer A, Beek PJ. Effects of sleep deprivation on event-related fields and alpha activity during rhythmic force production. Neurosci Lett 2005;388:27–32.
Boonstra TW, Daffertshofer A, Breakspear M, Beek PJ. Multivariate time–frequency analysis of electromagnetic brain activity during bimanual motor learning. Neuroimage 2007;36:370–7.
Chatrian GE, Petersen MC, Lazarete JA. The blocking of the Rolandic wicket rhythm and some central changes related to movement. Electroencephalogr Clin Neurophysiol 1959;11:497–510.
Cheyne D, Gaetz W, Garnero L, Lachaux JP, Ducorps A, Schwartz D, et al. Neuromagnetic imaging of cortical oscillations accompanying tactile stimulation. Brain Res Cogn Brain Res 2003;17:599–611.
de Munck JC, Goncalves SI, Huijboom L, Kuijer JP, Pouwels PJ, Heethaar RM, et al. The hemodynamic response of the alpha rhythm: an EEG/fMRI study. Neuroimage 2007;35:1142–51.
Delorme A, Makeig S. EEGLAB: an open source toolbox for analysis of single-trial EEG dynamics including independent component analysis. J Neurosci Methods 2004;134:9–21.
Desmedt JE, Robertson D. Differential enhancement of early and late components of the cerebral somatosensory evoked potentials during forced-paced cognitive tasks in man. J Physiol 1977;271:761–82.
Difrancesco MW, Holland SK, Szaflarski JP. Simultaneous EEG/functional magnetic resonance imaging at 4 Tesla: correlates of brain activity to spontaneous alpha rhythm during relaxation. J Clin Neurophysiol 2008;25:255–64.
Eimer M, Forster B, Van Velzen J. Anterior and posterior attentional control systems use different spatial reference frames: ERP evidence from covert tactile-spatial orienting. Psychophysiology 2003;40:924–33.
Ergenoglu T, Demiralp T, Bayraktaroglu Z, Ergen M, Beydagi H, Uresin Y. Alpha rhythm of the EEG modulates visual detection performance in humans. Brain Res Cogn Brain Res 2004;20:376–83.
Feige B, Scheffler K, Esposito F, Di Salle F, Hennig J, Seifritz E. Cortical and subcortical correlates of electroencephalographic alpha rhythm modulation. J Neurophysiol 2005;93:2864–72.
Garcia-Larrea L, Lukaszewicz AC, Mauguiere F. Somatosensory responses during selective spatial attention: the N120-to-N140 transition. Psychophysiology 1995;32:526–37.
Gastaut H. Etude 'lectrocorticographique de la r'activit' des rhythmes rolandiques. Rev Neurol Paris 1952;87:176–82.
Goldman RI, Stern JM, Engel Jr J, Cohen MS. Simultaneous EEG and fMRI of the alpha rhythm. Neuroreport 2002;13:2487–92.
Goncalves SI, de Munck JC, Pouwels PJ, Schoonhoven R, Kuijer JP, Maurits NM, et al. Correlating the alpha rhythm to BOLD using simultaneous EEG/fMRI: Inter-subject variability. Neuroimage 2005.
Hanslmayr S, Klimesch W, Sauseng P, Gruber W, Doppelmayr M, Freunberger R, et al. Visual discrimination performance is related to decreased alpha amplitude but increased phase locking. Neurosci Lett 2005a;375:64–8.
Hanslmayr S, Sauseng P, Doppelmayr M, Schabus M, Klimesch W. Increasing individual upper alpha power by neurofeedback improves cognitive performance in human subjects. Appl Psychophysiol Biofeedback 2005b;30:1–10.
Jasper H, Penfield W. Electrocorticograms in man: effect of voluntary movement upon the electrical activity of the precentral gyrus. Arch Psychiatr Z Neurol 1949;183:163–74.
Jensen O, Gelfand J, Kounios J, Lisman JE. Oscillations in the alpha band (9–12 Hz) increase with memory load during retention in a short-term memory task. Cerbral Cortex 2002;12:877–82.
Kenntner-Mabiala R, Andreatta M, Wieser MJ, Muhlberger A, Pauli P. Distinct effects of attention and affect on pain perception and somatosensory evoked potentials. Biol Psychol 2008;78:114–22.
Klimesch W. EEG-alpha rhythms and memory processes. Int J Psychophysiol 1997;26:319–40.
Klimesch W, Sauseng P, Gerloff C. Enhancing cognitive performance with repetitive transcranial magnetic stimulation at human individual alpha frequency. Eur J Neurosci 2003;17:1129–33.
Klimesch W, Sauseng P, Gruber W. The functional relevance of phase reset A comment to Risner et al. (2009): the visual evoked potential of surface alpha rhythm phase. Neuroimage 2009.
Klimesch W, Sauseng P, Hanslmayr S. EEG alpha oscillations: the inhibition-timing hypothesis. Brain Res Rev 2007;53:63–88.
Kuhlman WN. Functional topography of the human mu rhythm. Electroencephalogr Clin Neurophysiol 1978;44:83–93.
Laufs H, Kleinschmidt A, Beyerle A, Eger E, Salek-Haddadi A, Preibisch C, et al. EEG-correlated fMRI of human alpha activity. Neuroimage 2003a;19:1463–76.
Laufs H, Krakow K, Sterzer P, Eger E, Beyerle A, Salek-Haddadi A, et al. Electroencephalographic signatures of attentional and cognitive default modes in spontaneous brain activity fluctuations at rest. Proc Natl Acad Sci USA 2003b;100:11053–8.
Linkenkaer-Hansen K, Nikulin VV, Palva S, Ilmoniemi RJ, Palva JM. Prestimulus oscillations enhance psychophysical performance in humans. J Neurosci 2004;24:10186–90.
Makeig S, Westerfield M, Jung TP, Enghoff S, Townsend J, Courchesne E, et al. Dynamic brain sources of visual evoked responses. Science 2002;295:690–4.
Mazaheri A, Jensen O. Asymmetric amplitude modulations of brain oscillations generate slow evoked responses. J Neurosci 2008;28:7781–7.
McIntosh AR, Bookstein FL, Haxby JV, Grady CL. Spatial pattern analysis of functional brain images using partial least squares. Neuroimage 1996;3:143–57.
McIntosh AR, Chau WK, Protzner AB. Spatiotemporal analysis of event-related fMRI data using partial least squares. Neuroimage 2004;23:764–75.
McIntosh AR, Lobaugh NJ. Partial least squares analysis of neuroimaging data: applications and advances. Neuroimage 2004;23(Suppl. 1):S250–63.
Miltner W, Johnson Jr R, Braun C, Larbig W. Somatosensory event-related potentials to painful and non-painful stimuli: effects of attention. Pain 1989;38:303–12.
Moosmann M, Ritter P, Krastel I, Brink A, Thees S, Blankenburg F, et al. Correlates of alpha rhythm in functional magnetic resonance imaging and near infrared spectroscopy. Neuroimage 2003;20:145–58.
Mountcastle VB. Central nervous system mechanisms in the mechanoreceptive sensibility. In: Handbook of physiology. Bethesda, MD: American Psychological Association; 1984. pp. 789–878.
Nakajima Y, Imamura N. Relationships between attention effects and intensity effects on the cognitive N140 and P300 components of somatosensory ERPs. Clin Neurophysiol 2000;111:1711–8.
Neuper C, Wortz M, Pfurtscheller G. ERD/ERS patterns reflecting sensorimotor activation and deactivation. Prog Brain Res 2006;159:211–22.
Niedermeyer E, Lopes da Silva FH. Electroencephalography: basic principles, clinical applications, and related fields. Lippincott Williams & Wilkins; 2004.
Nikouline VV, Wikstrom H, Linkenkaer-Hansen K, Kesaniemi M, Ilmoniemi RJ, Huttunen J. Somatosensory evoked magnetic fields: relation to pre-stimulus mu rhythm. Clin Neurophysiol 2000;111:1227–33.
Nikulin VV, Linkenkaer-Hansen K, Nolte G, Lemm S, Muller KR, Ilmoniemi RJ, et al. A novel mechanism for evoked responses in the human brain. Eur J Neurosci 2007;25:3146–54.
Pfurtscheller G. Event-related synchronization (ERS): an electrophysiological correlate of cortical areas at rest. Electroencephalogr Clin Neurophysiol 1992;83:62–9.
Pfurtscheller G, Aranibar A. Changes in central EEG activity in relation to voluntary movement. I. Normal subjects. Prog Brain Res 1980;54:225–31.
Pfurtscheller G, Berghold A. Patterns of cortical activation during planning of voluntary movement. Electroencephalogr Clin Neurophysiol 1989;72:250–8.
Pineda JA. The functional significance of mu rhythms: translating "seeing" and "hearing" into "doing". Brain Res Brain Res Rev 2005;50:57–68.
Ray WJ, Cole HW. EEG alpha activity reflects attentional demands, and beta activity reflects emotional and cognitive processes. Science 1985;228:750–2.
Rihs TA, Michel CM, Thut G. Mechanisms of selective inhibition in visual spatial attention are indexed by alpha-band EEG synchronization. Eur J Neurosci 2007;25:603–10.
Risner ML, Aura CJ, Black JE, Gawne TJ. The visual evoked potential is independent of surface alpha rhythm phase. Neuroimage 2009.
Ritter P, Becker R. Detecting alpha rhythm phase reset by phase sorting: caveats to consider. Neuroimage 2009.
Ritter P, Moosmann M, Villringer A. Rolandic alpha and beta EEG rhythms' strengths are inversely related to fMRI-BOLD signal in primary somatosensory and motor cortex. Hum Brain Mapp 2009;30:1168–87.
Salmelin R, Hamalainen M, Kajola M, Hari R. Functional segregation of movement-related rhythmic activity in the human brain. Neuroimage 1995;2:237–43.
Salmelin R, Hari R. Spatiotemporal characteristics of sensorimotor neuromagnetic rhythms related to thumb movement. Neuroscience 1994;60:537–50.
Sauseng P, Klimesch W, Gruber WR, Hanslmayr S, Freunberger R, Doppelmayr M. Are event-related potential components generated by phase resetting of brain oscillations? A critical discussion. Neuroscience 2007;146:1435–44.
Sauseng P, Klimesch W, Stadler W, Schabus M, Doppelmayr M, Hanslmayr S, et al. A shift of visual spatial attention is selectively associated with human EEG alpha activity. Eur J Neurosci 2005;22:2917–26.
Sayers BM, Beagley HA, Henshall WR. The mechanism of auditory evoked EEG responses. Nature 1974;247:481–3.

Schubert R, Blankenburg F, Lemm S, Villringer A, Curio G. Now you feel it–now you don't: ERP correlates of somatosensory awareness. Psychophysiology 2006;43:31–40.

Schubert R, Haufe S, Blankenburg F, Villringer A, Curio G. Now you'll feel it-now you won't: EEG rhythms predict the effectiveness of perceptual masking. J Cogn Neurosci 2008.

Thut G, Nietzel A, Brandt SA, Pascual-Leone A. Alpha-band electroencephalographic activity over occipital cortex indexes visuospatial attention bias and predicts visual target detection. J Neurosci 2006;26:9494–502.

Worden MS, Foxe JJ, Wang N, Simpson GV. Anticipatory biasing of visuospatial attention indexed by retinotopically specific alpha-band electroencephalography increases over occipital cortex. J Neurosci 2000;20:RC63.

Zhang Y, Ding M. Detection of a weak somatosensory stimulus: role of the prestimulus mu rhythm and its top-down modulation. J Cogn Neurosci 2009.

Ziehe A, Muller KR, Nolte G, Mackert BM, Curio G. Artifact reduction in magnetoneurography based on time-delayed second-order correlations. IEEE Trans Biomed Eng 2000;47:75–87.

4.2 Study 2

- Becker, R., **Reinacher, M.**, Freyer, F., Villringer, A. & Ritter, P. How Ongoing Neuronal Oscillations Account for Evoked fMRI Variability. *The Journal of Neuroscience* **31**, 11016–11027 (2011).

Behavioral/Systems/Cognitive

How Ongoing Neuronal Oscillations Account for Evoked fMRI Variability

Robert Becker,[1] Matthias Reinacher,[1] Frank Freyer,[1] Arno Villringer,[1,2,3] and Petra Ritter[1,2,3]

[1]Bernstein Center for Computational Neuroscience Berlin and Bernstein Focus State Dependencies of Learning, Department of Neurology, Charité Universitaetsmedizin Berlin, Berlin, Germany, [2]Max Planck Institute for Human Cognitive and Brain Sciences, Leipzig, Germany, and [3]Berlin School of Mind and Brain and Mind and Brain Institute, Humboldt University Berlin, Berlin, Germany

Variability of evoked single-trial responses despite constant input or task is a feature of large-scale brain signals recorded by fMRI. Initial evidence signified relevance of fMRI signal variability for perception and behavior. Yet the underlying intrinsic neuronal sources have not been previously substantiated. Here, we address this issue using simultaneous EEG–fMRI and real-time classification of ongoing alpha-rhythm states triggering visual stimulation in human subjects. We investigated whether spontaneous neuronal oscillations—as reflected in the posterior alpha rhythm—account for variability of evoked fMRI responses. Based on previous work, we specifically hypothesized linear superposition of fMRI activity related to fluctuations of ongoing alpha rhythm and a visually evoked fMRI response. We observed that spontaneous alpha-rhythm power fluctuations largely explain evoked fMRI response variance in extrastriate, thalamic, and cerebellar areas. For extrastriate areas, we confirmed the linear superposition hypothesis. We hence linked evoked fMRI response variability to an intrinsic rhythm's power fluctuations. These findings contribute to our conceptual understanding of how brain rhythms can account for trial-by-trial variability in stimulus processing.

Introduction

Pronounced trial-to-trial variability is a universal feature of evoked responses across different species and recording modalities. Invasive animal recordings indicate evoked-response variance to be explained by neuronal background activity superimposed on fixed evoked responses (Arieli et al., 1996). In case of motor fMRI, fluctuating coherent background fMRI activity—constituting resting-state networks (Biswal et al., 1995; Raichle et al., 2001; Greicius et al., 2003; Beckmann et al., 2005)—linearly superimposes evoked responses (Fox et al., 2006), explaining much of the trial-by-trial variance. Since fMRI provides indirect measures of neuronal activity, it is unclear whether fluctuating signal parts reflect intrinsic neuronal activity. The fact of behavior and perception being comodulated with ongoing fMRI activity (Fox et al., 2007; Hesselmann et al., 2008) makes non-neuronal sources, e.g., respiration or heartbeat, seem unlikely (Birn, 2007); however, a proof for neuronal sources has not been previously provided.

Thus, while variations of evoked neuronal responses are explained by intrinsic neuronal-signal fluctuations and variations of evoked vascular (fMRI) responses by intrinsic vascular-signal fluctuations, the key question remains how fluctuations of the vascular-evoked fMRI-response are related to ongoing fluctuations in the neuronal domain. Although tight links between evoked neuronal activity and fMRI signal changes (Logothetis et al., 2001) and between spontaneous coherent fMRI signal fluctuations and intrinsic EEG rhythms (Mantini et al., 2007) exist, there has been no data available [with the single exception of a recent study by Scheeringa et al. (2011)] linking variability of fMRI stimulus responses to intrinsic neuronal signal amplitudes—the latter being noninvasively assessable by EEG. Hence, we used EEG–fMRI simultaneously (Ritter and Villringer, 2006; Laufs et al., 2008) to investigate neuronal underpinnings of evoked fMRI response variability.

In EEG, ongoing activity is related to variability of evoked responses. For example, the posterior alpha (8–12 Hz) rhythm covaries with features of the visual evoked potential (VEP) (Makeig et al., 2002; Becker et al., 2008; Mazaheri and Jensen, 2008). Functional relevance in terms of perception and behavior has been proposed for the alpha rhythm (Klimesch et al., 2006; Mathewson et al., 2009). Furthermore, this rhythm is associated with fMRI signal decreases in occipital areas (Goldman et al., 2002; Moosmann et al., 2003; Feige et al., 2005; de Munck et al., 2007) resembling visual resting-state networks (Damoiseaux et al., 2006; De Luca et al., 2006). Here, we examine whether alpha-rhythm-dependent fluctuations of fMRI background activity (fMRI-baseline) are superimposed on evoked fMRI responses. In case of such a mechanism, the alpha rhythm would represent a neuronal substrate of fMRI trial-to-trial variability.

Our working hypothesis was that ongoing alpha activity strength accounts for variance of sensory-evoked fMRI re-

Received Jan. 13, 2011; revised May 18, 2011; accepted May 22, 2011.

Author contributions: R.B., M.R., F.F., A.V., and P.R. designed research; R.B., M.R., F.F., and P.R. performed research; R.B., M.R., and P.R. contributed unpublished reagents/analytic tools; R.B., M.R., and P.R. analyzed data; R.B., M.R., F.F., A.V., and P.R. wrote the paper.

This work was supported by the German Federal Ministry of Education and Research (Berlin NeuroImaging Center, Bernstein Center for Computational Neuroscience, Bernstein Focus State Dependencies of Learning), the German Research Foundation (Berlin School of Mind and Brain), the Robert Bosch Foundation, and the James S. McDonnell Foundation (Brain NRG).

Correspondence should be addressed to either Robert Becker or Petra Ritter, Department of Neurology, Charité Universitaetsmedizin Berlin, Charitéplatz 1, 10117 Berlin, Germany. E-mail: robert.becker@charite.de or petra.ritter@charite.de.

DOI:10.1523/JNEUROSCI.0210-11.2011

 0270-6474/11/3111016-12$15.00/0

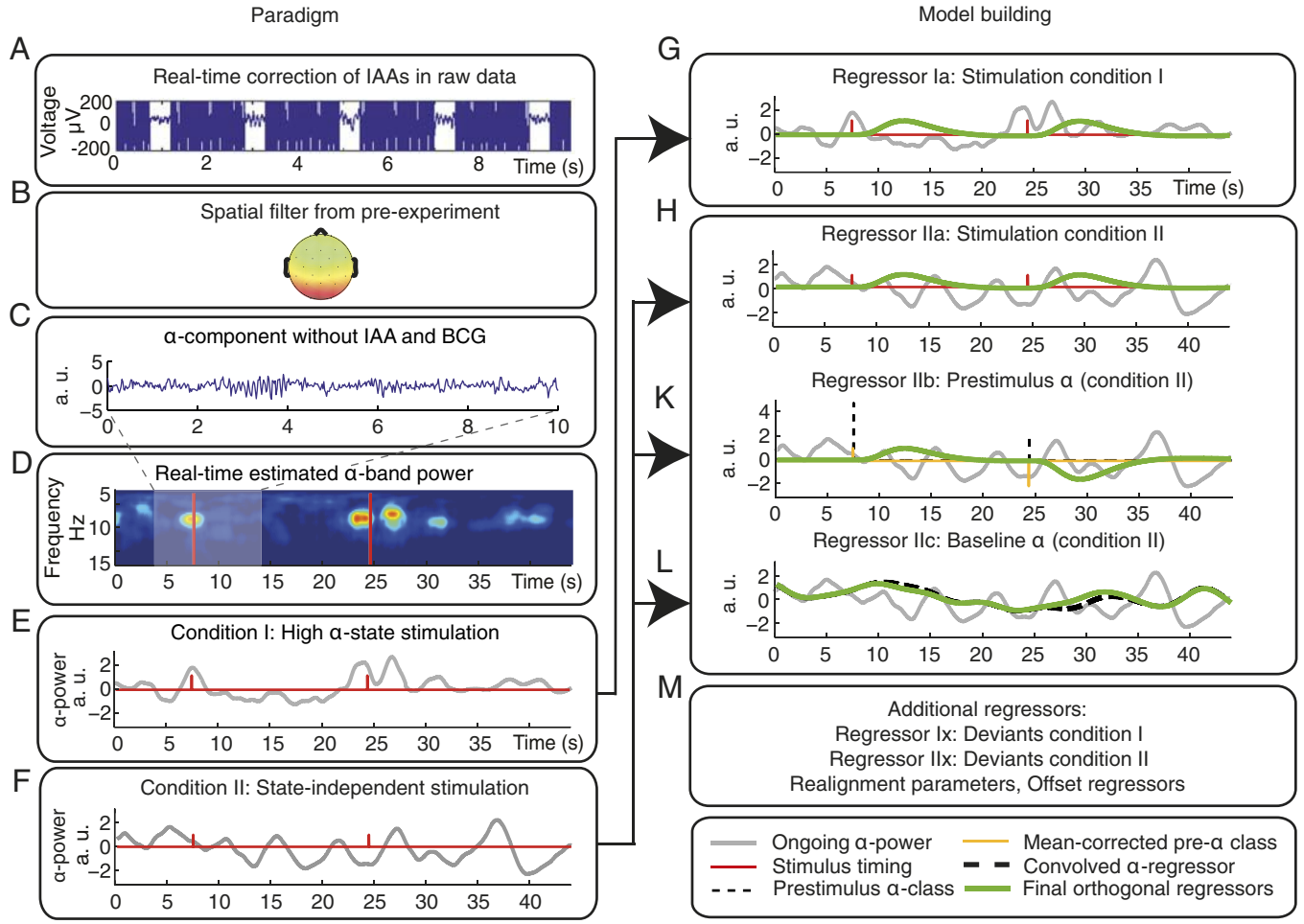

Figure 1. Scheme of the experimental setup (left) and of the resulting model for analysis (right). ***A***, First, IAAs were removed online. ***B***, Then we used the demixing matrix obtained from the pre-experiment as a spatial filter. ***C***, We extracted the posterior alpha-rhythm component and minimized signatures from other sources, such as heartbeat-related BCG. ***D***, On these data, a short-term FFT was applied to calculate alpha-band power online. ***E***, In the high alpha-state condition, stimulation was triggered when the current alpha-band power exceeded an adaptive threshold (condition I). ***F***, Trigger timings from high alpha-state stimulation condition (condition I) were recorded and used for the state-independent stimulation condition (condition II). ***G***, ***H***, ***K–M***, Model creation for fMRI analysis. Gray, Alpha power; green, final regressors. ***G***, ***H***, Calculation of stimulus regressor for conditions I (Regressor Ia) and II (Regressor IIa). Red, Unconvolved stick functions derived from stimulation. ***K***, Calculation of prestimulus alpha power regressor for condition II (Regressor IIb). Thin dashed line, Parameterized alpha power stick function; orange, after mean correction. Final regressor (green) is orthogonal to Regressor IIa. Regressor IIb is thought to probe the effect of fluctuating prestimulus alpha activity on the evoked fMRI response. ***L***, Calculation of ongoing alpha-power regressor (Regressor IIc). Thick dashed line, Ongoing alpha power convolved with HRF. Final regressor (green) is orthogonalized to Regressors IIa and IIb. Regressor IIc is supposed to probe stimulus-unrelated alpha activity, testing the effect of fluctuating alpha activity on the fMRI baseline. ***M***, The model comprises additional regressors representing deviant stimuli, realignment parameters, and constant offsets.

sponses. As linear superposition of ongoing and task-related brain signals has previously been observed across different time scales and imaging modalities (Arieli et al., 1996; Fox et al., 2006), we specifically tested whether linear superposition also holds true for fMRI responses to spontaneously fluctuating alpha power (i.e., neuronal activity-related fMRI-baseline fluctuations) and stimulus-evoked fMRI responses (hereafter called the superposition hypothesis). Furthermore, we tested whether ongoing alpha activity, as measured here, has functional relevance for behavior.

Materials and Methods

Experimental design and procedure

Simultaneous EEG–fMRI was acquired from 16 healthy subjects (seven females; mean age, 26.8 ± 2.9 years), with the final sample consisting of 12 subjects (for exclusion criteria, see BCG reduction, below). Written informed consent according to the Declaration of Helsinki was obtained from each subject before the investigation and the study was approved by the local ethics committee. An overview of the entire experimental setup and the resulting model is provided in Figure 1.

Pre-experiment

Before the main experiment, all subjects underwent an EEG experiment in the static magnetic field of the magnetic resonance (MR) system designed to modulate the power of the posterior alpha rhythm in a controlled fashion. Alpha rhythm was modulated by a blockwise eyes open/eyes closed task (12 blocks each consisting of 20 s eyes closed and 20 s eyes open; total duration, 8 min). On these data, we performed independent component analysis using temporal decorrelation source separation (TDSEP) (Ziehe et al., 2000), a computationally efficient method for extraction of independent components (ICs). This method has been successfully used for the separation of ongoing EEG rhythms (Ritter et al., 2009b). We examined the degree of correlation between the alpha band power of each resulting IC and the experimental protocol. In each subject, we identified the IC best representing the posterior alpha rhythm, i.e., responsive to eyes opening/closing as indicated by a maximum correlation coefficient. Subsequently, the resulting individual demixing matrices were transferred to the main experiment and the IC best representing the posterior alpha rhythm (henceforth termed "alpha IC") was extracted to enhance signal-to-noise ratio.

Main experiment

The main experiment consisted of a visual oddball task, requiring subjects to remain awake with eyes open, pay attention to the stimulus while focusing on the constantly shown fixation cross, and respond to deviant stimuli with the right-hand index finger. Visual evoked responses were elicited by projecting a circular black-and-white checkerboard onto an acrylic screen in the bore of the MR system. Duration of the stimulus was 900 ms. In 20% of cases, a deviant stimulus was shown, consisting of a contrast reversal of the circular checkerboard after 500 ms.

We used two experimental conditions in this experiment. In the high alpha-state stimulation condition, stimuli were applied during a state of high alpha-rhythm power, achieved by the method described in Real-time EEG alpha-state classification and stimulus triggering, below. In the state-independent stimulation condition, stimuli were applied independent of alpha-rhythm power, with stimulus timings replayed from condition I (see Single subject analyses and models, below) to maintain corresponding interstimulus intervals (ISIs) across conditions.

The experiment was split into eight blocks of 7 min each. Stimulus conditions were pseudorandomly assigned to these blocks to avoid order effects. Also, the sequences of stimulus triggers from high alpha-state stimulation runs being replayed in the state-independent stimulation runs were assigned in a pseudorandom fashion.

Data acquisition

EEG–fMRI

Simultaneous EEG–fMRI poses the challenge that the two major types of artifacts in the EEG, related to gradient switching during image acquisition and to heartbeat in the magnetic field, may critically interfere with real-time alpha-rhythm evaluation. Thus, we carefully minimized those artifacts in real time via two approaches before alpha-rhythm evaluation and used strict validation criteria to ensure adequate reduction of artifacts. Detailed procedures and validation of the real-time EEG are described in EEG system and recording parameters and in Validation of alpha-state-dependent triggering approach, below.

EEG system and recording parameters

EEG recordings were conducted with a 32-channel MR-compatible EEG system (BrainAmp MR Plus; Brain Products) and an MR-compatible EEG cap (EasyCap; FMS), using ring-type sintered silver chloride electrodes with iron-free copper leads. Twenty-one scalp electrodes were arranged according to the International 10–20 System with the reference located at electrode position FCz. In addition, one vertical electrooculogram, two horizontal electrooculogram, and two electrocardiogram channels were recorded. Impedances of all electrodes were kept below 10 kΩ using an abrasive electrolyte gel (Abralyt 2000; FMS). The EEG amplifier's recording range was ±16.38 mV at a resolution of 0.5 μV, capturing both low-amplitude EEG and high-amplitude image acquisition artifacts (IAAs) without reaching saturation. EEG sampling rate was 5 kHz. A hardware low-pass filter of 250 Hz was applied. To allow acquisition of the entire frequency spectrum of the physiological EEG as well as of IAAs, we enabled DC recording (Ritter et al., 2009a). To ensure time-invariant sampling of the IAA, we synchronized the EEG-sampling clock to the gradient-switching clock of the MR scanner (Anami et al., 2003; Freyer et al., 2009).

Real-time EEG alpha-state classification and stimulus triggering. Before evaluation of alpha states, we removed IAAs in real time using the IAA correction plug-in from the BrainVision RecView v1.0 software package (Brain Products), which performs online calculation of an artifact template based on a number of preceding IAA epochs (here, $n = 3$) and subsequent subtraction of this template from each following artifact epoch.

For online reduction of the other major artifact, the ballistocardiogram (BCG), we extracted the alpha IC from the IAA-corrected raw EEG data by applying the TDSEP-derived spatial filter from the pre-experiment. This maximizes sensitivity to the posterior alpha rhythm and reduces contribution of BCG and other sources of noise to the high alpha-state stimulation condition.

Next, alpha-band (8–12 Hz) power was calculated in real time by an in-house-developed RecView plug-in based on a real-time short-term fast Fourier transform (FFT) approach with a sliding (20 ms steps) time window of 4096 sample points/819.2 ms. The resulting value was compared with an adaptive baseline, which was defined as the average alpha power of the preceding 1 min time window. Visual stimulation was triggered when the current alpha-band power exceeded 2 SDs of the adaptive baseline. After each stimulus, a dead time (i.e., no stimulation) of 4–6 s ensured sufficiently long ISIs. The resulting median ISI for both high alpha-state stimulation and state-independent stimulation conditions amounted to 10.5 s (median absolute deviation: 4.9 s for high alpha state, 4.7 s for state-independent stimulation). For each stimulus condition, deviant stimuli (independent of ongoing alpha power) were triggered in 20% of total stimulations.

Behavioral data

To exclude condition-wise shifts in vigilance and attention as possible confounds for differences between the high alpha-state and state-independent stimulation conditions, we compared the response times for deviant stimuli of both stimulation conditions. A paired Student's t test was used, testing whether there was a within-subject effect of stimulus condition on response times. We also analyzed resulting hit rates for both conditions.

fMRI data acquisition

For fMRI recordings, we used a 1.5 T Siemens Vision MR scanner with a modified T2*-weighted BOLD-sensitive echo planar imaging sequence (stepping stone), which was specifically developed for EEG–fMRI acquisition (Anami et al., 2003). Recording parameters were as follows: repetition time, 3000 ms; acquisition time, 2090 ms; echo time, 39.29 ms; 22 slices covering the whole brain and acquired aligned to the anterior/posterior commissure; 135 volumes per run (eight runs per subject); voxel size, 3 × 3×5.5 mm (0.5 mm gap); flip angle, 90°; matrix, 64 × 64; field of view, 192 × 192 mm.

Data analysis

EEG preprocessing

For subsequent analyses, EEG data were offline corrected for IAAs and filtered (bandpass, 0.5–40 Hz) using BrainVision Analyzer v1.05 (Brain Products) software. All following analyses were performed in MATLAB v7.3 (Mathworks) and EEGLAB v5.03 (Delorme and Makeig, 2004). For handling in EEGLAB, data were down-sampled to 200 Hz.

Movement artifacts were rejected with EEGLAB using an exclusion threshold of 100 μV and improbability criteria, such as joint-probability and kurtosis-of-activity, as estimated with EEGLAB preset defaults. Of 105 ± 12 (mean ± SD) trials for the high alpha-state stimulation and 107 ± 11 trials for the state-independent stimulation, an average of 98 ± 15 and 99 ± 14 trials, respectively, were retained after artifact correction.

For all subsequent EEG analyses, we extracted the alpha IC using the demixing matrix from the pre-experiment. By back-projecting alpha ICs to occipital electrode position O2, polarity information and scaling in microvolt was regained. We then performed a time-frequency decomposition using a short-term FFT. The resulting data were used for validation of our approach (see Validation of alpha-state-dependent triggering approach, below) and to construct regressors for fMRI analysis (see Single subject fMRI analyses and models, below).

Validation of alpha-state-dependent triggering approach

To validate our alpha-state-dependent triggering approach, we analyzed spatial distribution of alpha ICs, evoked potentials, spectral EEG activity of both stimulus conditions before and after stimulus onset, and efficiency of BCG reduction. If not stated otherwise, all analyses are based on the individual alpha IC component back-projected to channel O2 as described above.

Spatial distribution of alpha ICs. For visualization of the spatial distribution of alpha ICs, topographies of single-subject alpha ICs were analyzed and an average across alpha IC weightings of all subjects was computed.

Analysis of evoked potentials. A grand-average evoked potential (EP) was calculated for each stimulation condition. To examine whether previously reported results of late EP modulations in the visual (Becker et al., 2008; Mazaheri and Jensen, 2008) and somatosensory (Reinacher et al.,

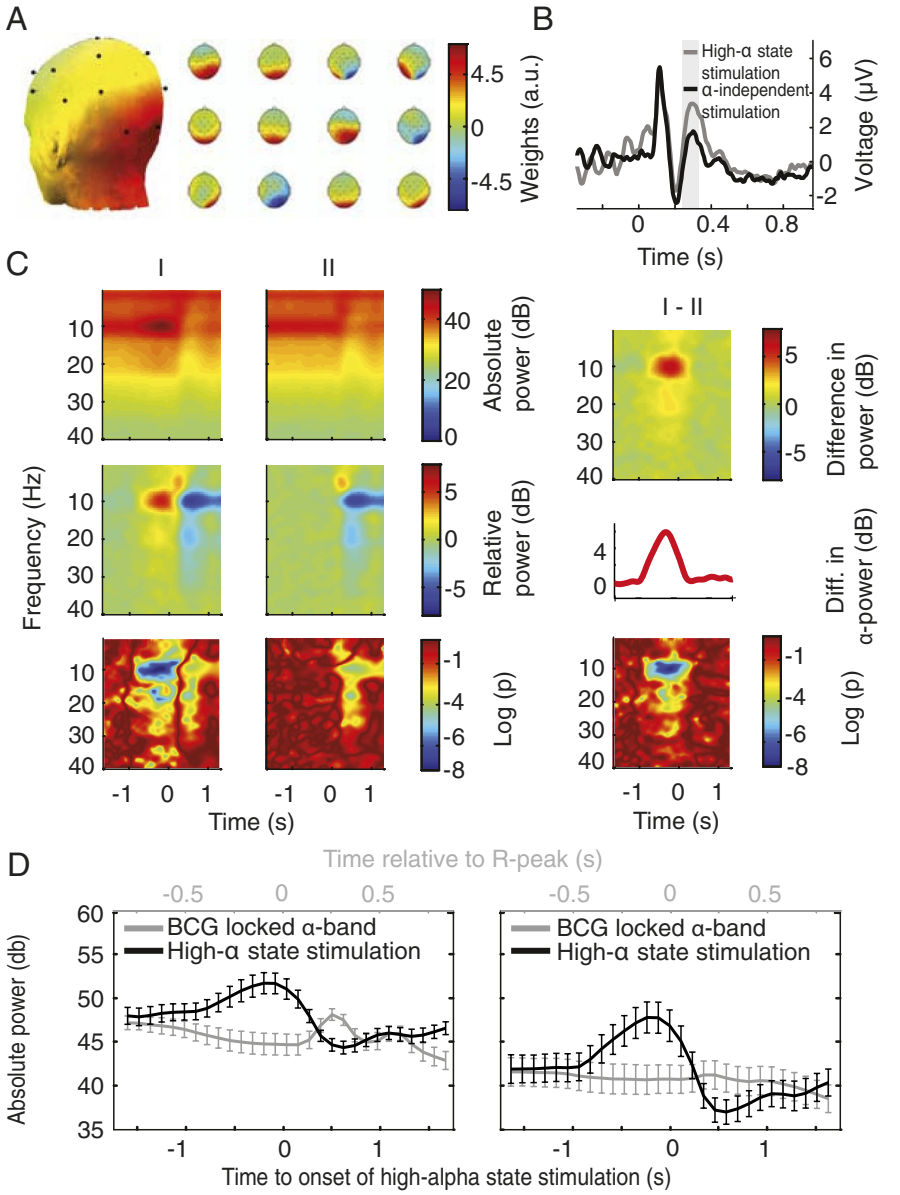

Figure 2. Validation of the online EEG-triggered stimulation approach. All analyses are based on the alpha-associated IC. ***A***, Left, Average posterior spatial distribution of alpha-associated IC. Right, Spatial distribution of alpha ICs for single subjects. Color bar represents weightings (arbitrary units). ***B***, Grand average EPs of the alpha IC for high alpha-state and state-independent stimulations reproducing previously reported amplitude increases of a late evoked component for the high alpha-state stimulation condition (window of analysis in gray, $p \leq 0.05$). ***C***, Grand average time-frequency plots of EEG data for stimulation and interstimulus conditions demonstrate proper alpha state-dependent triggering. Top and middle rows, Images depict same data without (top) and with (middle) baseline correction. Bottom row, Significance of time-frequency behavior, tested against a prestimulus baseline. Decadic logarithmized p values are color coded (e.g., -2 indicates $p < 10^{-2}$). Left column, High alpha-state stimulation; Middle column, state-independent stimulation; Right column, difference of time-frequency behavior between high alpha-state and state-independent stimulation conditions. Right column, middle row, Average prestimulus alpha-power increase (cf. Fig. 3). ***D***, Validation of alpha-rhythm extraction and efficient BCG reduction. Grand averages of EEG alpha-band power of IAA-corrected data locked to either high alpha-state stimulation (black) or the heartbeat-related R peak (gray) before (left) and after (right) applying the spatial filter from the pre-experiment, extracting the alpha IC. Alpha rhythm is maintained in the alpha IC while BCG is strongly reduced. Note the different time scales for the two averages.

2009) domains could be reproduced, a paired Student's t test over the average in the time window of 250–350 ms was performed.

Spectral activity of stimulus conditions. To ensure accuracy of our real-time stimulus triggering, we analyzed the time-frequency behavior of peristimulus data. To validate our triggering approach, we performed one-sample t test statistics on the time-frequency behavior for our two stimulus conditions and their difference.

BCG reduction. To assess the efficiency of the used spatial filter for the reduction of heartbeat-related BCG contamination (Debener et al., 2008) in our signal, we segmented data in a dual manner relative to the heartbeat-related R-peak and relative to high alpha-state stimulation. Event-related spectral perturbations within the alpha band were calculated using a short-term FFT time-frequency analysis and grand averages across all subjects were computed and compared (Fig. 2*D*). Ideally, there should be no increase in alpha-band power locked to the BCG (as defined by segmenting data relative to R-peak). We excluded any systematic relation between the timing of BCG and high-alpha state stimulation. This was achieved by a double-check approach. First, we calculated subject-wise χ^2 test of deviation from uniform distribution of R-peaks relative to high alpha-state stimulation onset (significance threshold, $p \leq 0.05$). This led to the exclusion of two subjects. Second, we calculated the power distance between the BCG–alpha response and the high alpha trigger and determined the threshold value up to which a systematic temporal relation was detected in at least one subject using the above mentioned χ^2 test. The limit value turned out to be 3.5 dB. Two additional subjects who failed to reach this threshold were also excluded. This highly conservative double-check approach resulted in a final sample of 12 subjects (mean, 26.8 ± 3.4 years), with an average distance measure of 5.9 dB ± 1.1 (SD), meaning that the average alpha power increase during the alpha triggering exceeded the maximum BCG-locked activity by almost 300%.

fMRI preprocessing

The fMRI data were preprocessed and analyzed using the software package SPM5 (www.fil.ion.ucl.ac.uk/spm). Preprocessing consisted of realignment for motion correction, normalization to the brain template of the Montreal Neurological Institute (MNI) supplied with SPM, resampling data to a resolution of 2 × 2 × 2 mm, and subsequent spatial smoothing with a kernel of 6 mm full-width-at-half-maximum. A temporal high-pass filter with a cutoff of 128 s was applied. The first five scans of each run were discarded to account for spin-saturation effects.

fMRI statistical analysis

Single subject analyses and models. We performed a regression analysis based on the general linear model for each individual subject (first-level analysis). For visualization of how regressors were calculated, see Figure 1. The model, i.e., the design matrix, designed for condition I sessions consisted of a high alpha-state stimulation (Regressor Ia) and a response to deviants (Regressor Ix). For condition II sessions, the design matrix consisted of an alpha state-independent stimulation (Regressor IIa), a prestimulus alpha power (Regressor IIb), an alpha baseline (Regressor IIc), and a response to deviants (Regressor IIx).

For both stimulus conditions, stimulus onsets were modeled by stick-like Dirac functions convolved with the canonical hemodynamic response function (HRF) exhibiting a delay of 5 s relative to event onset (Regressors Ia and IIa). Additional temporal and dispersion derivatives of this response function were added, yielding a basis set. Furthermore,

for condition II sessions, two different types of fluctuating alpha activity were examined for their effect on the fMRI signal.

First, the effect of fluctuating prestimulus alpha power on the fMRI stimulus response was examined (Regressor IIb). Depending on the prestimulus alpha power level, a parametric event-related regressor (*z*-scored alpha power was grouped into discrete classes with a range of 1–7 after mean correction from −3 to +3; resulting scaled Dirac functions were convolved with a basis set of HRFs) was calculated in addition (and orthogonal) to the standard fixed-amplitude stimulus response regressor (IIa). In case prestimulus alpha power affects the evoked response, this parametric prestimulus alpha power regressor will explain a significant part of the variance of the data.

Second, we were also interested in fMRI correlates of ongoing stimulus-unrelated alpha-power variations, i.e., the alpha-rhythm power-related fMRI baseline modulations (Regressor IIc). This alpha baseline regressor was calculated by convolving continuous alpha-band power fluctuations during condition II with a basis set of HRFs. The resulting functions were orthogonalized, first to the stimulus regressors and then to the prestimulus alpha regressors described above.

This model was complemented by adding the set of six translational and rotational realignment parameters and constant session offsets. It was then fitted to the fMRI data and, based on the estimated parameter values (effect sizes), contrast images were calculated as follows: for condition I: high alpha-state stimulus response (contrast on Regressor Ia); for condition II: state-independent stimulus response (contrast on Regressor IIa), prestimulus alpha response modulation (contrast on Regressor IIb), alpha-dependent baseline modulation (contrast on Regressor IIc); and the difference between stimulus responses of the two conditions: the high-alpha state stimulus response modulation (Regressor Ia vs IIa).

Group level analyses. Based on these single-subject contrasts, we calculated a group-level random-effects analysis, allowing inferences on the whole population.

To analyze alpha-state-dependent effects on the visual-evoked fMRI activity, regions exhibiting significant responses to visual stimulation under either stimulation condition were defined as visually responsive regions-of-interest [ROI; comprising all significantly activated voxels of both conditions with $p \leq 0.0003$, corrected for multiple comparisons based on false discovery rate (FDR), extent threshold 60 voxels]. This visual ROI was used as a mask for all further analyses.

For the high-alpha state stimulus-response modulation, the alpha-dependent baseline modulation, and the prestimulus alpha activity correlation, we used a statistical peak threshold of $t > 2.9$ and an extent threshold of 10 voxels, guaranteeing an FDR-corrected threshold of $p < 0.04$ in all conditions.

To test our linear superposition hypothesis, we looked for areas in which the alpha-dependent fMRI baseline and stimulus response were systematically modulated in the same manner. To derive a statistical measure for the existence and systematic occurrence of brain regions with such equally directed alpha-dependent baseline- and stimulus-response modulations, we performed a conjunction analysis that explicitly included only voxels found active in both contrasts, using the same previously defined initial threshold of $t > 2.9$ for each condition.

fMRI response functions. By using the estimated hemodynamic alpha impulse response function for the ongoing alpha regressor, we were able to predict the corresponding hemodynamic baseline modulation for the high-alpha state that was observed in our alpha-dependent stimulus condition (condition I). This procedure is explained in Figure 3. The resulting predicted hemodynamic response curve (comparable to the difference between high-alpha and average-alpha stimulation responses) is termed high alpha-state baseline modulation. Its amplitude was compared with the observed high alpha-state stimulus-response modulation. For the case that the baseline modulations (as predicted to occur during the high alpha state) account for the complete observed fMRI stimulus response variability, i.e., in case of linear superposition, both curves are expected to match. In turn, differences between the observed and the predicted response give an estimate of the degree of nonadditivity.

Single-trial correlation between prestimulus alpha activity and the evoked fMRI response. Finally, we tested whether alpha activity affects stimulus responses also on a trial-by-trial basis. To this end, for the alpha-independent stimulation (condition II) we examined those areas exhibiting both alpha-dependent baseline (Regressor IIc) and stimulus response modulations (Regressor Ia–Regressor IIa), as identified by individual conjunction analysis (using a subject-wise adaptive threshold of $p < 0.05$ or smaller to identify individual peak clusters of <450 voxels). We tested whether prestimulus alpha-based predicted-fMRI signal modulations (i.e., fitted Regressor IIb) account for the observed fMRI stimulus-response modulations on a trial-by-trial basis. Time series of the respective individually determined voxels were collapsed to yield average time series for each subject using the Marsbar toolbox for SPM (http://marsbar.sourceforge.net). Then, within subjects, we correlated the predicted effect of prestimulus alpha power with the observed data (with realignment parameters regressed out). Data points of 0 to 9 s after stimulation were included in this correlation analysis.

Results

This results section is divided into two parts. The first part, comprised of EEG and behavioral data, focuses on the general validation of our approach from a methodological and experimental-design perspective. The second part, based on the (EEG-related) fMRI data, deals with the main results of the study.

EEG and behavioral results

Validation of alpha-state-dependent triggering approach

Spatial distribution of alpha ICs. Figure 2*A*, left, depicts the average distribution of the alpha IC with a clear posterior focus. Figure 2*A*, right, shows the corresponding single subject ICs (please note that for single IC maps, depicted weightings have arbitrary polarity).

Evoked potentials. As was previously reported from related EEG and magnetoencephalography studies (Jasiukaitis and Hakerem, 1988; Becker et al., 2008; Mazaheri and Jensen, 2008), late evoked-component amplitudes were significantly increased in the high alpha-state stimulation condition ($p \leq 0.05$) (Fig. 2*B*).

Spectral activity of stimulus and interstimulus conditions. In all subjects, a pronounced and frequency-specific increase of prestimulus alpha-band activity for the high alpha-state stimulation condition was observed. Figure 2*C*, top row, shows absolute magnitudes of spectral activity; the middle row depicts baseline-corrected data (corrected in a prestimulus window of −2 to −1 s before stimulus onset). For the high alpha-state stimulation (Fig. 2*C*, left), power increases preceding stimulation were restricted to the alpha band, verifying that stimulation was effectively triggered by high alpha states. The alpha band increase starts at −800 ms before actual stimulation with a significance of $p < 1 \times 10^{-5}$ throughout the prestimulus period (Fig. 2*C*, bottom). In contrast, poststimulus power increases below the alpha band reflect the EP and decreases in the alpha band reflect the classical alpha rhythm event-related desynchronization (ERD) due to stimulation, which also occurs for state-independent stimulation (Fig. 2*C*, middle column). Figure 2*C*, right, shows the difference between high alpha-state stimulation and state-independent stimulation, i.e., the increase of prestimulus alpha power.

BCG reduction. How relevant the use of the alpha IC is for reduction of BCG-locked activity is shown in Figure 2*D*. The left plot shows the relation of BCG-locked and -triggered alpha activity without use of the alpha IC (i.e., channel data); the right plot shows the effect of using the alpha IC for triggering. This indicates efficient reduction of BCG activity after use of the spatial filter from the pre-experiment and extraction of the alpha IC.

Consideration of eye movements. Regarding the issue of possible alpha rhythm-related eye movements, comparing artifact detection rate in EEG across stimulus conditions did not indicate a systematic accumulation of eye movement-related responses before the alpha-

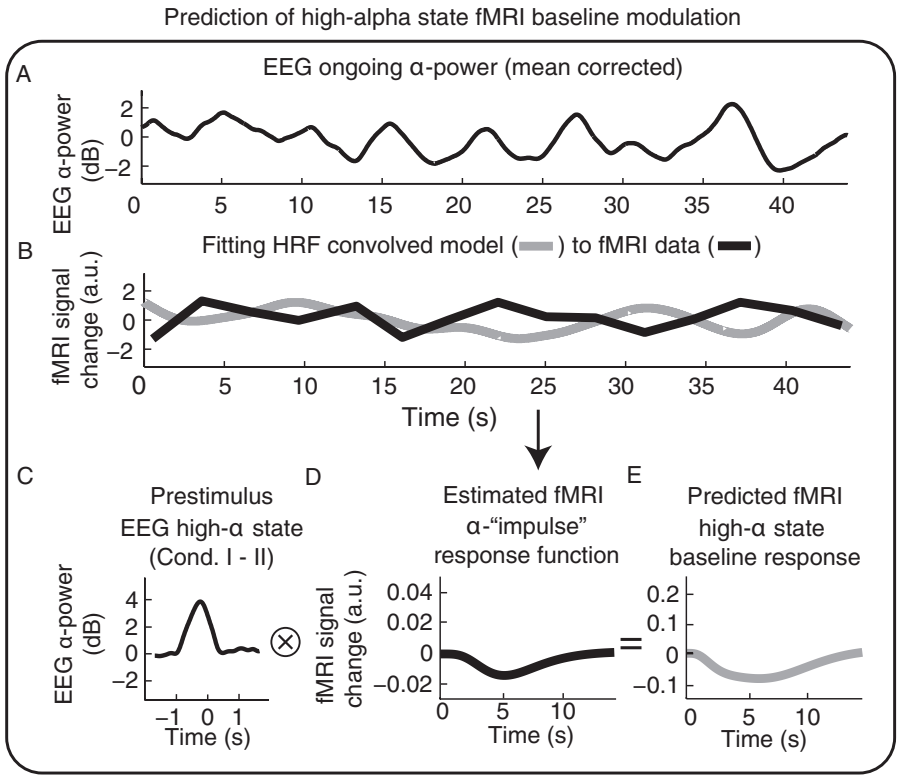

Figure 3. How we used observed alpha-dependent fMRI baseline modulations to predict high alpha-state fMRI baseline modulations. ***A***, Ongoing alpha power (condition II). ***B***, Regressor IIc (i.e., ongoing alpha power convolved with the canonical HRF+ derivatives, orthogonalized to Regressors IIa and IIb) is fitted to the data to estimate beta magnitudes. ***C***, Prestimulus alpha power increase found in the high alpha condition relative to control condition (Fig. 2*C*). ***D***, Estimation of the alpha-rhythm power impulse-response function by scaling HRF+ derivatives with the beta values obtained in ***B***. With the generic hemodynamic impulse response function, we can predict an fMRI response to any arbitrary alpha-power behavior. ***E***, We predicted fMRI responses to prestimulus high alpha-rhythm power signals by convolving the curves depicted in ***C*** and ***D***. Resulting predictions were compared with the observed high alpha fMRI stimulus-response modulations (Fig. 6, blue and red curves).

triggered stimulation. Also, a more specific time-frequency analysis of frontal electrodes did not reveal any systematic effects during alpha-triggered stimulation.

Response times

Mean response times for deviant stimuli were 489 ms for the high alpha-state stimulation condition and 497 ms for the state-independent stimulation condition. Within subjects, the average difference was not significant (mean, 9 ms; SD across subjects, 53 ms; $p = 0.59$). Hit rate was 95.77% (high alpha-state condition) and 94.86% (state-independent condition). This indicates corresponding levels of vigilance and attention across stimulus conditions.

Deviants differed from nondeviant visual stimuli (consisting of 900 ms black-and-white checkerboard presentations) by a contrast reversal after 500 ms. Hence, reaction times can be related either to the alpha-rhythm power before stimulus-response onset or to the alpha-rhythm power before the response to contrast reversal. In the latter case, desynchronized alpha activity, i.e., lower alpha-rhythm power, due to the preceding 500 ms checkerboard stimulus will be present. In addition, the amount of alpha-rhythm power change, i.e., ERD, can be related to behavior. We did all three analyses. In a time window from −250 to 250 ms around the contrast reversal in the deviant, a subject-wise correlation analysis of alpha power and reaction times revealed no significant correlation different from zero [mean correlation coefficient (cc) = -0.04 ± 0.05 (SEM), $p = 0.45$, Student's t test], whereas a (negative) correlation (mean cc = -0.16 ± 0.04, $p = 0.001$) exists for the time −1000 to −500 ms before contrast reversal, i.e., in the 500 ms window before stimulation onset. With respect to alpha ERD, we found an equally directed correlation (mean cc = -0.11 ± 0.03, $p = 0.005$). Notably deviant stimuli were not triggered dependent on alpha power in either condition, but rather were generated independent of alpha activity after a pseudorandomized delay, so this does not constitute a difference across conditions.

fMRI results

All group level fMRI maps reported in the following are based on a statistical threshold of $t > 2.9$, with $p < 0.04$ (FDR corrected) if not stated otherwise. The main fMRI map yielded by conjunction analysis (henceforth referred to as map purple) of alpha-dependent stimulus response (map red) and baseline modulations (map blue) is also based on the same statistical threshold.

Group level analyses: statistical parametric maps for alpha-dependent stimulus response modulation (condition I vs II)

We first examined whether fMRI stimulus responses were altered when stimulation occurred in the high alpha state (condition I–condition II). Within the visual ROI (Fig. 4*A*, gray areas), we identified reduced stimulus-response amplitudes for the high alpha state (compared with the control condition, i.e., alpha state-independent stimulation) (for response curves, see Fig. 4*B*) in bilateral occipitoparietal cortex, cuneus [Brodmann area (BA) 18, 19], bilateral thalamus, and left cerebellum (map red; $p < 0.04$, FDR corrected) (Fig. 4*A*; Table 1). At the same statistical threshold, no positive high alpha-state activations were found.

Statistical parametric maps for alpha-dependent baseline response modulation

Next, we examined the effect of the ongoing alpha activity on the fMRI baseline (i.e., alpha-dependent baseline modulation). Also here, we only found regions with significantly reduced fMRI baseline signal in response to increased alpha activity. They were observed in bilateral occipital areas (BAs 17, 18, 19) and bilateral cerebellum (map blue; $p < 0.03$ FDR corrected) (Fig. 5; Table 1).

Statistical parametric maps for alpha-dependent baseline and stimulus-response comodulations

At this stage, our results provided evidence of alpha rhythm-dependent fMRI baseline and stimulus-response alterations—more precisely, deactivations—however, they did not yet directly address the superposition hypothesis, which states that fMRI-baseline modulations related to the alpha rhythm add linearly to a fixed evoked response and thus are responsible for the observed stimulus-evoked fMRI response modulations. To this end, we first examined—on a qualitative basis—to what degree a spatial overlap exists for areas that are systematically modulated by the alpha rhythm in the same way during stimulation and nonstimulation periods, using a conjunction analysis. Analogous to the resulting

statistical maps of the separate analyses (for alpha baseline and stimulus response modulation), we identified areas showing a significant deactivating effect in both conditions (i.e., in and between stimulations, map purple; $p < 0.04$, FDR corrected) (Fig. 6*A*,*B*, Table 1). These areas comprise bilateral cuneus (BA 18), left fusiform gyrus (left BA 19), and cerebellum.

fMRI-response functions

For a further quantitative test of our linear superposition hypothesis, we extracted magnitudes of high alpha-state stimulus and baseline fMRI modulations by estimating average HRFs. Of particular interest are the response curves in the areas that exhibit alpha-dependent comodulations of the baseline and the stimulus response (Figs. 4*A*, 5). Here, equal magnitudes of the two curves would imply the hypothesized linear superposition, i.e., alpha-dependent fMRI baseline modulations accounting for the observed alpha-dependent fMRI stimulus-response modulations. In other words, fMRI stimulus response variability could be explained by a linear superposition of alpha-dependent fMRI baseline modulations and a fixed visually evoked fMRI response (Fig. 6*C*). By necessity, in map purple, the areas exhibiting both high alpha-state stimulus response modulations and alpha-dependent baseline modulations—both being deactivations—will only yield negative responses. However, their amplitudes do not necessarily match each other. Notably, our results (Fig. 6*C*, red and blue curves) show that magnitudes of both types of response curves are highly similar in map purple. We also analyzed response curves separately for each cluster in all three maps. For map purple, alpha-dependent baseline and stimulus-response curves matched for all clusters—so that the average curves shown in Figure 6*C* fully reflect what we also see on single-cluster level. The same results were found for the clusters of map blue. With respect to map red, we found a differential behavior (Fig. 7). Those areas of map red that were part of map purple, i.e., the conjunction result, exhibited response curves that matched in amplitude (including the largest statistically significant cluster, observed in the right extrastriate cortex). Those areas, however, that were located outside of map purple, such as thalamus and cerebellar areas at the margins of map purple, exhibited a stronger deactivation to high-alpha stimuli, as predicted by less pronounced (and nonsignificant) alpha-dependent baseline modulations, meaning that here amplitudes of baseline and response modulations did not match.

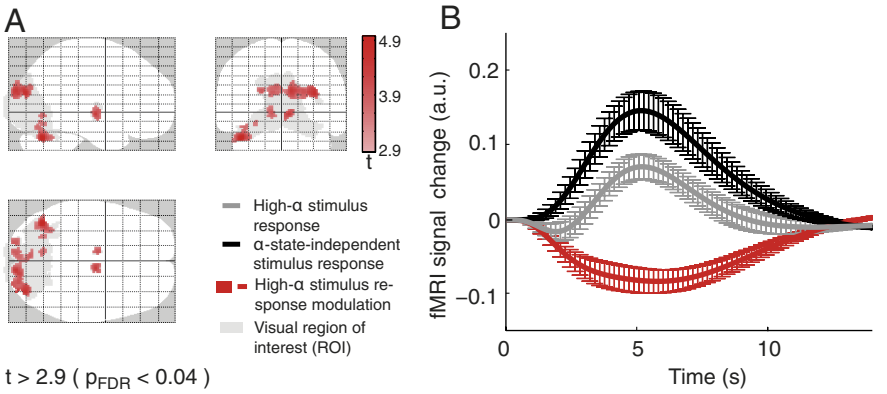

Figure 4. fMRI results for alpha-dependent stimulus response modulation [$t > 2.9$; $p < 0.04$, FDR corrected (p_{FDR}); extent threshold 10 voxels]. ***A***, The observed deactivations (red) within the visual ROI (gray) are projected onto a glass brain template. For corresponding *z*-values and MNI coordinates with anatomical labeling, see Table 1. ***B***, The resulting response curves for the identified clusters, depicting the high alpha-state stimulus response, the alpha-independent stimulus response, and their difference (error bars indicating SEM across subjects).

Table 1. fMRI results of random-effects group analyses ($n = 12$) for alpha-dependent stimulus response modulation, alpha-dependent baseline modulation, their conjunction, and prestimulus alpha-dependent responses

Anatomical region	Hemisphere	Coordinates *x*	*y*	*z*	Cluster size	*t* value	*z* value
Alpha-dependent stimulus-response modulation (map red)							
Cerebellum	L	−42	−66	−28	155	5.00	4.29
Middle occipital gyrus/cuneus (BA 18)	R	34	−82	20	453	4.51	3.95
Thalamus	R	8	−10	−2	51	4.19	3.73
Thalamus	L	−10	−8	0	29	3.70	3.36
Middle occipital gyrus/cuneus (BA 18)	L	−20	−92	22	32	3.60	3.28
Cerebellum	L	−10	−64	−4	17	3.32	3.06
Cerebellum/fusiform gyrus (BA 19)	L	−26	−66	−12	15	3.06	2.85
Alpha-dependent baseline modulation (map blue)							
Cerebellum	L	−28	−78	−16	429	4.82	4.16
Middle occipital gyrus/cuneus (BA 18/19)	L	−24	−96	24	56	4.52	3.96
Cerebellum/lingual gyrus (BA 18)	R	26	−84	−20	186	4.50	3.94
Cuneus/middle occipital gyrus (BA 18)	L	−18	−102	−16	69	4.02	3.60
Cuneus/middle occipital gyrus (BA 18/19)	R	24	−92	18	97	3.69	3.35
Cuneus/lingual gyrus (BA 17/18)	R	6	−98	4	120	3.41	3.14
Cuneus/lingual gyrus (BA 17/18)	R	22	−102	4	12	3.37	3.1
Conjunction analysis on alpha-dependent responses (map purple)							
Cuneus/middle occipital gyrus (BA 18)	R	22	−90	20	68	3.60	3.28
Cuneus/middle occipital gyrus (BA 18)	L	−10	−94	24	22	3.41	3.13
Cuneus/middle occipital gyrus (BA 18)	L	−20	−94	24	32	3.32	3.06
Cuneus/middle occipital gyrus (BA 18)	R	12	−94	26	4	3.09	2.88
Fusiform gyrus (BA 19)/cerebellum	L	−28	−66	−12	8	3.06	2.85
Prestimulus alpha response (map orange)							
Cuneus (BA 18)	R	2	−80	32	372	5.06	4.33
Cerebellum/lingual gyrus (BA 18)	L	−36	−70	−24	694	4.64	4.04
Cuneus/middle occipital gyrus (BA 18)	R	28	−82	24	96	4.54	3.97
Cuneus/middle occipital gyrus (BA 18/19)	L	−22	−92	24	47	4.44	3.91
Cerebellum/fusiform gyrus (BA 19)	R	24	−70	−20	298	4.21	3.74

Statistical parametric maps for trial-by-trial prestimulus alpha-dependent stimulus-response modulations

In addition to the observed alpha-triggered stimulus response modulation, we also investigated whether significant alpha-dependent stimulus response modulations exist for fluctuating prestimulus alpha activity (in condition II). In Figure 8, the resulting areas showing significant deactivations are depicted ($p < 0.02$, FDR corrected), comprising bilateral inferior and superior occipital clusters (map orange). A further conjunction of this prestimulus alpha analysis with the alpha-triggered stimulus response and the alpha baseline modulation did not change the outcome in terms of identified areas (data not shown). This supports the notion that alpha-triggered response modulations and the trial-by-trial alpha-dependent response modulations originate from the same functional network.

Single-trial correlation between prestimulus alpha activity and the evoked fMRI response

As it became apparent from the conjunction analysis, a close relation between alpha-dependent stimulus response and baseline modulations exists. To further support this finding, we performed additional single-subject analyses correlating the predicted (i.e., modeled and fitted) fMRI effect of prestimulus alpha and single-trial evoked fMRI responses. For this analysis, we examined areas exhibiting conjoint effects of both alpha-dependent stimulus response modulation and alpha-dependent baseline modulation in single subjects. Results of all subjects are depicted in Figure 9 (one scatter plot

per subject). A clear alpha-dependency of the fMRI stimulus response across the entire continuum of prestimulus alpha power can be observed (mean cc = 0.30; range across subjects, 0.12–0.48). This provides further positive evidence that variability of the evoked fMRI response can be explained by the ongoing alpha power on a trial-by-trial basis.

In summary, our results link fMRI variance and ongoing neuronal activity. During high alpha-state stimulation, a robust effect, i.e., a decrease of the fMRI stimulus response compared with state-independent stimulation, is revealed (Fig. 4*A*,*B*). A corresponding decrease of the fMRI baseline due to spontaneous alpha fluctuations can be observed (Fig. 5). These two alpha-dependent effects appear to share a common network of regions (Fig. 6*A*,*B*), with their hemodynamic responses matching in size (Fig. 6*C*). This supports the idea of linear superposition of hemodynamic responses to ongoing alpha and a fixed evoked stimulus response. Further positive evidence for linear superposition is provided by single-trial analysis (during state-independent stimulation) identifying a negative linear correlation of prestimulus alpha power and fMRI evoked responses in every subject (Figs. 8, 9).

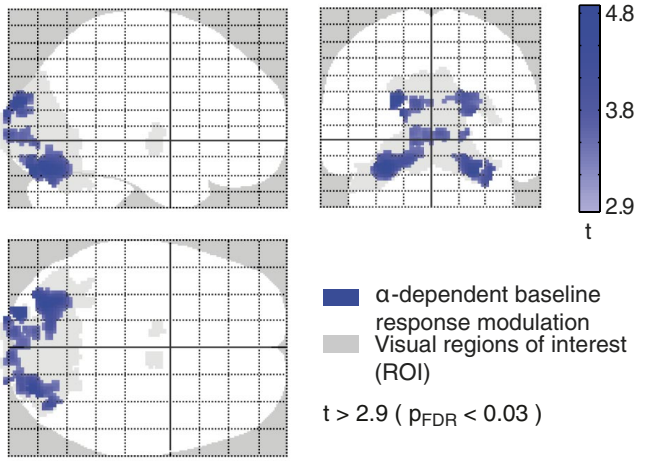

Figure 5. fMRI results for alpha-dependent baseline response modulation [$t > 2.9$; $p < 0.03$, FDR corrected (p_{FDR}); extent threshold 10 voxels]. The observed deactivations (blue) within the visual ROI (gray) projected onto a glass brain template. For corresponding *z*-values and MNI coordinates with anatomical labeling, see Table 1.

Discussion

In this study, we provide the anticipated and requested (Birn, 2007) evidence for the assumption that intrinsic neuronal activity is indeed responsible for intrinsic fMRI fluctuations superimposed on evoked fMRI responses (Fox et al., 2006).

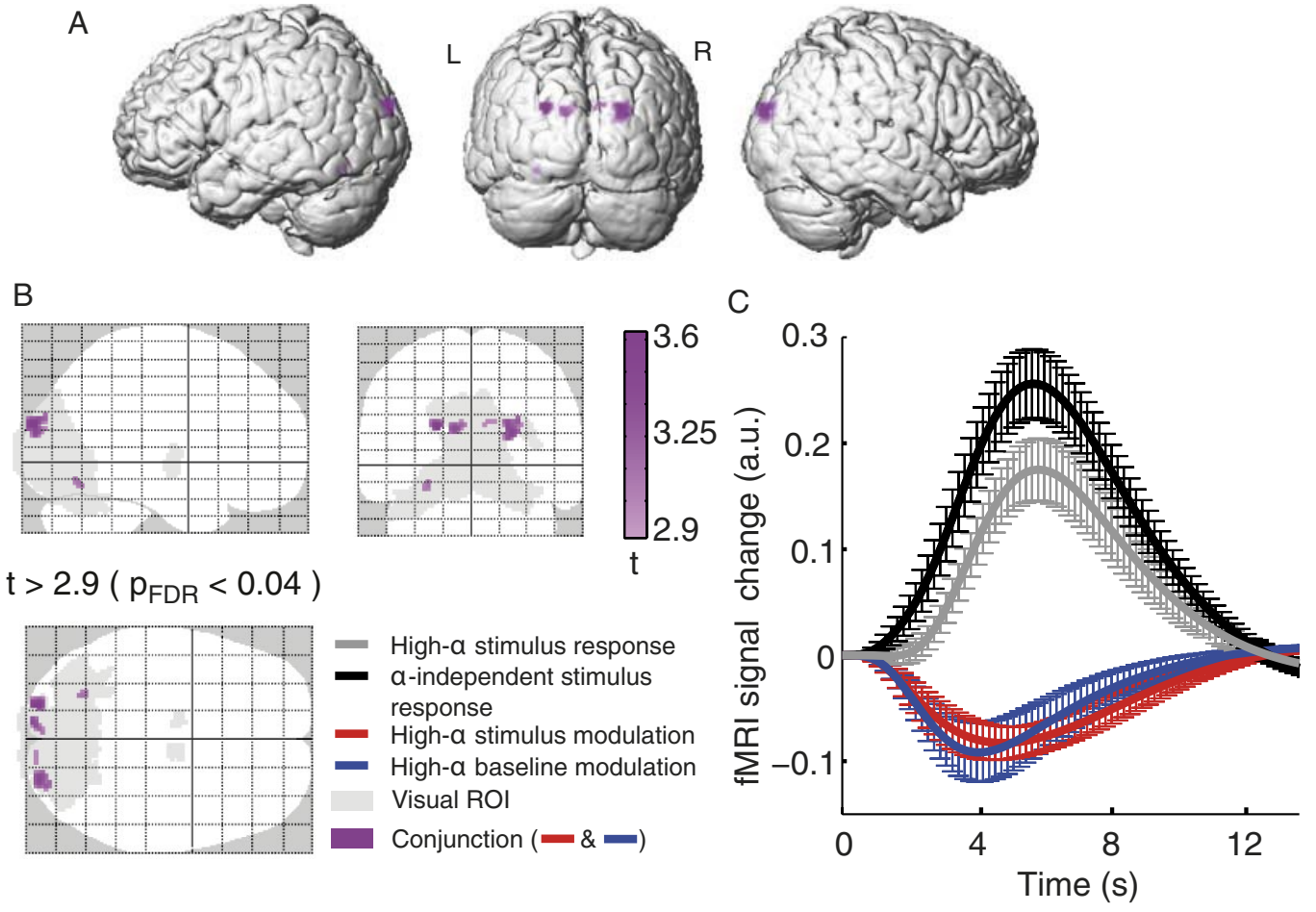

Figure 6. fMRI results of conjunction analysis. ***A***, ***B***, Occipital and occipitoparietal clusters deactivating during high-alpha activity during both stimulation and nonstimulation periods [$t > 2.9$; $p < 0.04$, FDR corrected (p_{FDR}); purple] depicted on a typical brain (Colin single-subject MNI brain template) and on a glass brain, together with the visual ROI (gray). ***C***, In these areas, the observed difference in evoked fMRI responses due to high alpha stimulation (gray line) compared with state-independent stimulation (black line; difference depicted by red line) can be explained by the modulation of the fMRI baseline due to high alpha during nonstimulation periods (blue). Error bars indicate SEM across subjects. For corresponding *z* values and MNI coordinates with anatomical labeling, see Table 1.

Excluding possible confounds

EEG–fMRI is an artifact-prone method potentially leading to erroneous inferences (Ritter et al., 2009a). We implemented several strategies to exclude such confounds, as detailed in the Materials and Methods and Results, above. Both kinds of MR-related artifacts were reduced efficiently by a spatial-filter approach [capable of identifying even subtle mu rhythm fMRI correlates (Ritter et al., 2009b)] and an optimized EEG–fMRI setup (Freyer et al., 2009).

Due to relatively short nonstimulation periods, the ongoing alpha activity assessed here might differ qualitatively from alpha activity assessed during continuous rest. However, by orthogonalizing alpha baseline regressors to stimulus and prestimulus alpha regressors, we ensured that the identified fMRI correlates reflect ongoing nonstimulus-locked alpha power changes. Notably, observed fMRI correlates of orthogonalized regressors correspond to previous resting-state findings in terms of location and response character.

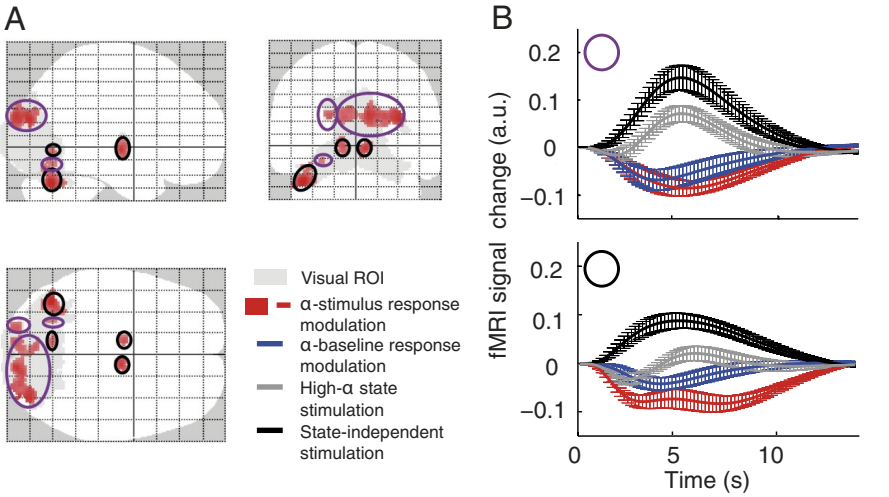

Figure 7. ***A***, Within the map of suprathreshold high alpha-state stimulus-response modulations, i.e., map red, two kinds of clusters can be identified. ***B***, In one set of cortical areas (purple rings in ***A***), the observed modulation during high alpha-state stimulation can be explained by baseline modulations caused by high alpha states (top). In the other set (black rings in ***A***), including thalamic and cerebellar areas outside the conjunction map, the observed effect cannot be explained by baseline modulations (bottom).

Considerations on neurophysiology

In the cat visual cortex, broadband ongoing membrane potentials correlate linearly with evoked postsynaptic membrane potentials (Azouz and Gray, 1999). Without excluding nonlinear scenarios, our main finding agrees with such linear superposition of ongoing and evoked activities on the neuronal level and subsequent linear transformation of summed neuronal signals into hemodynamic responses. In accordance with previous studies (Goldman et al., 2002; Moosmann et al., 2003; Feige et al., 2005; de Munck et al., 2007), intrinsic alpha rhythm negatively correlates with fMRI signals in extrastriate areas, indicating decreases of net neuronal activity during high alpha states (Ritter et al., 2002). This baseline effect seems to add linearly to fixed visually evoked fMRI responses, finally leading to the observed decrease of alpha-triggered fMRI stimulus responses.

Regarding the EEG, present and earlier findings also suggest linear superposition between ongoing alpha rhythm and fixed evoked responses for early VEP components at ~100 ms poststimulus-time (P100) (Mazaheri and Jensen, 2006; Becker et al., 2008) and positive relations between prestimulus alpha-rhythm power and late evoked components (~300 ms poststimulus). These findings agree well with the notion that the VEP–P100 component is generated in extrastriate visual cortex (Schroeder et al., 1998) for which our fMRI data indicate linear superposition. How does the finding of linear superposition in extrastriate visual areas relate to invasive animal recordings reporting linear superposition in striate visual cortex (Arieli et al., 1996; Azouz and Gray, 1999)? One likely explanation is that alpha-rhythm ICs in our study only contained minor alpha activity from striate cortex due to this structure's deep location and unfavorable potential orientations. Accordingly, many EEG–fMRI studies report extrastriate fMRI correlates of EEG–alpha activity (Goldman et al., 2002; Moosmann et al., 2003; Feige et al., 2005; Gonçalves et al., 2006; de Munck et al., 2007). Our findings do not exclude the possibility of similar effects in primary visual areas. What they do suggest is that ongoing alpha activity, as measured here, explains evoked activity in secondary visual areas best, being in accordance with a recent study of Scheeringa et al. (2011).

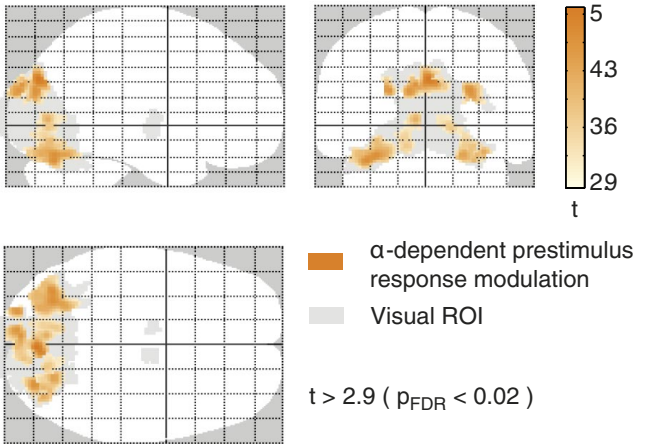

Figure 8. fMRI results of single-trial prestimulus alpha correlation analysis, testing the effect of fluctuating prestimulus alpha power on the single-trial evoked fMRI response [$t > 2.9$; $p < 0.02$, FDR corrected (p_{FDR}); extent threshold 10 voxels]. Found deactivations are depicted on a glass brain (orange; visual ROI, gray). For corresponding z values and MNI coordinates with anatomical labeling, see Table 1.

Complementary to the latter study, we also analyzed subcortical areas such as thalamus and cerebellum, where we identified significant alpha-dependent fMRI stimulus-response modulations but no corresponding baseline modulations. Here, the linear superposition hypothesis does not hold true. The theory of linear superposition is also linked to the (possibly simplified) assumption of linear neurovascular coupling. While some studies report nonlinear neurovascular coupling for specific brain areas and stimulus conditions (Huettel et al., 2004), less is known about possible nonlinear couplings of ongoing EEG activity and fMRI baseline responses. Empirical and theoretical studies suggest U-shaped, i.e., nonlinear, relationships of ongoing activity and behavior (Linkenkaer-Hansen et al., 2004) and between ongoing activity and evoked EEG responses (Rajagovindan and Ding, 2011). Such phenomena may account for some of the nonlinearities we have observed. In terms of sta-

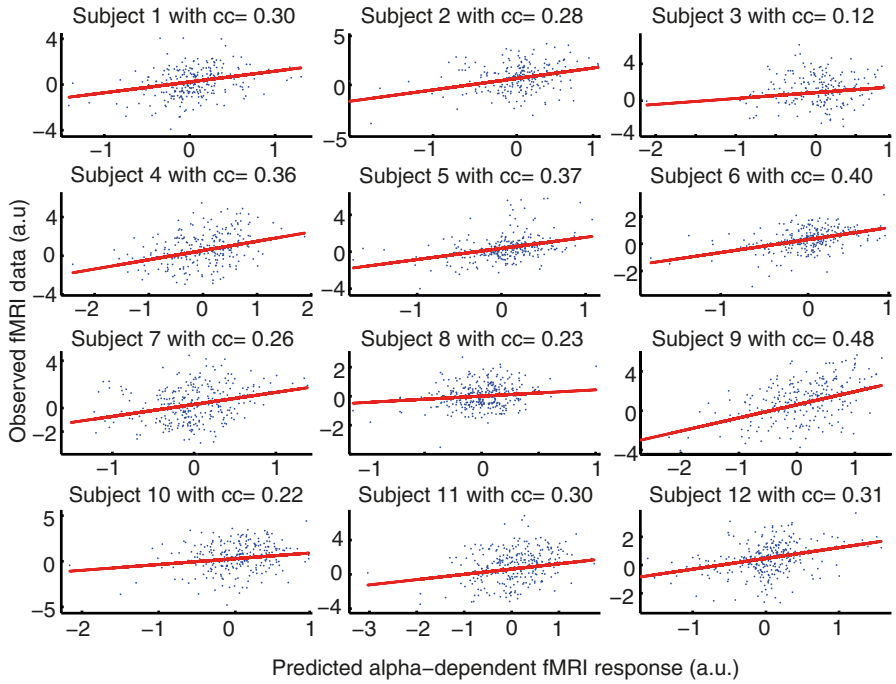

Figure 9. Single-trial correlation between prestimulus alpha power-based predictions of fMRI signal modulations (*x*-axis) and actually observed evoked fMRI responses (*y*-axis) for all individual subjects. The inverse relation between alpha power and fMRI signal is accounted for by model fitting. Hence the fitted model yields a positive correlation with the fMRI signal. A clear alpha dependency of the fMRI stimulus response across the entire continuum of prestimulus alpha power can be observed.

tistical robustness, our prevailing finding is linear superposition of ongoing and evoked fMRI responses.

Functional implications

Linear superposition occurs mainly in secondary visual (extrastriate) cortex, including occipitoparietal visual association areas important for visuospatial attention (Yantis et al., 2002; Tuch et al., 2005). As information passes through visual hierarchies from striate via extrastriate to the visual association cortex, increasing levels of specialization of processing occur (Haxby et al., 1991). The areas identified here (extrastriate occipitoparietal cortex, including cuneus), of which the stimulus-response behavior is modulated by ongoing alpha activity, point to alpha-dependent modulations of higher visual functions.

A proposed mechanism linking alpha band oscillatory activity and modulation of visual processing is gating by inhibition (Jensen and Mazaheri, 2010). Accumulating evidence supports this theory. For example, power of prestimulus alpha band oscillations is inversely related to cortical excitability (Romei et al., 2008). Spatial attention is tightly related to alpha-rhythm power and the latter to cortical excitability. Spatial attention-related top-down regulations of stimulus-related excitability have recently been shown for somatosensory areas (Schubert et al., 2008). Other studies demonstrated that high prestimulus alpha-rhythm power in somatosensory cortex reduces perception of somatosensory (Schubert et al., 2009) and painful (Babiloni et al., 2006) stimuli. This is in line with findings in the visual system, where spontaneous power fluctuations of prestimulus alpha rhythm are inversely related to perceptual performance (Ergenoglu et al., 2004; van Dijk et al., 2008; Busch et al., 2009).

While the present study was not conceived to investigate relations between alpha-rhythm power and behavior, it is worth mentioning that even for the sparsely inserted deviant trials requiring behavioral responses, we found a relation between alpha rhythm and behavior, adding evidence to the notion of the alpha rhythm's functional role. Given the low number of trials and the particularity of deviant stimuli (the contrast reversal falling into windows where alpha ERD is already present), it was beyond the scope of this study to further identify exact mechanisms underlying the observed behavioral effects (for related debates, see Klimesch et al. 2006). Notably, it supports the notion that linear-superposition mechanisms, as observed here, and functional roles of ongoing activity are not mutually exclusive, as also shown previously by fMRI (Fox et al., 2007). While spatial attention modulates alpha-rhythm power (Thut et al., 2006; Rajagovindan and Ding, 2011) and firing rates of neurons (Rajagovindan and Ding, 2011), it does not affect early VEPs (Gomez Gonzalez et al., 1994; Clark and Hillyard, 1996; Noesselt et al., 2002). Attention may be mediated through modulation of synchrony of neuronal oscillations (Mitchell et al., 2009). In humans, nonrelevant neurons coding nonattended receptive fields presumably synchronize in the alpha band. With their increasing engagement in oscillatory networks, responsiveness of neurons to external inputs decreases (Buzsáki and Draguhn, 2004) along with reduced synaptic transmissions and decreased fMRI activity. In case of stimulation, the thus modulated baseline would add linearly to visually evoked responses. How can this be reconciled with the fact that later components of the VEP covary with prestimulus alpha-rhythm power (Becker et al., 2008) and also with attention (Noesselt et al., 2002)? These effects were expected to introduce deviations from linear superposition given the temporal low-pass filtering properties of fMRI and hence blurring of early and late responses. Possible explanations are differences in location and the recently proposed origin of such late components, i.e., alpha-rhythm amplitude asymmetry (Nikulin et al., 2007; Mazaheri and Jensen, 2008). This would represent a mechanism probably not associated with hemodynamic responses (other than prestimulus alpha-related fMRI activity) and hence poses one possible scenario reconcilable with our present findings [and the recent findings of Scheeringa et al. (2011)].

Another functional role of ongoing oscillations with respect to state-dependent processing may be the integration of bottom-up and top-down processes in line with the theories of predictive coding and hierarchical inference (Friston, 2003). In real life, we often have feature-based and spatial foreknowledge. These sources of information are presumably used in concert to optimize the allocation of attention and eye movements (Egner et al., 2008). The finding of state-dependency of evoked responses is also compatible with the theory of preferred cortical states (Tsodyks et al., 1999), implying the existence of intrinsic facilitative neuronal modes.

Outlook

We demonstrated the role of the posterior alpha rhythm for variability of fMRI stimulus responses. Our findings, however, do not

exclude the presence of additional intrinsic sources of evoked-response variability as proposed, for example, in Truccolo et al. (2002). Apart from the alpha rhythm, we expect other neuronal signatures already known to contribute to fMRI signal variability under resting condition (Laufs et al., 2003; Giraud et al., 2007; Mantini et al., 2007; Nir et al., 2007) to further explain fMRI evoked-response variability. Also, complementary to our results on amplitude-dependent effects, a link between alpha-rhythm phase and fMRI stimulus-evoked responses has recently been revealed (Scheeringa et al., 2011). Thus, in the wake of future multimodal studies, we may appreciate additional forms of integration of intrinsic neuronal context, sensation, and action constituting the foundation of adaptive behavior.

From a theoretical perspective, large-scale neural-systems models indicate the importance of local dynamics, anatomical connectivity, and noise for the emergence of resting-state patterns in general (Deco et al., 2011) and the alpha rhythm in particular (Freyer et al., 2011). By illuminating underlying physiological parameters that are otherwise inaccessible to noninvasive recordings, those modeling approaches may contribute to a deeper understanding of state-dependent information processing in humans.

References

Anami K, Mori T, Tanaka F, Kawagoe Y, Okamoto J, Yarita M, Ohnishi T, Yumoto M, Matsuda H, Saitoh O (2003) Stepping stone sampling for retrieving artifact-free electroencephalogram during functional magnetic resonance imaging. Neuroimage 19:281–295.

Arieli A, Sterkin A, Grinvald A, Aertsen A (1996) Dynamics of ongoing activity: explanation of the large variability in evoked cortical responses. Science 273:1868–1871.

Azouz R, Gray CM (1999) Cellular mechanisms contributing to response variability of cortical neurons in vivo. J Neurosci 19:2209–2223.

Babiloni C, Brancucci A, Del Percio C, Capotosto P, Arendt-Nielsen L, Chen AC, Rossini PM (2006) Anticipatory electroencephalography alpha rhythm predicts subjective perception of pain intensity. J Pain 7:709–717.

Becker R, Ritter P, Villringer A (2008) Influence of ongoing alpha rhythm on the visual evoked potential. Neuroimage 39:707–716.

Beckmann CF, DeLuca M, Devlin JT, Smith SM (2005) Investigations into resting-state connectivity using independent component analysis. Philos Trans R Soc Lond B Biol Sci 360:1001–1013.

Birn RM (2007) The behavioral significance of spontaneous fluctuations in brain activity. Neuron 56:8–9.

Biswal B, Yetkin FZ, Haughton VM, Hyde JS (1995) Functional connectivity in the motor cortex of resting human brain using echo-planar MRI. Magn Reson Med 34:537–541.

Busch NA, Dubois J, VanRullen R (2009) The phase of ongoing EEG oscillations predicts visual perception. J Neurosci 29:7869–7876.

Buzsáki G, Draguhn A (2004) Neuronal oscillations in cortical networks. Science 304:1926–1929.

Clark VP, Hillyard SA (1996) Spatial selective attention affects early extrastriate but not striate components of the visual evoked potential. J Cogn Neurosci 8:387–402.

Damoiseaux JS, Rombouts SA, Barkhof F, Scheltens P, Stam CJ, Smith SM, Beckmann CF (2006) Consistent resting-state networks across healthy subjects. Proc Natl Acad Sci U S A 103:13848–13853.

Debener S, Mullinger KJ, Niazy RK, Bowtell RW (2008) Properties of the ballistocardiogram artefact as revealed by EEG recordings at 1.5, 3 and 7 T static magnetic field strength. Int J Psychophysiol 67:189–199.

Deco G, Jirsa VK, McIntosh AR (2011) Emerging concepts for the dynamical organization of resting-state activity in the brain. Nat Rev Neurosci 12:43–56.

Delorme A, Makeig S (2004) EEGLAB: an open source toolbox for analysis of single-trial EEG dynamics including independent component analysis. J Neurosci Methods 134:9–21.

De Luca M, Beckmann CF, De Stefano N, Matthews PM, Smith SM (2006) fMRI resting state networks define distinct modes of long-distance interactions in the human brain. Neuroimage 29:1359–1367.

de Munck JC, Gonçalves SI, Huijboom L, Kuijer JP, Pouwels PJ, Heethaar RM, Lopes da Silva FH (2007) The hemodynamic response of the alpha rhythm: an EEG/fMRI study. Neuroimage 35: 1142–1151.

Egner T, Monti JM, Trittschuh EH, Wieneke CA, Hirsch J, Mesulam MM (2008) Neural integration of top-down spatial and feature-based information in visual search. J Neurosci 28:6141–6151.

Ergenoglu T, Demiralp T, Bayraktaroglu Z, Ergen M, Beydagi H, Uresin Y (2004) Alpha rhythm of the EEG modulates visual detection performance in humans. Brain Res Cogn Brain Res 20:376–383.

Feige B, Scheffler K, Esposito F, Di Salle F, Hennig J, Seifritz E (2005) Cortical and subcortical correlates of electroencephalographic alpha rhythm modulation. J Neurophysiol 93:2864–2872.

Fox MD, Snyder AZ, Zacks JM, Raichle ME (2006) Coherent spontaneous activity accounts for trial-to-trial variability in human evoked brain responses. Nat Neurosci 9:23–25.

Fox MD, Snyder AZ, Vincent JL, Raichle ME (2007) Intrinsic fluctuations within cortical systems account for intertrial variability in human behavior. Neuron 56:171–184.

Freyer F, Becker R, Anami K, Curio G, Villringer A, Ritter P (2009) Ultrahigh-frequency EEG during fMRI: pushing the limits of imaging-artifact correction. Neuroimage 48:94–108.

Freyer F, Roberts JA, Becker R, Robinson PA, Ritter P, Breakspear M (2011) Biophysical mechanisms of multistability in resting state cortical rhythms. J Neurosci 31:6353–6361.

Friston K (2003) Learning and inference in the brain. Neural Netw 16:1325–1352.

Giraud AL, Kleinschmidt A, Poeppel D, Lund TE, Frackowiak RS, Laufs H (2007) Endogenous cortical rhythms determine cerebral specialization for speech perception and production. Neuron 56:1127–1134.

Goldman RI, Stern JM, Engel J Jr, Cohen MS (2002) Simultaneous EEG and fMRI of the alpha rhythm. Neuroreport 13:2487–2492.

Gomez Gonzalez CM, Clark VP, Fan S, Luck SJ, Hillyard SA (1994) Sources of attention-sensitive visual event-related potentials. Brain Topogr 7:41–51.

Gonçalves SI, de Munck JC, Pouwels PJ, Schoonhoven R, Kuijer JP, Maurits NM, Hoogduin JM, Van Someren EJ, Heethaar RM, Lopes da Silva FH (2006) Correlating the alpha rhythm to BOLD using simultaneous EEG/fMRI: Inter-subject variability. Neuroimage 30:203–213.

Greicius MD, Krasnow B, Reiss AL, Menon V (2003) Functional connectivity in the resting brain: a network analysis of the default mode hypothesis. Proc Natl Acad Sci U S A 100:253–258.

Haxby JV, Grady CL, Horwitz B, Ungerleider LG, Mishkin M, Carson RE, Herscovitch P, Schapiro MB, Rapoport SI (1991) Dissociation of object and spatial visual processing pathways in human extrastriate cortex. Proc Natl Acad Sci U S A 88:1621–1625.

Hesselmann G, Kell CA, Eger E, Kleinschmidt A (2008) Spontaneous local variations in ongoing neural activity bias perceptual decisions. Proc Natl Acad Sci U S A 105:10984–10989.

Huettel SA, McKeown MJ, Song AW, Hart S, Spencer DD, Allison T, McCarthy G (2004) Linking hemodynamic and electrophysiological measures of brain activity: evidence from functional MRI and intracranial field potentials. Cereb Cortex 14:165–173.

Jasiukaitis P, Hakerem G (1988) The effect of prestimulus alpha activity on the P300. Psychophysiology 25:157–165.

Jensen O, Mazaheri A (2010) Shaping functional architecture by oscillatory alpha activity: gating by inhibition. Front Hum Neurosci 4:186.

Klimesch W, Doppelmayr M, Hanslmayr S (2006) Upper alpha ERD and absolute power: their meaning for memory performance. Prog Brain Res 159:151–165.

Laufs H, Krakow K, Sterzer P, Eger E, Beyerle A, Salek-Haddadi A, Kleinschmidt A (2003) Electroencephalographic signatures of attentional and cognitive default modes in spontaneous brain activity fluctuations at rest. Proc Natl Acad Sci U S A 100:11053–11058.

Laufs H, Daunizeau J, Carmichael DW, Kleinschmidt A (2008) Recent advances in recording electrophysiological data simultaneously with magnetic resonance imaging. Neuroimage 40:515–528.

Linkenkaer-Hansen K, Nikulin VV, Palva S, Ilmoniemi RJ, Palva JM (2004) Prestimulus oscillations enhance psychophysical performance in humans. J Neurosci 24:10186–10190.

Logothetis NK, Pauls J, Augath M, Trinath T, Oeltermann A (2001) Neurophysiological investigation of the basis of the fMRI signal. Nature 412:150–157.

Makeig S, Westerfield M, Jung TP, Enghoff S, Townsend J, Courchesne E, Sejnowski TJ (2002) Dynamic brain sources of visual evoked responses. Science 295:690–694.

Mantini D, Perrucci MG, Del Gratta C, Romani GL, Corbetta M (2007) Electrophysiological signatures of resting state networks in the human brain. Proc Natl Acad Sci U S A 104:13170–13175.

Mathewson KE, Gratton G, Fabiani M, Beck DM, Ro T (2009) To see or not to see: prestimulus alpha phase predicts visual awareness. J Neurosci 29:2725–2732.

Mazaheri A, Jensen O (2006) Posterior alpha activity is not phase-reset by visual stimuli. Proc Natl Acad Sci U S A 103:2948–2952.

Mazaheri A, Jensen O (2008) Asymmetric amplitude modulations of brain oscillations generate slow evoked responses. J Neurosci 28:7781–7787.

Mitchell JF, Sundberg KA, Reynolds JH (2009) Spatial attention decorrelates intrinsic activity fluctuations in macaque area V4. Neuron 63: 879–888.

Moosmann M, Ritter P, Krastel I, Brink A, Thees S, Blankenburg F, Taskin B, Obrig H, Villringer A (2003) Correlates of alpha rhythm in functional magnetic resonance imaging and near infrared spectroscopy. Neuroimage 20:145–158.

Nikulin VV, Linkenkaer-Hansen K, Nolte G, Lemm S, Müller KR, Ilmoniemi RJ, Curio G (2007) A novel mechanism for evoked responses in the human brain. Eur J Neurosci 25:3146–3154.

Nir Y, Fisch L, Mukamel R, Gelbard-Sagiv H, Arieli A, Fried I, Malach R (2007) Coupling between neuronal firing rate, gamma LFP, and BOLD fMRI is related to interneuronal correlations. Curr Biol 17:1275–1285.

Noesselt T, Hillyard SA, Woldorff MG, Schoenfeld A, Hagner T, Jäncke L, Tempelmann C, Hinrichs H, Heinze HJ (2002) Delayed striate cortical activation during spatial attention. Neuron 35:575–587.

Raichle ME, MacLeod AM, Snyder AZ, Powers WJ, Gusnard DA, Shulman GL (2001) A default mode of brain function. Proc Natl Acad Sci U S A 98:676–682.

Rajagovindan R, Ding M (2011) From prestimulus alpha oscillation to visual-evoked response: an inverted-U function and its attentional modulation. J Cogn Neurosci 23:1379–1394.

Reinacher M, Becker R, Villringer A, Ritter P (2009) Oscillatory brain states interact with late cognitive components of the somatosensory evoked potential. J Neurosci Methods 183:49–56.

Ritter P, Villringer A (2006) Simultaneous EEG-fMRI. Neurosci Biobehav Rev 30:823–838.

Ritter P, Villringer A, Tomita M, Kanno I, Hamel E (2002) Inhibition and functional magnetic resonance imaging. In: Brain activation and CBF control, pp 213–222. Amsterdam: Elsevier.

Ritter P, Becker R, Freyer F, Villringer A (2009a) EEG quality: the image acquisition artefact. In: EEG-fMRI - Physiological Basis, Technique, and Applications (Mulert C, Lemieux L, eds), pp 153–171. New York: Springer.

Ritter P, Moosmann M, Villringer A (2009b) Rolandic alpha and beta EEG rhythms' strengths are inversely related to fMRI-BOLD signal in primary somatosensory and motor cortex. Hum Brain Mapp 30:1168–1187.

Romei V, Brodbeck V, Michel C, Amedi A, Pascual-Leone A, Thut G (2008) Spontaneous fluctuations in posterior alpha-band EEG activity reflect variability in excitability of human visual areas. Cereb Cortex 18:2010–2018.

Scheeringa R, Mazaheri A, Bojak I, Norris DG, Kleinschmidt A (2011) Modulation of visually evoked cortical fMRI responses by phase of ongoing occipital alpha oscillations. J Neurosci 31:3813–3820.

Schroeder CE, Mehta AD, Givre SJ (1998) A spatiotemporal profile of visual system activation revealed by current source density analysis in the awake macaque. Cereb Cortex 8:575–592.

Schubert R, Ritter P, Wustenberg T, Preuschhof C, Curio G, Sommer W, Villringer A (2008) Spatial attention related SEP amplitude modulations covary with BOLD signal in S1: a simultaneous EEG-fMRI study. Cereb Cortex 18:2686–2700.

Schubert R, Haufe S, Blankenburg F, Villringer A, Curio G (2009) Now you'll feel it, now you won't: EEG rhythms predict the effectiveness of perceptual masking. J Cogn Neurosci 21:2407–2419.

Thut G, Nietzel A, Brandt SA, Pascual-Leone A (2006) Alpha-band electroencephalographic activity over occipital cortex indexes visuospatial attention bias and predicts visual target detection. J Neurosci 26:9494–9502.

Truccolo WA, Ding M, Knuth KH, Nakamura R, Bressler SL (2002) Trial-to-trial variability of cortical evoked responses: implications for the analysis of functional connectivity. Clin Neurophysiol 113:206–226.

Tsodyks M, Kenet T, Grinvald A, Arieli A (1999) Linking spontaneous activity of single cortical neurons and the underlying functional architecture. Science 286:1943–1946.

Tuch DS, Salat DH, Wisco JJ, Zaleta AK, Hevelone ND, Rosas HD (2005) Choice reaction time performance correlates with diffusion anisotropy in white matter pathways supporting visuospatial attention. Proc Natl Acad Sci U S A 102:12212–12217.

van Dijk H, Schoffelen JM, Oostenveld R, Jensen O (2008) Prestimulus oscillatory activity in the alpha band predicts visual discrimination ability. J Neurosci 28:1816–1823.

Yantis S, Schwarzbach J, Serences JT, Carlson RL, Steinmetz MA, Pekar JJ, Courtney SM (2002) Transient neural activity in human parietal cortex during spatial attention shifts. Nat Neurosci 5:995–1002.

Ziehe A, Müller KR, Nolte G, Mackert BM, Curio G (2000) Artifact reduction in magnetoneurography based on time-delayed second-order correlations. IEEE Trans Biomed Eng 47:75–87.

4.3 Study 3

- Freyer, F., **Reinacher, M.**, Nolte, G., Dinse, H. R. & Ritter, P. Repetitive tactile stimulation changes resting–state functional connectivity—implications for treatment of sensorimotor decline. *Frontiers in Human Neuroscience* **6**, Article 144 (2012).

frontiers in
HUMAN NEUROSCIENCE

ORIGINAL RESEARCH ARTICLE
published: 23 May 2012
doi: 10.3389/fnhum.2012.00144

Repetitive tactile stimulation changes resting-state functional connectivity—implications for treatment of sensorimotor decline

Frank Freyer[1,2,4], Matthias Reinacher[1,2], Guido Nolte[3], Hubert R. Dinse[4] and Petra Ritter[1,2,5,6]*

[1] *Bernstein Focus State Dependencies of Learning and Bernstein Center for Computational Neuroscience, Berlin, Germany*
[2] *Department of Neurology, Charité University Medicine, Berlin, Germany*
[3] *Department of Neurophysiology and Pathophysiology, University Medical Center Hamburg-Eppendorf, Hamburg, Germany*
[4] *Institute for Neuroinformatics, Neural Plasticity Lab, Ruhr-University Bochum, Germany*
[5] *Max Planck Institute for Human Cognitive and Brain Sciences, Leipzig, Germany*
[6] *Berlin School of Mind and Brain and Mind and Brain Institute, Humboldt University, Berlin, Germany*

Edited by:
Burkhard Pleger, Max Planck Institute for Human Cognitive and Brain Sciences, Germany

Reviewed by:
Sarang S. Dalal, INSERM, France
Andreas Daffertshofer, VU University Amsterdam, Netherlands

***Correspondence:**
Petra Ritter, Department of Neurology, Charité Universitaetsmedizin Berlin, Charitéplatz 1, 10117 Berlin, Germany.
e-mail: petra.ritter@charite.de

Neurological disorders and physiological aging can lead to a decline of perceptual abilities. In contrast to the conventional therapeutic approach that comprises intensive training and practicing, passive repetitive sensory stimulation (RSS) has recently gained increasing attention as an alternative to countervail the sensory decline by improving perceptual abilities without the need of active participation. A particularly effective type of high-frequency RSS, utilizing Hebbian learning principles, improves perceptual acuity as well as sensorimotor functions and has been successfully applied to treat chronic stroke patients and elderly subjects. High-frequency RSS has been shown to induce plastic changes of somatosensory cortex such as representational map reorganization, but its impact on the brain's ongoing network activity and resting-state functional connectivity has not been investigated so far. Here, we applied high-frequency RSS in healthy human subjects and analyzed resting state Electroencephalography (EEG) functional connectivity patterns before and after RSS by means of imaginary coherency (ImCoh), a frequency-specific connectivity measure which is known to reduce over-estimation biases due to volume conduction and common reference. Thirty minutes of passive high-frequency RSS lead to significant ImCoh-changes of the resting state mu-rhythm in the individual upper alpha frequency band within distributed sensory and motor cortical areas. These stimulation induced distributed functional connectivity changes likely underlie the previously observed improvement in sensorimotor integration.

Keywords: EEG, resting state, functional connectivity, sensory stimulation, plasticity, sensorimotor, mu-rhythm, ongoing activity

INTRODUCTION

Pathological changes in neuronal functioning lead to a decline of perceptual and sensory abilities. The most obvious cause is a damage of sensory brain areas due to trauma or stroke (Carey et al., 1993; Feys et al., 1998; Rosamond et al., 2007), but also a variety of neurological disorders such as Parkinson's disease (Koller, 1984; Sathian et al., 1997) or dystonia (Tinazzi et al., 2003; Stamelou et al., 2011) can affect perceptual and sensory function, possibly by a dysfunction of the sensorimotor network (Silberstein et al., 2005; Tamura et al., 2009; Litvak et al., 2011). In addition, a more natural but progressive decline of perceptual and sensory capacity develops with increasing age, not only in the visual and auditory, but also in the somatosensory system (Kalisch et al., 2009). Therapeutic strategies to treat the decline of perceptual abilities, which often impacts also motor function, usually comprise intensive and repeated mass training of the respective sensory modality (Sawaki et al., 2003; Kornatz et al., 2005).

A highly efficient alternative approach consists of passive repetitive sensory stimulation (RSS), which has been shown to enhance sensory abilities in chronic stroke patients (Powell et al., 1999; Conforto et al., 2002, 2007; Sawaki et al., 2006; Smith et al., 2009). RSS is a form of repetitive stimulation, following the idea of Hebbian learning: synchronous neural activity that is instrumental to drive plastic changes, is evoked by tactile "co"-activation of the skin, or electrical co-activation of the peripheral nerves of the fingers. Several studies have shown that after such type of stimulation, tactile discrimination abilities were improved and cortical representation of the respective skin area was enlarged (Godde et al., 2000; Pleger et al., 2001, 2003; Dinse et al., 2003). Evidence for the Hebbian nature of coactivation-related learning comes in addition from the fact that, when using a modified version of the coactivation protocol consisting of a single, small stimulation site instead of one large area, no changes in perception or cortical maps occur (Pleger et al., 2003; Ragert et al., 2008). This implies that spatial summation requirements

indicative of cooperative processes need to be fulfilled to drive behavioral changes.

High-frequency RSS enhances sensory and motor abilities in post-stroke patients suffering from sensory loss (Smith et al., 2009), and counteracts age-related declines of perceptual discrimination abilities (Dinse et al., 2006) and sensorimotor performance (Kalisch et al., 2008, 2010). Several studies have related the effectiveness of RSS to an induction of neural plasticity in the somatosensory system (Pleger et al., 2001, 2003; Dinse et al., 2003). However, these findings focus predominantly on cortical representations of *evoked* sensory neuronal activity (e.g., an altered representation of the stimulated hand area in primary somatosensory cortex). Less is known about the impact of RSS on *global* connectivity features of the involved neuronal network during the *resting state*. Illuminating this relationship would be particularly helpful in order to account for the improvement of sensorimotor integration observed in chronic stroke patients (Smith et al., 2009) and elderly subjects (Kalisch et al., 2008, 2010), since changes in sensorimotor integration most likely correspond to changes of long-range interactions between sensory, motor, and association areas (Diamond et al., 2008; Aronoff et al., 2010; Mao et al., 2011).

One way to assess the functional interactions between these distant but coordinated brain areas is to analyze resting state functional connectivity, which reflects a measure of correlations between spatially distant ongoing neuronal dynamics. To investigate the impact of RSS on resting state functional connectivity was the aim of this study. We applied high-frequency RSS in healthy subjects and recorded resting state activity by means of non-invasive Electroencephalography (EEG) before and after the RSS procedure. As a measure of functional connectivity we analyzed changes in EEG imaginary coherency (ImCoh), which can be used to assess frequency-specific interactions between distinct brain areas and unlike the conventional measure of (magnitude squared) coherence has the advantage to reduce overestimation errors due to common references, volume conduction, and cross-talk (Nolte et al., 2004; Guggisberg et al., 2008). The sensorimotor system is known to exhibit dominant resting state rhythms (Salmelin and Hari, 1994b) that peak in the alpha (8–12 Hz) and beta (13–29 Hz) band, the former known as mu-rhythm or rolandic alpha rhythm (Gastaut, 1952; Kuhlman, 1978), the latter as rolandic beta rhythm (Pfurtscheller, 1981, 1992; Salmelin and Hari, 1994a). While the rolandic beta rhythm has a stronger link to the precentral motor cortex, the mu-rhythm is more tightly related to the somatosensory postcentral cortex (Salmelin et al., 1995; Ritter et al., 2009). Given the previously reported positive impact of high-frequency RSS on the sensorimotor abilities in stroke patients (Smith et al., 2009) and elderly subjects (Kalisch et al., 2008, 2010), we hypothesized that RSS might induce changes of functional connectivity within the respective sensorimotor cortical network, and therefore, focused analysis on the alpha and beta frequency bands.

MATERIALS AND METHODS

SUBJECTS AND EXPERIMENTAL SCHEDULE

Thirty-three healthy, right-handed subjects (three male, 26.1 ± 4.0 years) participated in the study. The study was performed in compliance with the relevant laws and institutional guidelines and approved by the ethics committee of the Charité University Medicine Berlin. In the *pre*-session, 15 min of resting state EEG was recorded using a 64-channel EEG system (BrainAmp, Brain Products, 0.1–250 Hz hardware bandpass filter, 59 scalp channels arranged according to the International 10–20 System, two ECG channel, and one vertical EOG channel, all referenced against FCz, impedances $<5\,k\Omega$, sampling rate 5 kHz). During the whole session subjects were sitting in a quiet and dimly lit room and were instructed to stay awake and watch a silent animal documentary on a distant computer screen, which allowed maintaining a high state of vigilance while still minimizing eye movements. During the *RSS*-session high-frequency somatosensory stimuli were delivered for 30 min to the right index finger (IF) of the subject (see section "*High-frequency RSS*" for details of the stimulation protocol). EEG was continuously recorded during RSS and was used to identify EEG somatosensory signal components (see section "*EEG pre-processing*"). In the *post*-session, 30 min after RSS terminated, another 15 min of resting state EEG was recorded, with all settings identical to the *pre*-session.

HIGH-FREQUENCY RSS

Two types of previously reported somatosensory RSS stimuli were used (electrical or vibrotactile). In 21 subjects, two disposable surface electrodes with an area of 15 × 20 mm were attached to the palmar skin of the right IF, with the positive electrode applied to the distal and the negative electrode applied to the proximal phalanxes (Smith et al., 2009; Kalisch et al., 2010). In 12 subjects, a small loudspeaker diaphragm with a diameter of ∼8 mm was mounted to the tip of the right IF and was used to transmit the tactile stimuli to the skin (Godde et al., 2000; Pleger et al., 2001; Dinse et al., 2003). Stimulation trains consisted of 20 single pulses within 1 s (i.e., a repetition rate of 20 Hz) with an inter-train interval of 5 s. Duration of the RSS protocol was 30 min, resulting in a total number of 6000 pulses. RSS stimuli were applied at 50% above perception threshold.

PSYCHOPHYSICAL MEASUREMENTS

Behavioral impact of RSS was assessed by testing tactile discrimination performance via a two-alternative forced-choice simultaneous spatial two-point-discrimination (2PD) paradigm. This data was in fact acquired in the context of another study and not used for any further analysis, but is reported here for the sake of completeness. In every subject, 2PD was performed before and after RSS, for the right stimulated and left control IF. For details of the 2PD procedure please refer to previous studies using the identical protocol (Godde et al., 2000; Pleger et al., 2001; Dinse et al., 2003).

EEG—PRE-PROCESSING

All EEG data analysis was carried out using MATLAB v7.6.0 and the EEGLAB toolbox (Delorme and Makeig, 2004). EEG was down-sampled to 100 Hz and filtered (1–40 Hz) to remove slow drifts and line-noise and to improve the frequency specificity of subsequent post-processing techniques. EEG data were visually inspected and segments containing gross artifacts (due to movements or bad electrode impedances) were excluded. In all datasets

such segments constituted less than 2% of the data, indicating an overall sufficient data quality. For each subject, EEG datasets of all three sessions (*Pre, RSS, Post*) were merged and submitted to an independent component analysis (ICA). ICA linearly unmixes the original EEG channel data into a sum of maximally temporally independent and spatially fixed components (Bell and Sejnowski, 1995; Makeig et al., 1996). Characteristics of the resulting independent components (ICs) were obtained by the following analyses: for *pre*- and *post*-sessions, we calculated resting state power spectra using Welch's methods, where the time series is divided into overlapping, Hamming-windowed segments, the squared magnitude of the discrete Fourier transform is computed for all segments and then averaged. Segments had 50% overlap and a window length of two seconds (i.e., twice the number of data points sampled every second), resulting in a frequency resolution of 0.5 Hz. For the *RSS* session, we calculated two types of activity: stimulus-locked activity, i.e., the somatosensory-evoked potentials (SEP), reflecting evoked activity, and the event-related spectral perturbation (ERSP), reflecting frequency-resolved induced oscillatory activity [please refer to (Delorme and Makeig, 2004) for a detailed description of ERSP calculation]. ICA was used for further identification of artifacts. Time-courses, spectra, and topographic distributions of all ICs were inspected to identify components that reflected eye movement, scalp muscle artifacts and movement artifacts. These ICs were removed from the data. Furthermore, in each subject an IC was identified that represents activity related to sensorimotor activity and in particular to the somatosensory processing of the high-frequency RSS stimulus (further termed somato-IC). The somato-IC was identified by four criteria: (1) a somatosensory topography of the component map, (2) an alpha (8–12 Hz) frequency peak in the component spectrum (a beta peak is usually expected, but was not obligatory), (3) a significant SEP, and (4) a significant event-related desynchronization in the alpha frequency band of the ERSP images. If more than one somato-IC was identified in one subject, the first in order (explaining the most variance) was chosen.

For each subject, the individual alpha peak frequency of the rolandic rhythm was determined (further termed Iαf) as the frequency in the power spectrum of the somato-IC showing the maximum value within the broad alpha (8–12 Hz) band (Klimesch, 1996; Klimesch et al., 2006). We defined three subbands with reference to Iαf: peak (Iαf − 0.5 Hz–Iαf + 0.5 Hz), lower (Iαf – 1.5 Hz–Iαf), and upper (Iαf–Iαf + 1.5 Hz) alpha frequency band. This subdivision was motivated by previous studies showing that the broad alpha band can be divided into a lower and an upper sub-band, which exhibit different functional properties (Klimesch et al., 1994, 1997, 2006; Rohm et al., 2001; Doppelmayr et al., 2002). Additionally the beta band was defined as 13–29 Hz (since a beta peak was not identifiable in every subject, no individual beta peak frequency was calculated). Our approach to identify components extracted by the ICA related to somatosensory processing had the primary goal of ensuring that the RSS was conducted correctly. However, we performed all subsequent analyses in channel space and not in component space because we did not want to bias our analysis a priori only to ongoing activity related to the somatosensory system. A considerable fraction of rhythmic brain activity relevant to our hypothesis might be hidden in other components that were not categorized as somato-ICs.

EEG—IMAGINARY COHERENCY

Functional connectivity was assessed by means of ImCoh. Introduced by Nolte et al., this connectivity estimate is known to reduce overestimation biases inherent in many other measures of EEG functional connectivity, such as absolute coherence, phase locking, or synchronization likelihood (Nolte et al., 2004; Guggisberg et al., 2008). In these measures, spurious interactions with zero time lag arise due to common references, cross-talk, and volume conduction. In contrast, ImCoh only captures "true" interactions that occur with a certain time lag, omitting all spurious zero time lag interactions. ImCoh is defined as the imaginary part of coherency $C_{ij}(f)$, which is a complex measure of the linear relationship between two time series $\hat{x}_i(t)$ and $\hat{x}_j(t)$ at a certain frequency *f*. $C_{ij}(f)$ is defined as the normalized cross-spectrum between the two signals (which in our case are the time series of two EEG channels *i* and *j*):

$$C_{ij}(f) = \frac{S_{ij}(f)}{\left(S_{ii}(f)S_{jj}(f)\right)^{1/2}},$$

where $S_{ij}(f) \equiv \langle x_i(f)x_j^*(f)\rangle$ is the cross-spectrum, * is the complex conjugate, $\langle\,\rangle$ is the expectation value, and $x_i(f), x_j(f)$ are the complex Fourier transforms of $\hat{x}_i(t), \hat{x}_j(t)$.

With $n = 59$ scalp channels available, there are $\frac{n(n-1)}{2} = 1711$ possible ImCoh values, since C is antisymmetric with vanishing diagonal. ImCoh was calculated separately for each subject, recording session, and channel pair combination. The 15 min EEG time series was partitioned into overlapping (50%) segments with a window length of 2 s, which resulted in a frequency resolution of 0.5 Hz. ImCoh values for each of the four frequency bands (three alpha sub-bands and beta band) were calculated by averaging the ImCoh of the respective frequencies. For each channel pair, changes of ImCoh between *pre*- and *post*-session were tested for significance using Student's *t*-tests. In order to allow appropriate use of a parametric statistical test, *Fisher's Z*-transformation was used to normalize the distribution of ImCoh data (see Nolte et al., 2004 for details on the transformation of complex coherency). After transformation normality of the distribution was confirmed by an Anderson–Darling test.

CORRECTION FOR MULTIPLE COMPARISONS

The large number of tested channel pairs increases the probability that one or more null hypotheses are mistakenly rejected, also known as the family-wise error rate (FWER). Thus, a correction for multiple comparisons is needed before a statement with respect to statistical significance can be made. Due to the possible redundancy between neighboring channels, a classical Bonferroni correction is a too conservative approach. An established alternative is the false discovery rate (FDR), which is a less conservative and more powerful method for controlling the FWER (Benjamini and Hochberg, 1995).

FDR calculates the expected proportion of false positives (type I error) among all significant hypotheses $H_1 \ldots H_m$.

Their corresponding P-values $P_1 \ldots P_m$ are sorted in increasing order and for a given threshold α the largest $P(i)$ such that $P(i) \leq \frac{i}{m}\alpha$, is identified. Then all hypotheses $H_1 \ldots H_i$ are rejected. Here, we used the generalized Benjamini–Hochberg–Yekutieli procedure which controls the FDR under arbitrary dependence assumptions by using $P(i) \leq \frac{i}{m\sum_{j=1}^{m} 1/j}\alpha$ and thus is guaranteed to be accurate for any test dependency structure, i.e., even if the tests are positively or negatively correlated (Benjamini and Yekutieli, 2001).

RESULTS

EEG—IDENTIFICATION OF SENSORIMOTOR COMPONENTS

We aimed to investigate the impact of high-frequency RSS on resting state functional connectivity in the sensorimotor system. As a first step we used ICA to identify EEG components in each subject that reflect sensorimotor activity (somato-ICs), including the response to the RSS (for definition of criteria see Materials and Methods section "*EEG—pre-processing*"). **Figure 1** shows the properties of a somato-IC in a representative subject. The distribution of the component's weights shows a clear sensorimotor topography (**Figure 1A**). Its resting state frequency spectrum exhibits distinct peaks in the alpha and beta frequency bands, which reflect the ongoing rolandic rhythms (**Figure 1C**). The component shows both an evoked and an induced response to the RSS (**Figures 1B** and **D**).

In seven subjects we could not identify any somato-IC. Neither did they show any somatosensory features (SEP, ERD, spectral alpha peak) in channel space. In fact all subjects that showed an EEG response to the RSS in channel space yielded at least one somato-IC. There might be several reasons why these subjects did not respond to stimulation, at least in terms of a measurable EEG response. The stimulation amplitude was set to 50% above perception threshold, which was determined in an iterative manner via the subjects' feedback. It is conceivable that in some cases, the amplitude of the stimulation might have been too low to induce any EEG response (and also any perceptual learning). Another possibility is a malfunction of the stimulation device. Since we could not exclude technical failure or a bad setting of the stimulation amplitude we excluded these subjects. Importantly the exclusion was based on the absence of their EEG response, not on the basis of their behavioral results. Nevertheless, these subjects did not show any behavioral improvement (mean $\pm$ SD two-point-discrimination threshold changes of the right stimulated IF were $-1.03 \pm 7.27\%, p < 0.8125$, Wilcoxon-Signed Rank test).

The final subject group was still large enough to perform proper group analyses and statistics (26 subjects, 3 male,

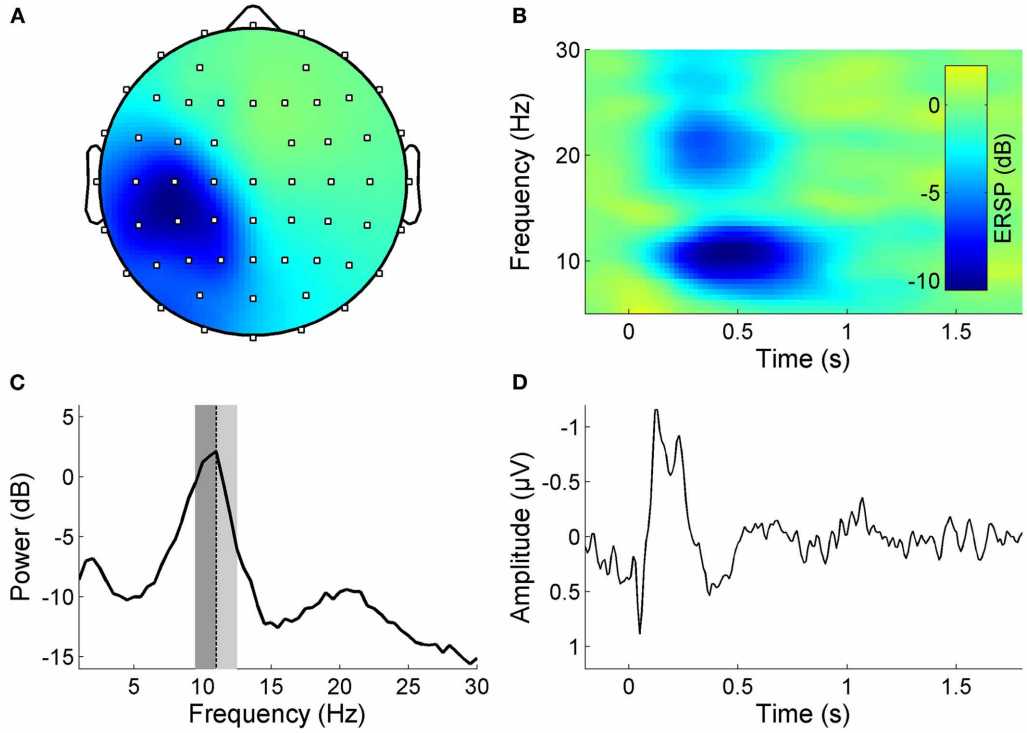

FIGURE 1 | Properties of a somato-IC reflecting sensorimotor activity in a representative subject. (A) Scalp map projection of IC weights (dots display channel locations, color-coding as in panel **B**, but unitless). The projection shows a lateralized somatosensory topography with a peak contralateral to the stimulation site. **(B)** Time-frequency image showing ERSP, which is the relative change in event-related power at different frequencies, time-locked to the high-frequency RSS which starts at time point zero and is sustained for one second. Note the pronounced ERD in the alpha and beta frequency band during stimulation. **(C)** Mean log power spectrum with distinct peaks in the alpha and beta frequency band. Individual alpha frequency Iα f indicated as dotted lines, lower/upper alpha bands relative to Iαf are indicated as dark/light gray areas. **(D)** Corresponding time-locked average SEP.

26.1 ± 4.0 years). All remaining subjects exhibited a clear alpha peak in the resting state spectrum of their primary somato-IC. The group mean (±SD) peak frequency in the alpha band was 9.9 ± 1.35 Hz.

Prior to further analysis, ICs representing eye movement, scalp muscle artifacts, and movement artifacts were removed from the data. The mean ± SD number of ICs removed from data was 2.19 ± 0.89, which corresponds to 3.7 ± 1.5% of the total 59 ICs per subject. Although the total number of discarded ICs limits the maximum number of independent coherencies, the removal of these non-physiological and non-neuronal ICs increases the overall sensitivity for coherencies based on neuronal processes.

EEG—FUNCTIONAL CONNECTIVITY CHANGES

To assess the impact of RSS on resting state functional connectivity, we analyzed ImCoh before and after the RSS procedure. **Figure 2** shows an overview of the frequency-resolved (1–40 Hz, resolution 0.5 Hz) statistical dispersion of ImCoh-spectra. Depicted are the standard deviations (SD) across all subjects and all channel pairs for *pre*- and *post*-sessions and for the difference spectra *post-pre* indicating the change between the two sessions. Before calculating the SD, spectra of all subjects were shifted so that their alpha peak frequencies coincide at 10 Hz (e.g., if a subject exhibits an alpha peak frequency of 11.5 Hz, the spectrum is shifted 1.5 Hz to the left). This visualization corresponds to the band-specific analyses, which we performed based on individual peak frequencies (Klimesch, 1996; Klimesch et al., 2006). The original alpha peak frequencies of all subjects are indicated in **Figure 2A** as black dots. The most pronounced change of ImCoh is clearly visible in the alpha frequency band (8–12 Hz). A first hint to the location of the alpha ImCoh change is given when looking at the SD of ImCoh spectra of channel pairs in specific regions-of-interest (ROIs). A separate display for frontal, central, and occipital channels reveals that the main effect originates from central channels, with maximal changes in the alpha and beta frequency bands (**Figure 2D**). This fits to the sensory modality of the RSS stimulation, since the sensorimotor system is known to exhibit oscillatory activity in these bands (Kuhlman, 1978; Pfurtscheller, 1981, 2006).

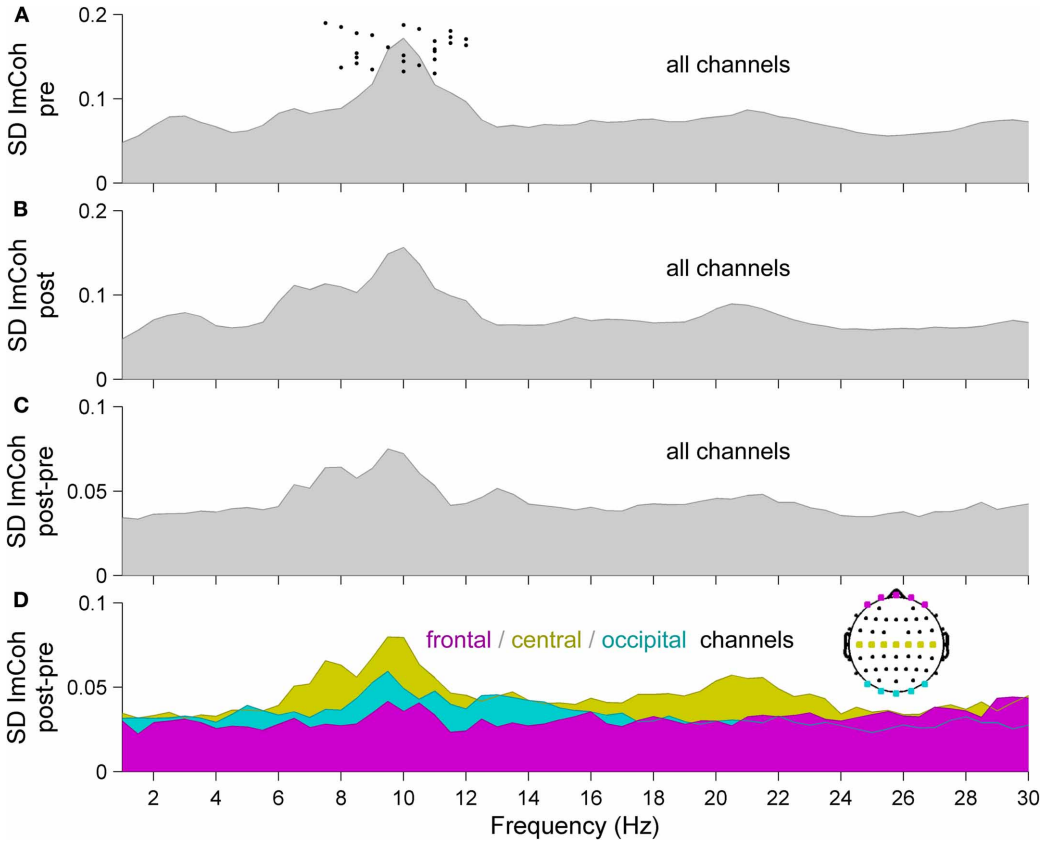

FIGURE 2 | Statistical dispersion of ImCoh-spectra for (A) pre- and (B) post-sessions and for (C, D) difference spectra post-pre, indicating the change between the two sessions. (A–C) Standard deviations (SD) across all subjects and all scalp channels. Before calculating the SD, spectra of all subjects were shifted so that their alpha peak frequencies coincide at 10 Hz. Original alpha peak frequencies of all subjects are indicated as dots in panel **A**. **(D)** SD of ImCoh difference spectra from panel **C**, but separately for three sub-groups of channels, indicated in the head plot (magenta: frontal, yellow: central, cyan: occipital). Since ImCoh is antisymmetric ($im(C_{ij}(f)) = -im(C_{ji}(f))$) only the upper off-diagonal elements of the imaginary part of the coherency matrix are shown. Normality of distributions was confirmed by Anderson–Darling tests, allowing the use of SD as a measure of statistical dispersion.

Please note that **Figure 2** is purely illustrative and does not allow for any statistical interpretation. Therefore next, we analyzed which of the changes of ImCoh between *pre*- and *post*-sessions were statistically significant. Given the sensory modality of the applied RSS, we focused on the ongoing oscillatory activity in the alpha (8–12 Hz) and beta (13–29 Hz) frequency bands. Also, given the known distinct functional roles of different alpha sub-bands (Klimesch and Doppelmayr, 1997; Pfurtscheller et al., 2000; Klimesch et al., 2003; Sadaghiani et al., 2010), we additionally defined three alpha sub-bands (peak, lower and upper band), which were determined in each subject according to their individual peak frequencies (see Materials and Methods section for details). Of all analyzed frequency bands, we found the maximum connectivity change in the upper alpha frequency band. **Figure 3** shows the group results for this band. A pronounced change of ImCoh can be seen over central cortical areas contralateral to the somatosensory stimulation. This change is highly significant (**Figures 3B** and **C**). **Figure 3D** shows significant channel pairs after FDR-correction for multiple comparisons, which were: C1–C3, C1–C5, C1–CP5, CP1–CP3, CP1–CP5, CP3–C1, FC1–FT7. In the other analyzed alpha and beta frequency bands, we also found significant changes of ImCoh, but they were only marginal and after FDR-correction for multiple comparisons confined to isolated single channel pairs (lower alpha band: no significant changes, peak alpha band: C1–C3, beta band: FC3-TP7).

Although our data allows only limited claims regarding the exact cortical source of the change in resting state functional connectivity, they indicate that the main change is possibly related to activity in the sensorimotor cortex. First, the peak of change is located over central electrodes contralateral to the somatosensory stimulation site, indicating that the change in functional connectivity is produced by the repetitive somatosensory stimulation. Secondly, the main change in functional connectivity is reflected in a change of ImCoh in the alpha band, which, due to the location, most certainly corresponds to mu-rhythm activity, which is the dominant resting state rhythm of the sensorimotor system. The observed connectivity changes exhibited a predominant medio-lateral orientation and are distributed over frontoparietal sensorimotor cortex (**Figure 3E**). According to Koessler et al. (2009), who estimated the cranio-cerebral correlations between surface EEG channel positions and the underlying cortical fissures, our main effect reflects connectivity changes between precentral gyrus and postcentral/inferior parietal gyrus (channel C1

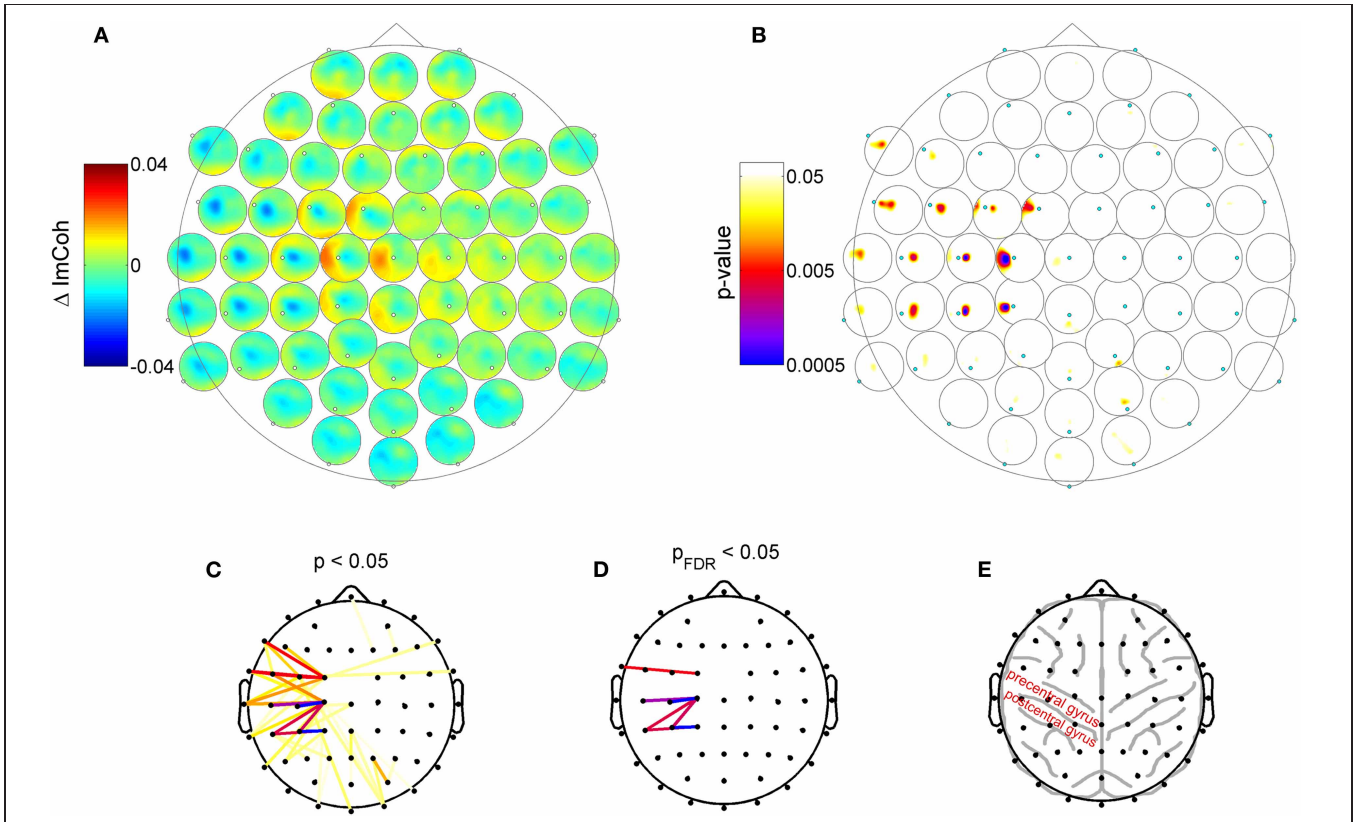

FIGURE 3 | Change of resting state functional connectivity after high-frequency RSS. (A) ImCoh difference between *pre*- and *post*-session (before and after RSS). Dots: Channel relative to which ImCoh is shown. **(B)** Corresponding *p*-values indicating statistically significant changes of ImCoh. A cluster of significant connectivity changes is located over contralateral central areas. **(C)** Different visualization of data shown in panel **B**. Dots indicate channel locations, lines indicate channel pairs with statistically significant ImCoh changes (color coding as in panel **B**). **(D)** Same as panel **C**, but only significant ImCoh changes after FDR-correction for multiple comparisons. **(E)** Outline of typical locations of cortex gyri and sulci, indicating that the main change of ImCoh is located over pre- and post-central cortical areas.

to channels C3, C5, Cp1), and within postcentral/inferior parietal gyrus (channel CP1 to CP3, CP5).

INCREASED TACTILE ACUITY AFTER RSS

RSS led to a significant reduction of the 2PD threshold (*post-hoc* difference post-pre $= -0.24$ mm, $p < 4.67 \times 10^{-6}$, paired Student's t-test) for the stimulated right IF, while threshold of the left control IF remained unchanged (difference post-pre $= -0.0058$ mm, $p < 0.906$). These results are closely in line with earlier studies using the identical stimulation protocol as used in our current study (Godde et al., 2000; Pleger et al., 2001; Dinse et al., 2003). While 2PD data was measured here to ensure stimulation efficacy and for further analysis in the context of another study, we do not believe it is an effective test for changes in functional connectivity between distant brain regions, and hence did not further analyze behavioral data in the scope of this study. We plan to follow up on the link between functional connectivity changes and behavior by testing e.g., sensorimotor integration by means of motor tasks (Smith et al., 2009).

DISCUSSION

We investigated the impact of a specific form of intermittent high-frequency RSS on the network characteristics of the brain. In particular, we analyzed resting-state functional connectivity and found effects within sensorimotor areas which are known to be relevant for sensorimotor processing and integration (Diamond et al., 2008; Aronoff et al., 2010; Mao et al., 2011). The here-used RSS paradigm is known to evoke Hebbian-like learning processes and as a consequence causes both an improvement in tactile acuity (Godde et al., 2000) and a cortical reorganization of the somatosensory representational maps (Pleger et al., 2001, 2003; Dinse et al., 2003).

Similar improvements in tactile discrimination as well as in cortical representation can be induced by repetitive transcranial magnetic stimulation (rTMS). The approaches of RSS and of rTMS share a common conceptual idea: to adapt stimulation protocols typically used in studies of synaptic plasticity at a cellular level in order to alter perception and behavior in human individuals. Crucial to this approach is the observation that changes induced in this way are bidirectional depending on stimulation frequency. Both low frequency repetitive stimulation as well as low frequency rTMS have been shown to reduce cortical excitability in parallel to impairment of behavior. In contrast, high-frequency, intermittent stimulation enhances excitability, which is associated with improvement of performance (Siebner and Rothwell, 2003; Ragert et al., 2004; Tegenthoff et al., 2005; Reis et al., 2008; Dinse, 2011). What makes exposure-based learning different to rTMS is the fact that in contrast to rTMS, the use of sensory stimuli employs the natural sensory pathway to reach a particular cortical area, and that this allows application of highly specific stimulus features such as orientation or luminance, which has been shown to induce specific learning effects for those features (Beste et al., 2011), an option not possible for rTMS.

Please note that we referred to the effects of passive stimulation as "learning processes." The rationale for this is based on previous studies showing that the effects of repetitive stimulation depend on NMDA-receptor activation (Dinse et al., 2003), thus demonstrating that the effects of passive stimulation are mediated by very basic mechanisms underlying synaptic plasticity, and on empirical findings showing facilitation of intracortical excitability (Hoffken et al., 2007). We therefore argue that the effects of passive stimulation are based on modifications of synaptic efficacy and transmission, both fundamental principles underlying "learning". In a more general view, learning is defined as the acquisition of new knowledge, behaviors, skills, values, preferences or understanding, and may involve synthesizing different types of information. Apparently, the term "learning" is rather broadly defined. Given such a broad definition, in our view the outcome of persistent improvement observed following passive stimulation qualifies as learning.

High-frequency RSS was previously proposed as therapeutic approach to treat the decline and loss of sensory abilities (Kalisch et al., 2008, 2010; Smith et al., 2009). Additionally, high frequency RSS has been shown to improve sensorimotor abilities such as haptic and fine motor performance in elderly subjects (Kalisch et al., 2008, 2010). It has, therefore, successfully been applied in stroke patients to improve motor test results and to stabilize motor training effects over a longer time course (Smith et al., 2009). These data implicate that a purely passive sensory repetitive stimulation protocol has a pronounced impact on the network characteristics of the sensorimotor system, and point to the importance of sensory input and sensorimotor integration for the outcome of motor-training rehabilitation paradigms. Here, we provide neurophysiological evidence supporting these recent behavioral results. We show that high-frequency RSS not only changes sensory function and evoked activity in somatosensory areas (Pleger et al., 2001, 2003; Dinse et al., 2003), but also significantly affects resting-state functional connectivity between brain areas engaged in sensorimotor integration processes.

As a means of assessing functional connectivity, we examined coherency changes of ongoing oscillatory activity in human EEG. Although the approach of using ImCoh as a measure of functional connectivity is fairly new (Nolte et al., 2004), it has been applied in a wide variety of studies of different clinical and neuroscientific context (Guggisberg et al., 2008; Cole et al., 2010; Hinkley et al., 2010, 2011; Gonzalez et al., 2011; Martino et al., 2011; Nicolas et al., 2011; Sander et al., 2011).

Our results show that a brief application of RSS alters functional connectivity of the sensorimotor system. Connectivity changes had a mainly medio-lateral orientation, which principally is in line with earlier findings indicating a change of the center of gravity of somatosensory-evoked activity in medio-lateral direction in EEG and fMRI data (Pleger et al., 2001, 2003). In contrast to those previous results, however, the here-reported changes of functional connectivity were present during the resting state, i.e., in the absence of any explicit sensorimotor stimuli and are distributed over EEG channels which are located over pre- and post-central cortex (Koessler et al., 2009)—suggesting an involvement of not only sensory but also motor areas.

Hence, the here reported connectivity changes might be related to the findings by Smith et al. (2009) and Kalisch et al. (2008, 2010), who observed enhanced sensorimotor integration,

enhanced information transfer, and enhanced learning after RSS. Furthermore, our findings might not only be related to these studies on stroke rehabilitation and physiological aging, but possibly apply to a variety of pathologies associated with sensory loss and motor function impairment.

The observed effect is based on changes in oscillatory coupling of ongoing EEG rhythms, with the main finding being in the upper alpha band (∼10–12 Hz). The alpha rhythm is one of the most prominent oscillatory hallmarks of the resting human brain. The amplitude of alpha-band oscillations exhibits temporal correlations and spatial coherency, over long-range distances (Nunez et al., 2001; Freyer et al., 2009a, 2011), which makes them eligible for the investigation of the brain's network characteristics. The most prominent alpha rhythm is related to the visual system and plays a strong functional role in the processing of visual stimuli (Makeig et al., 2002; Kirschfeld, 2005; Hanslmayr et al., 2007; Becker et al., 2008, 2011; Ritter and Becker, 2009; Scheeringa et al., 2011). However, the changes in functional connectivity in the present study relates to alpha activity that is distinct from the "classic" occipital alpha rhythm, which dominates the EEG when the subject is at rest with eyes closed. In the present case, the subjects had their eyes open, which leads to a strong attenuation of the occipital alpha rhythm. As can be seen in **Figure 2D**, alpha band ImCoh changes in occipital electrodes were much less pronounced than in central electrodes. In fact, the change in the alpha band is not stronger than in any other of the investigated frequencies indicating that it does not exceed noise level. Given the clear peak in central channels and the modality of the stimulus, the present finding most likely reflects the alpha band activity of the sensorimotor system, i.e., the mu-rhythm (Gastaut, 1952; Kuhlman, 1978).

Evidence for a functional role of the mu-rhythm is plenty. For example, intermediate amplitudes of the rhythm facilitate somatosensory stimulus perception in near-threshold stimulation conditions (Linkenkaer-Hansen et al., 2004). Pre-stimulus mu-rhythm amplitude predicts detection of a target stimulus against stronger masking stimuli (Schubert et al., 2009). The rhythm is also involved in higher cognitive processes, as indicated by studies showing a modulation of the mu-rhythm by attention (Jones et al., 2010; Anderson and Ding, 2011) and by the numerous application of mu-rhythm-based brain computer interfaces (Blankertz et al., 2007; Muller et al., 2008; Yuan and He, 2009; Pfurtscheller et al., 2010; Boulay et al., 2011). Combined EEG-fMRI studies have shown the mu-rhythm to be negatively correlated to the BOLD signal in primary somatosensory and motor cortex (Ritter et al., 2009), indicating less net neuronal activity, which is well in line with the recently proposed theory that alpha band rhythms serve a "gating-by-inhibition" (Klimesch et al., 2007; Jensen and Mazaheri, 2010). Finally, mu-rhythm has been shown to exhibit a functional connection to stimulus-induced brain signals in remote brain areas, thus providing evidence for long-range connectivity (Reinacher et al., 2009). But what might be the role of this rhythm in sensorimotor integration? Here, we speculate that the observed RSS-induced change in oscillatory coupling between distant sensorimotor areas reflects enhanced effectiveness of neuronal information transfer and sensorimotor integration, possibly via a modified feedback loop between motor and sensory areas, which in turn lead to the observed improvement of behavioral sensorimotor abilities. In order to provide a more detailed account of the mechanisms that link changes in oscillatory resting-state dynamics, altered connectivity, and improved somatosensory capabilities, comprehensive approaches combining advanced multimodal empirical data acquisition capable to also monitor ultrahigh frequency activity (Ritter et al., 2008; Freyer et al., 2009b), spatiotemporal nesting analysis (Schultze-Kraft et al., 2011), multivariate approaches (McIntosh et al., 1996; Boonstra et al., 2007; Krishnan et al., 2011), and computational modeling will be employed in the future.

CONCLUSIONS

Here we provide evidence for the impact of passive sensory stimulation on the resting state functional connectivity in the human brain. We show that 30 min of RSS leads to significant coherency changes of the ongoing mu-rhythm, the dominant resting state rhythm of the sensorimotor system. These changes might constitute a neurophysiological substrate for the previously observed improvements in sensorimotor training in response to RSS (Kalisch et al., 2008, 2010; Smith et al., 2009). Functional connectivity measures provide tools for assessing network interactions in the human brain, and may thus be used to study efficacy of different sensory and motor training paradigms.

ACKNOWLEDGMENTS

The authors acknowledge the support of the German Ministry of Education and Research (Bernstein Focus State Dependencies of Learning 01GQ0971: Frank Freyer, Matthias Reinacher, Hubert R. Dinse, Petra Ritter), the James S. McDonnell Foundation (Brain Network Recovery Group JSMF22002082: Petra Ritter), the Max-Planck Society (Minerva Program: Petra Ritter).

REFERENCES

Anderson, K. L., and Ding, M. (2011). Attentional modulation of the somatosensory mu rhythm. *Neuroscience* 180, 165–180.

Aronoff, R., Matyas, F., Mateo, C., Ciron, C., Schneider, B., and Petersen, C. C. (2010). Long-range connectivity of mouse primary somatosensory barrel cortex. *Eur. J. Neurosci.* 31, 2221–2233.

Becker, R., Reinacher, M., Freyer, F., Villringer, A., and Ritter, P. (2011). How ongoing neuronal oscillations account for evoked fMRI variability. *J. Neurosci.* 31, 11016–11027.

Becker, R., Ritter, P., and Villringer, A. (2008). Influence of ongoing alpha rhythm on the visual evoked potential. *Neuroimage* 39, 707–716.

Bell, A. J., and Sejnowski, T. J. (1995). An information maximization approach to blind separation and blind deconvolution. *Neural Comput.* 7, 1129–1159.

Benjamini, Y., and Hochberg, Y. (1995). Controlling the false discovery rate – a practical and powerful approach to multiple testing. *J. R. Stat. Soc. B* 57, 289–300.

Benjamini, Y., and Yekutieli, D. (2001). The control of the false discovery rate in multiple testing under dependency. *Ann. Stat.* 29, 1165–1188.

Beste, C., Wascher, E., Gunturkun, O., and Dinse, H. R. (2011). Improvement and impairment of visually guided behavior through LTP- and LTD-like exposure-based visual learning. *Curr. Biol.* 21, 876–882.

Blankertz, B., Dornhege, G., Krauledat, M., Muller, K. R., and Curio, G. (2007). The non-invasive berlin brain-computer interface: fast acquisition of effective performance

in untrained subjects. *Neuroimage* 37, 539–550.

Boonstra, T. W., Daffertshofer, A., Breakspear, M., and Beek, P. J. (2007). Multivariate time-frequency analysis of electromagnetic brain activity during bimanual motor learning. *Neuroimage* 36, 370–377.

Boulay, C. B., Sarnacki, W. A., Wolpaw, J. R., and McFarland, D. J. (2011). Trained modulation of sensorimotor rhythms can affect reaction time. *Clin. Neurophysiol.* 122, 1820–1826.

Carey, L. M., Matyas, T. A., and Oke, L. E. (1993). Sensory loss in stroke patients – effective training of tactile and proprioceptive discrimination. *Arch. Phys. Med. Rehabil.* 74, 602–611.

Cole, M. W., Bagic, A., Kass, R., and Schneider, W. (2010). Prefrontal dynamics underlying rapid instructed task learning reverse with practice. *J. Neurosci.* 30, 14245–14254.

Conforto, A. B., Cohen, L. G., Dos Santos, R. L., Scaff, M., and Marie, S. K. (2007). Effects of somatosensory stimulation on motor function in chronic cortico-subcortical strokes. *J. Neurol.* 254, 333–339.

Conforto, A. B., Kaelin-Lang, A., and Cohen, L. G. (2002). Increase in hand muscle strength of stroke patients after somatosensory stimulation. *Ann. Neurol.* 51, 122–125.

Delorme, A., and Makeig, S. (2004). EEGLAB: an open source toolbox for analysis of single-trial EEG dynamics including independent component analysis. *J. Neurosci. Methods* 134, 9–21.

Diamond, M. E., Von Heimendahl, M., Knutsen, P. M., Kleinfeld, D., and Ahissar, E. (2008). 'Where' and 'what' in the whisker sensorimotor system. *Nat. Rev. Neurosci.* 9, 601–612.

Dinse, H. R. (2011). Choosing to improve or to impair. *Clin. Neurophysiol.* doi: 10.1016/j.clinph.2011.10.011. [Epub ahead of print].

Dinse, H. R., Kleibel, N., Kalisch, T., Ragert, P., Wilimzig, C., and Tegenthoff, M. (2006). Tactile coactivation resets age-related decline of human tactile discrimination. *Ann. Neurol.* 60, 88–94.

Dinse, H. R., Ragert, P., Pleger, B., Schwenkreis, P., and Tegenthoff, M. (2003). Pharmacological modulation of perceptual learning and associated cortical reorganization. *Science* 301, 91–94.

Doppelmayr, M., Klimesch, W., Stadler, W., Pollhuber, D., and Heine, C. (2002). EEG alpha power and intelligence. *Intelligence* 30, 289–302.

Feys, H. M., De Weerdt, W. J., Selz, B. E., Steck, G. A. C., Spichiger, R., Vereeck, L. E., Putman, K. D., and van Hoydonck, G. A. (1998). Effect of a therapeutic intervention for the hemiplegic upper limb in the acute phase after stroke – A single-blind, randomized, controlled multicenter trial. *Stroke* 29, 785–792.

Freyer, F., Aquino, K., Robinson, P. A., Ritter, P., and Breakspear, M. (2009a). Bistability and non-Gaussian fluctuations in spontaneous cortical activity. *J. Neurosci.* 29, 8512–8524.

Freyer, F., Becker, R., Anami, K., Curio, G., Villringer, A., and Ritter, P. (2009b). Ultrahigh-frequency EEG during fMRI: pushing the limits of imaging-artifact correction. *Neuroimage* 48, 94–108.

Freyer, F., Roberts, J. A., Becker, R., Robinson, P. A., Ritter, P., and Breakspear, M. (2011). Biophysical mechanisms of multistability in resting-state cortical rhythms. *J. Neurosci.* 31, 6353–6361.

Gastaut, H. (1952). Electrocorticographic study of the reactivity of rolandic rhythm. *Rev. Neurol. (Paris)* 87, 176–182.

Godde, B., Stauffenberg, B., Spengler, F., and Dinse, H. R. (2000). Tactile coactivation-induced changes in spatial discrimination performance. *J. Neurosci.* 20, 1597–1604.

Gonzalez, J. J., Manas, S., De Vera, L., Mendez, L. D., Lopez, S., Garrido, J. M., and Pereda, E. (2011). Assessment of electroencephalographic functional connectivity in term and preterm neonates. *Clin. Neurophysiol.* 122, 696–702.

Guggisberg, A. G., Honma, S. M., Findlay, A. M., Dalal, S. S., Kirsch, H. E., Berger, M. S., and Nagarajan, S. S. (2008). Mapping functional connectivity in patients with brain lesions. *Ann. Neurol.* 63, 193–203.

Hanslmayr, S., Aslan, A., Staudigl, T., Klimesch, W., Herrmann, C. S., and Bauml, K. H. (2007). Prestimulus oscillations predict visual perception performance between and within subjects. *Neuroimage* 37, 1465–1473.

Hinkley, L. B., Owen, J. P., Fisher, M., Findlay, A. M., Vinogradov, S., and Nagarajan, S. S. (2010). Cognitive impairments in schizophrenia as assessed through activation and connectivity measures of magnetoencephalography (MEG) data. *Front. Hum. Neurosci.* 3:73. doi: 10.3389/neuro.09.073.2009

Hinkley, L. B., Vinogradov, S., Guggisberg, A. G., Fisher, M., Findlay, A. M., and Nagarajan, S. S. (2011). Clinical symptoms and alpha band resting-state functional connectivity imaging in patients with schizophrenia: implications for novel approaches to treatment. *Biol. Psychiatry* 70, 1134–1142.

Hoffken, O., Veit, M., Knossalla, F., Lissek, S., Bliem, B., Ragert, P., Dinse, H. R., and Tegenthoff, M. (2007). Sustained increase of somatosensory cortex excitability by tactile coactivation studied by paired median nerve stimulation in humans correlates with perceptual gain. *J. Physiol.* 584, 463–471.

Jensen, O., and Mazaheri, A. (2010). Shaping functional architecture by oscillatory alpha activity: gating by inhibition. *Front. Hum. Neurosci.* 4:186. doi: 10.3389/fnhum.2010.00186

Jones, S. R., Kerr, C. E., Wan, Q., Pritchett, D. L., Hamalainen, M., and Moore, C. I. (2010). Cued spatial attention drives functionally relevant modulation of the mu rhythm in primary somatosensory cortex. *J. Neurosci.* 30, 13760–13765.

Kalisch, T., Ragert, P., Schwenkreis, P., Dinse, H. R., and Tegenthoff, M. (2009). Impaired tactile acuity in old age is accompanied by enlarged hand representations in somatosensory cortex. *Cereb. Cortex* 19, 1530–1538.

Kalisch, T., Tegenthoff, M., and Dinse, H. R. (2008). Improvement of sensorimotor functions in old age by passive sensory stimulation. *Clin. Interv. Aging* 3, 673–690.

Kalisch, T., Tegenthoff, M., and Dinse, H. R. (2010). Repetitive electric stimulation elicits enduring improvement of sensorimotor performance in seniors. *Neural Plast.* 2010, 690531.

Kirschfeld, K. (2005). The physical basis of alpha waves in the electroencephalogram and the origin of the "berger effect". *Biol. Cybern.* 92, 177–185.

Klimesch, W. (1996). Memory processes, brain oscillations and EEG synchronization. *Int. J. Psychophysiol.* 24, 61–100.

Klimesch, W., and Doppelmayr, M. (1997). Upper alpha desynchronization, semantic memory, and task difficulty. *J. Psychophysiol.* 11, 373–374.

Klimesch, W., Doppelmayr, M., and Hanslmayr, S. (2006). Upper alpha ERD and absolute power: their meaning for memory performance. *Prog. Brain Res.* 159, 151–165.

Klimesch, W., Doppelmayr, M., Pachinger, T., and Ripper, B. (1997). Brain oscillations and human memory: EEG correlates in the upper alpha and theta band. *Neurosci. Lett.* 238, 9–12.

Klimesch, W., Sauseng, P., and Gerloff, C. (2003). Enhancing cognitive performance with repetitive transcranial magnetic stimulation at human individual alpha frequency. *Eur. J. Neurosci.* 17, 1129–1133.

Klimesch, W., Sauseng, P., and Hanslmayr, S. (2007). EEG alpha oscillations: the inhibition-timing hypothesis. *Brain Res. Rev.* 53, 63–88.

Klimesch, W., Schimke, H., and Schwaiger, J. (1994). Episodic and semantic memory – an analysis in the eeg theta-band and alpha-band. *Electroencephalogr. Clin. Neurophysiol.* 91, 428–441.

Koessler, L., Maillard, L., Benhadid, A., Vignal, J. P., Felblinger, J., Vespignani, H., and Braun, M. (2009). Automated cortical projection of EEG sensors: anatomical correlation via the international 10-10 system. *Neuroimage* 46, 64–72.

Koller, W. C. (1984). Sensory symptoms in parkinson's disease. *Neurology* 34, 957–959.

Kornatz, K. W., Christou, E. A., and Enoka, R. M. (2005). Practice reduces motor unit discharge variability in a hand muscle and improves manual dexterity in old adults. *J. Appl. Physiol.* 98, 2072–2080.

Krishnan, A., Williams, L. J., McIntosh, A. R., and Abdi, H. (2011). Partial least squares (PLS) methods for neuroimaging: a tutorial and review. *Neuroimage* 56, 455–475.

Kuhlman, W. N. (1978). Functional topography of the human mu rhythm. *Electroencephalogr. Clin. Neurophysiol.* 44, 83–93.

Linkenkaer-Hansen, K., Nikulin, V. V., Palva, S., Ilmoniemi, R. J., and Palva, J. M. (2004). Prestimulus oscillations enhance psychophysical performance in humans. *J. Neurosci.* 24, 10186–10190.

Litvak, V., Jha, A., Eusebio, A., Oostenveld, R., Foltynie, T., Limousin, P., Zrinzo, L., Hariz, M. I., Friston, K., and Brown, P. (2011). Resting oscillatory cortico-subthalamic connectivity in patients with parkinson's disease. *Brain* 134, 359–374.

Makeig, S., Jung, T. P., Bell, A. J., Ghahremani, D., and Sejnowski, T. J. (1996). Blind separation of event-related brain response components. *Psychophysiology* 33, S58.

Makeig, S., Westerfield, M., Jung, T. P., Enghoff, S., Townsend, J., Courchesne, E., and Sejnowski, T. J. (2002). Dynamic brain sources of visual evoked responses. *Science* 295, 690–694.

Mao, T. Y., Kusefoglu, D., Hooks, B. M., Huber, D., Petreanu, L., and Svoboda, K. (2011). Long-range neuronal circuits underlying the interaction between sensory and motor cortex. *Neuron* 72, 111–123.

Martino, J., Honma, S. M., Findlay, A. M., Guggisberg, A. G., Owen, J. P., Kirsch, H. E., Berger, M. S., and Nagarajan, S. S. (2011). Resting functional connectivity in patients with brain tumors in eloquent areas. *Ann. Neurol.* 69, 521–532.

McIntosh, A. R., Bookstein, F. L., Haxby, J. V., and Grady, C. L. (1996). Spatial pattern analysis of functional brain images using partial least squares. *Neuroimage* 3, 143–157.

Muller, K. R., Tangermann, M., Dornhege, G., Krauledat, M., Curio, G., and Blankertz, B. (2008). Machine learning for real-time single-trial EEG-analysis: from brain-computer interfacing to mental state monitoring. *J. Neurosci. Methods* 167, 82–90.

Nicolas, M. J., Lopez-Azcarate, J., Valencia, M., Alegre, M., Perez-Alcazar, M., Iriarte, J., and Artieda, J. (2011). Ketamine-induced oscillations in the motor circuit of the rat basal ganglia. *PLoS ONE* 6:e21814. doi: 10.1371/journal.pone.0021814

Nolte, G., Bai, O., Wheaton, L., Mari, Z., Vorbach, S., and Hallett, M. (2004). Identifying true brain interaction from EEG data using the imaginary part of coherency. *Clin. Neurophysiol.* 115, 2292–2307.

Nunez, P. L., Wingeier, B. M., and Silberstein, R. B. (2001). Spatial-temporal structures of human alpha rhythms: theory, microcurrent sources, multiscale measurements, and global binding of local networks. *Hum. Brain Mapp.* 13, 125–164.

Pfurtscheller, G. (1981). Central beta rhythm during sensorimotor activities in man. *Electroencephalogr. Clin. Neurophysiol.* 51, 253–264.

Pfurtscheller, G. (1992). Event-related synchronization (ERS): an electrophysiological correlate of cortical areas at rest. *Electroencephalogr. Clin. Neurophysiol.* 83, 62–69.

Pfurtscheller, G. (2006). The cortical activation model (CAM). *Prog. Brain Res.* 159, 19–27.

Pfurtscheller, G., Allison, B. Z., Brunner, C., Bauernfeind, G., Solis-Escalante, T., Scherer, R., Zander, T. O., Mueller-Putz, G., Neuper, C., and Birbaumer, N. (2010). The hybrid BCI. *Front. Neurosci.* 4:30. doi: 10.3389/fnpro.2010.00003

Pfurtscheller, G., Neuper, C., and Krausz, G. (2000). Functional dissociation of lower and upper frequency mu rhythms in relation to voluntary limb movement. *Clin. Neurophysiol.* 111, 1873–1879.

Pleger, B., Dinse, H. R., Ragert, P., Schwenkreis, P., Malin, J. P., and Tegenthoff, M. (2001). Shifts in cortical representations predict human discrimination improvement. *Proc. Natl. Acad. Sci. U.S.A.* 98, 12255–12260.

Pleger, B., Foerster, A. F., Ragert, P., Dinse, H. R., Schwenkreis, P., Malin, J. P., Nicolas, V., and Tegenthoff, M. (2003). Functional imaging of perceptual learning in human primary and secondary somatosensory cortex. *Neuron* 40, 643–653.

Powell, J., Pandyan, A. D., Granat, M., Cameron, M., and Stott, D. J. (1999). Electrical stimulation of wrist extensors in poststroke hemiplegia. *Stroke* 30, 1384–1389.

Ragert, P., Becker, M., Tegenthoff, M., Pleger, B., and Dinse, H. R. (2004). Sustained increase of somatosensory cortex excitability by 5 Hz repetitive transcranial magnetic stimulation studied by paired median nerve stimulation in humans. *Neurosci. Lett.* 356, 91–94.

Ragert, P., Kalisch, T., Bliem, B., Franzkowiak, S., and Dinse, H. R. (2008). Differential effects of tactile high- and low-frequency stimulation on tactile discrimination in human subjects. *BMC Neurosci.* 9, 9.

Reinacher, M., Becker, R., Villringer, A., and Ritter, P. (2009). Oscillatory brain states interact with late cognitive components of the somatosensory evoked potential. *J. Neurosci. Methods* 183, 49–56.

Reis, J., Swayne, O. B., Vandermeeren, Y., Camus, M., Dimyan, M. A., Harris-Love, M., Perez, M. A., Ragert, P., Rothwell, J. C., and Cohen, L. G. (2008). Contribution of transcranial magnetic stimulation to the understanding of cortical mechanisms involved in motor control. *J. Physiol.* 586, 325–351.

Ritter, P., and Becker, R. (2009). Detecting alpha rhythm phase reset by phase sorting: caveats to consider. *Neuroimage* 47, 1–4.

Ritter, P., Freyer, F., Curio, G., and Villringer, A. (2008). High-frequency (600 Hz) population spikes in human EEG delineate thalamic and cortical fMRI activation sites. *Neuroimage* 42, 483–490.

Ritter, P., Moosmann, M., and Villringer, A. (2009). Rolandic alpha and beta EEG rhythms' strengths are inversely related to fMRI-BOLD signal in primary somatosensory and motor cortex. *Hum. Brain Mapp.* 30, 1168–1187.

Rohm, D., Klimesch, W., Haider, H., and Doppelmayr, M. (2001). The role of theta and alpha oscillations for language comprehension in the human electroencephalogram. *Neurosci. Lett.* 310, 137–140.

Rosamond, W., Flegal, K., Friday, G., Furie, K., Go, A., Greenlund, K., Haase, N., Ho, M., Howard, V., Kissela, B., Kittner, S., Lloyd-Jones, D., McDermott, M., Meigs, J., Moy, C., Nichol, G., O'Donnell, C. J., Roger, V., Rumsfeld, J., Sorlie, P., Steinberger, J., Thom, T., Wasserthiel-Smoller, S., Hong, Y. L., and Assoc, A. H. (2007). Heart disease and stroke statistics – 2007 update – a report from the american heart association statistics committee and stroke statistics subcommittee. *Circulation* 115, E69–E171.

Sadaghiani, S., Scheeringa, R., Lehongre, K., Morillon, B., Giraud, A. L., and Kleinschmidt, A. (2010). Intrinsic connectivity networks, alpha oscillations, and tonic alertness: a simultaneous electroencephalography/functional magnetic resonance imaging study. *J. Neurosci.* 30, 10243–10250.

Salmelin, R., Hamalainen, M., Kajola, M., and Hari, R. (1995). Functional segregation of movement-related rhythmic activity in the human brain. *Neuroimage* 2, 237–243.

Salmelin, R., and Hari, R. (1994a). Characterization of spontaneous MEG rhythms in healthy adults. *Electroencephalogr. Clin. Neurophysiol.* 91, 237–248.

Salmelin, R., and Hari, R. (1994b). Spatiotemporal characteristics of sensorimotor neuromagnetic rhythms related to thumb movement. *Neuroscience* 60, 537–550.

Sander, T. H., Leistner, S., Geisler, F., Mackert, B. M., and Trahms, L. (2011). Characterization of motor and somatosensory function for stroke patients. *Physiol. Meas.* 32, 1737–1746.

Sathian, K., Zangaladze, A., Green, J., Vitek, J. L., and Delong, M. R. (1997). Tactile spatial acuity and roughness discrimination: impairments due to aging and parkinson's disease. *Neurology* 49, 168–177.

Sawaki, L., Wu, C. W., Kaelin-Lang, A., and Cohen, L. G. (2006). Effects of somatosensory stimulation on use-dependent plasticity in chronic stroke. *Stroke* 37, 246–247.

Sawaki, L., Yaseen, Z., Kopylev, L., and Cohen, L. G. (2003). Age-dependent changes in the ability to encode a novel elementary motor memory. *Ann. Neurol.* 53, 521–524.

Scheeringa, R., Mazaheri, A., Bojak, I., Norris, D. G., and Kleinschmidt, A. (2011). Modulation of visually evoked cortical fMRI responses by phase of ongoing occipital alpha oscillations. *J. Neurosci.* 31, 3813–3820.

Schubert, R., Haufe, S., Blankenburg, F., Villringer, A., and Curio, G. (2009). Now you'll feel it, now you won't: EEG rhythms predict the effectiveness of perceptual masking. *J. Cogn. Neurosci.* 21, 2407–2419.

Schultze-Kraft, M., Becker, R., Breakspear, M., and Ritter, P. (2011). Exploiting the potential of three dimensional spatial wavelet analysis to explore nesting of temporal oscillations and spatial variance in simultaneous EEG-fMRI data. *Prog. Biophys. Mol. Biol.* 105, 67–79.

Siebner, H. R., and Rothwell, J. (2003). Transcranial magnetic stimulation: new insights into representational cortical plasticity. *Exp. Brain Res.* 148, 1–16.

Silberstein, P., Pogosyan, A., Kuhn, A. A., Hotton, G., Tisch, S., Kupsch, A., Dowsey-Limousin, P., Hariz, M. I., and Brown, P. (2005). Cortico-cortical coupling in parkinson's disease and its modulation by therapy. *Brain* 128, 1277–1291.

Smith, P. S., Dinse, H. R., Kalisch, T., Johnson, M., and Walker-Batson, D. (2009). Effects of repetitive electrical stimulation to treat sensory loss in persons poststroke. *Arch. Phys. Med. Rehabil.* 90, 2108–2111.

Stamelou, M., Edwards, M. J., Hallett, M., and Bhatia, K. P. (2011). The non-motor syndrome of primary dystonia: clinical and pathophysiological implications. *Brain* doi: 10.1093/brain/awr224. [Epub ahead of print].

Tamura, Y., Ueki, Y., Lin, P., Vorbach, S., Mima, T., Kakigi, R., and Hallett, M. (2009). Disordered plasticity in the primary somatosensory cortex in focal hand dystonia. *Brain* 132, 749–755.

Tegenthoff, M., Ragert, P., Pleger, B., Schwenkreis, P., Forster, A. F., Nicolas, V., and Dinse, H. R. (2005). Improvement of tactile discrimination performance and enlargement of cortical somatosensory maps after 5 Hz rTMS. *PLoS Biol.* 3:e362. doi: 10.1371/journal.pbio.0030362

Tinazzi, M., Rosso, T., and Fiaschi, A. (2003). Role of the somatosensory system in primary dystonia. *Mov. Disord.* 18, 605–622.

Yuan, H., and He, B. (2009). Cortical imaging of sensorimotor rhythms for BCI applications. *Conf. Proc. IEEE Eng. Med. Biol. Soc.* 2009, 4539–4542.

Conflict of Interest Statement: The authors declare that the research was conducted in the absence of any commercial or financial relationships that could be construed as a potential conflict of interest.

Received: 15 December 2012; accepted: 08 May 2012; published online: 23 May 2012.

Citation: Freyer F, Reinacher M, Nolte G, Dinse HR and Ritter P (2012) Repetitive tactile stimulation changes resting-state functional connectivity—implications for treatment of sensorimotor decline. Front. Hum. Neurosci. ***6****:144. doi: 10.3389/fnhum.2012.00144*

5 Curriculum Vitae

Mein Lebenslauf wird aus datenschutzrechtlichen Gründen in der elektronischen Version meiner Arbeit nicht veröffentlicht.

For privacy reasons, this electronic version of my thesis does not contain my CV.

6 Complete list of publications

6.1 Articles in peer-reviewed journals

- **Reinacher, M.**, Becker, R., Villringer, A. & Ritter, P. Oscillatory brain states interact with late cognitive components of the somatosensory evoked potential. *Journal of Neuroscience Methods* **183**, 49–56 (2009).

- Becker, R., **Reinacher, M.**, Freyer, F., Villringer, A. & Ritter, P. How Ongoing Neuronal Oscillations Account for Evoked fMRI Variability. *The Journal of Neuroscience* **31**, 11016–11027 (2011).

- Freyer, F., **Reinacher, M.**, Nolte, G., Dinse, H. R. & Ritter, P. Repetitive tactile stimulation changes resting–state functional connectivity—implications for treatment of sensorimotor decline. *Frontiers in Human Neuroscience* **6**, Article 144 (2012).

6.2 Presentations at international conferences

- **Reinacher, M.**, Becker, R., Villringer, A., & Ritter, P. Ongoing rolandic alpha rhythm modulates evoked responses to vibrotactile stimuli. Program No. 723.2/F4. 2009 Neuroscience Meeting Planner. Chicago, IL: Society for Neuroscience, 2009. Online.

- Ritter, P., Schirner, M., **Reinacher, M.**, Rothmeier S., Schwarz, J., McIntosh, A., & Jirsa, V. Merging computational models and multimodal imaging data using The Virtual Brain. 2012 Meeting of the Organization for the Mapping of the Human Brain, Beijing, China.

7 Selbstständigkeitserklärung

Ich, Matthias Reinacher, erkläre, dass ich die vorgelegte Dissertation mit dem Thema: "Relationships of ongoing activity, stimulus response variability, and behavioral performance in the human brain" selbst verfasst und keine anderen als die angegebenen Quellen und Hilfsmittel benutzt, ohne die (unzulässige) Hilfe Dritter verfasst und auch in Teilen keine Kopien anderer Arbeiten dargestellt habe.

Datum _____

Unterschrift _____

8 Acknowledgements

This thesis would not have been possible without the support of numerous people at Charité University Medicine and the Bernstein Center for Computational Neuroscience in Berlin.

First, I would like to thank my supervisor PD Dr. Petra Ritter, whose ongoing support and critical expertise has been invaluable for the genesis of this thesis.

I would like to thank all former and current members of the lab, especially Robert Becker and Frank Freyer, who supported this work with both their own outstanding work and by providing valuable feedback. They also became friends.

I would like to thank my parents, for providing me with great education and a scientific world view, and for the freedom to pursue my own ideas and goals.

Lastly and most importantly, I would like to thank my partner, who supported me throughout this process and without whom this would not have been possible.

Berlin, July 15, 2012
Matthias Reinacher